UNIVERSITY OF MANITOBA

Experimental Study of a Novel Actively Assisted Bipedal Walker – Simulation, Modeling and Experiment

By

Nishant Balakrishnan, B.Sc.

A Thesis submitted to the faculty of Graduate Studies of

The University of Manitoba

In partial fulfillment of the requirements of the degree of

MASTER OF SCIENCE

Department of Mechanical and Manufacturing Engineering
University of Manitoba
Winnipeg, Manitoba

Abstract

This thesis covers the study of an actively assisted passive walker with discontinuous and impulsive actuation. The dynamics of the passive and active portions are derived, and a comprehensive mathematical model is proposed. An actuation method is also proposed to study the use of multiple discrete actuation events in a walking gait. Two key cases are considered: actuation at the stance point and at the EA point of a non-kneed walker. An experimental walker was designed that is capable of passive walking and has an experimental implementation of the proposed actuation system. A thorough characterization of the model is then performed, with experimental validation to show that: at high ramp angles, energy injection results in an increase in BOA of ∼38% on a stable walking gait at a C_t of 0.086, and at low ramp angles, injection results in a stride length increase of ∼29% at a C_t of 0.06.

Acknowledgment

I would like to offer thanks to my advisor, Dr. C. Wu for her unfaltering support, guidance, and faith. The contributions to my education from this research have been immense and it was possible thanks to the guidance I received. Through my education I was able to learn to push the boundaries of my knowledge and can honestly say I couldn't have seen myself producing this document the way it is when I started without the help of Dr. C. Wu.

I would like to offer thanks to Dr. S. Balakrishnan for technical guidance, facilities, support, and his never-ending ability to solve the toughest problems; I definitely couldn't have done it without you.

I would also like to offer thanks to M. Alghooneh, C. Fry Skyora, I. Penner, D. Tataryn, R. Earley and all of the other people who helped me solve any and all of the technical difficulties I ran into and for graciously allowing me to bounce ideas off of them.

I would finally like to thank the Natural Sciences and Engineering Research Council of Canada (NSERC) for their support of Dr. C. Wu through the Industrial Research Chair Program, and their personal support of my graduate education through the CGS research scholarship. Without the support of NSERC, projects like this would not be possible.

Table of Contents

List of Figures

List of Tables

Lexicon – Mathematical Terms

$\boldsymbol{\alpha}$ – Angular acceleration of the hipshaft of the walker

$\boldsymbol{\omega_i}$ – Angular velocity of the limb with index *i* in the walker system.

$\boldsymbol{\vartheta_i}$ – Leg angle of the limb with index *i* in the walker system.

$\boldsymbol{a}$ – Lower leg portion of NK-Walker model, analogous to shank.

$\boldsymbol{b}$ – Upper leg portion of NK-Walker model, analogous to thigh.

$\boldsymbol{d_1}$ – Upper portion of K-Walker shank

$\boldsymbol{d_2}$ – Lower portion of K-Walker thigh

$\boldsymbol{L}$ – Total leg length (K-walker or NK-Walker)

$\boldsymbol{L_s}$ – K-Walker shank length

$\boldsymbol{L_t}$ – K-Walker thigh length

$\boldsymbol{I_i}$ – Index inertia of each portion of the hip actuation mechanism, taken about the hip.

$\boldsymbol{I_O}$ – Total inertia of the hip actuator assembly, taken about the hip.

$\boldsymbol{M}$ – Total lumped mass at the hip of the NK-Walker model.

$\boldsymbol{m}$ – Total lumped mass on each leg of the NK-Walker model.

$\boldsymbol{m_T}$ – Total lumped mass at each thigh of the K-Walker model.

$\boldsymbol{m_S}$ – Total lumped mass at each shank of the K-Walker model.

$\boldsymbol{m_H}$ – Total lumped mass at the hip of the K-Walker model, same as M on the NK-Walker.

$\boldsymbol{C_t}$ – Total non-dimensional cost of transport of the walker

$\boldsymbol{C_{mt}}$ – Cost of transport of the walker considering only mechanical energy into the system

$\boldsymbol{C_{et}}$ – Cost of transport of the walker considering only actuation energy into the system

$\boldsymbol{f}$ – Discrete map representing the stride function of the walker, taken as a map of

$\boldsymbol{P_{input}}$ – Total power input to the system over a single stride (active or passive).

$\boldsymbol{E_{input}}$ – Total energy input to the system over a single stride (active or passive).

$\overrightarrow{\boldsymbol{\theta_m}}$ – Fixed points angles of the stride function, represent period 1 gait cycle ϑ_i.

$\overrightarrow{\omega_m}$ – Fixed points angular velocities of the stride function, represent period 1 gait cycle ω_i.

L(ω) – The magnitude of the angular momentum delivered via actuation, as a function of *ω.*

$\mathbf{r_g}$ – Radius of gyration, measured using only the leg mass and the inertia of the leg.

$\mathbf{x_m}$ – Mass center location, measured as a distance down from the hip along the leg axis.

$\boldsymbol{\omega}$ – The angular velocity of the hipshaft of the walker.

$\boldsymbol{\omega_t}$ – The terminal value for the angular velocity of the hipshaft of the walker.

$\boldsymbol{T(\omega)}$ – Torque as a function of time for the actuator.

$\boldsymbol{K_t}$ – The torque slope coefficient for the motor (specific to PMDC motors selected).

$\boldsymbol{I_A}$ – Net actuator inertia, taken as the sum of all declutched inertial components

$\boldsymbol{\tau}$ – Time constant for actuation, taken as the rest time between MTGE gait events.

$\boldsymbol{\tau_s}$ – Step period, measured for a single step only from one heelstrike to the next.

$\boldsymbol{f_0}$ – Natural frequency of the swing leg, experimentally measured value.

$\boldsymbol{y_h}$ – Peak hip motion (vertical), calculated for a specific gait only.

$\boldsymbol{L_S}$ – Stride length of the walker (measured for a single step), experimental or simulation.

$\boldsymbol{\theta_S}$ – Stance angle of a stable period 1 cycle gait, taken as the sum of $\overrightarrow{\theta_m}$

Fr – Froude number, non-dimensional walking velocity (experimentally derived).

γ – Fixed ramp angle for passive and hybrid walking gaits.

Lexicon - Concepts

Active Systems – A system has dynamics influenced by inertial forces, as well as an external force other than gravity. Systems (in the context of this thesis) will only be considered active if the energy injection into the system results in a change in system dynamics.

Passive Systems – A system has dynamics influenced by inertial forces, and no other forces with the exception of gravity. Typically employs the principles of passive dynamics to respond to disturbances.

Passive Dynamic Walking – A type of walking mechanism that is capable of walking *passively* on a ramp of fixed slope.

Human Bipedal Simulacrum – A mechanism that exhibits bipedal walking behavior but of a form not strictly found in nature or human bipedal locomotion. Devices of this nature are meant to provide understanding into similar systems, even If they are not a simulation of a real life system.

Natural Dynamics – The simple inertial response of a system described by Newtonian Dynamics. Typically used to describe systems that have a desirable response when undergoing inertial forcing or free response based on a set of initial conditions.

Stance Leg – The leg of the walker that is supporting the weight of the walker on it, and is the pivot point on the ground for the walker.

Swing Leg – The leg of the walker that is not supporting weight during the swing phase and is undergoing a swinging type motion.

Planar Walker – A walker with a mechanism requiring the walker to walk without any yaw motion of the hips, typically in the form of a four legged walker frame with the two outer legs linked and the two inner legs linked.

3D Walker – A walker that has hip motion and therefore moves in a 3 dimensional path (hip yaw motion), similar to a human walking gait.

N-Cycle Gait – A gait that repeats with a periodicity of *N*. Typically only gaits with N = 1 or N = 2 are studied in the field of passive dynamic walking.

Gait Cycle – A type of bipedal walking behavior that is comparable to human walking that occurs cyclically in a system.

Gait Event – A part of the gait cycle of a walker where the walker undergoes a drastic change in dynamics. These are typically impact type events that occur in a walking gait.

Heel Strike – A gait event when the swing leg of the walker contacts the ground and becomes the stance leg in the case of a periodic gait.

Knee Lock – A gait event where the knee of the walker is prevented from hyper-extension. This can only occur in walkers with a knee is not strictly necessary with some walker designs.

Stride Function – A discrete mapping utilized by the walker simulation model to map a set of pre-heelstrike initial angles and angular velocities through the dynamics of the chosen walker model to their post heelstrike counterparts.

Actuator Impedance – The dynamic response of an actuator to external forcing when the actuator is either disabled or in a state that is dormant. When a joint is said to have zero impedance, the dynamics of the joint are completely unaffected by the actuator attached to the joint.

Launch Target – A set of physical conditions corresponding to the fixed point of a walker gait for a given ramp angle that are used as a baseline to launch the walker.

SEA – Acronym for *Series Elastic Actuator*, a type of actuator that is typically employed on systems where joint impedance is of concern. Typically employs an elastic element between the actuator and the joint to assist in masking actuator impedance.

MTGE – Acronym for *Modified Transitional Gait Event*, a novel actuation method proposed in this research that utilized existing gait events to mask actuation forces (in the case of a simple MTGE) or creates new gait events for actuation that have a similar form (impulsive) to existing gait events.

BOA – Acronym for *Basin of Attraction*, the region surround the fixed point of a dynamical system that converges to the fixed point when an initial condition is started within it.

Chapter 1

Introduction

1.1 Motivation

Passive dynamics is a relatively complex field of research that is primarily focused on the behavior of systems responding to inertial disturbances. One key focus of this type of research is to use it to produce a desired motion from the system with a variety of initial conditions [1] via natural dynamics. This means that the system will respond in a desirable way to a disturbance (potentially to counter act it) or will produce a desired motion from an inertial disturbance which may come from within the system itself. A typical example of this is a passive bipedal walker, a device which can produce a cyclic bipedal walking gait by using the system's natural response to gravitational force and the systems own inertia. This generally takes the form of a small passive or active robot or mechanism that is placed on an inclined surface and is capable of walking down the surface in a controlled manner with a periodic bipedal gait [2].

There are a wide variety of reasons why there is keen research interest in harnessing natural dynamics, but one of the most basic is that devices utilizing natural dynamics have been shown to be substantially more energy efficient than devices employing traditional trajectory planning based control. An example of this is a passive dynamic biped vs. a trajectory control based biped such as Honda's ASIMO biped. While both can produce stable walking motions, a

purely passive biped on a slope of only 2˚ can produce a walking gait that is nearly 93 times more efficient than the one produced by ASIMO [3]. On the surface, this would make it seem as though the passive walker is substantially better than a traditionally controlled one, but in reality there are limitations inherent to passive walkers that must be considered. One of the simplest issues, is that a passive walker can only walk under a very specific set of initial conditions (which encompass a narrow region of the state-space of the walker system), and can only walk under these conditions if the right system parameters are also used. This includes having carefully set inertial properties of the walker legs, as well as the need for a relatively fixed rate of energy input (normally via a carefully controlled ramp angle). The most common solution to this is to try and vary the response of the walker via joint actuation governed by a control system.

In terms of practical applications, the first step is to look at the overall approach of the research instead of merely observing the direct outcome of it. The direct outcome of passive walking research is to produce a machine capable of bipedal walking gaits, but that is not to say the outcome is a simulation of a typical humanoid bipedal gait. In human walking, thousands of energy impulses control and shape each step, which is quite different from the outcome of a simple system responding to only gravitational energy. This means that the direct outcome does not have a strong link to humanoid bipedal walking, and the application of the research towards that end is significantly limited by this. If instead the overall approach of the research is considered, a different application can be seen where the research is very relevant: the fundamental study of the effect of energy injection on a passive system.

In terms of fundamental research on passive systems, there have been countless studies on very simple systems like an inverted pendulum with the focus being placed on the controlling a system with relatively simple passive dynamics. In most real world applications however, the passive dynamics of a physical system are not simple to study, and often governed by non-linear dynamics. In the case of a passive walking system, the dynamics are relatively complex but if system can produce a stable walking gait then the dynamics of the system are at least predictable. This offers a middle ground to study passive dynamics that is more complex than what would be found in a system that trivializes the dynamics (such as an inverted pendulum),

but is still less complex than many real life systems. These systems can also be studied as partially passive systems, where active elements (energy injection components) can be added to change the behaviour of the system without changing the passive dynamics substantially. The study of such middle-ground systems opens up the potential to study more complex system and the capacity to extend the developed control concepts to subsets of more complex systems. Examples of where partially passive systems could be implemented include the fields of robotics and prosthetic design. To achieve these goals however, the first step is to understand the idea of actuating a passive system, as discussed next.

1.2 Actuation of Passive Systems

One issue with actuation in a system that has passive dynamics comes down to a simple concept: joint impedance. The motion of a zero joint impedance planar walker is governed by the Newtonian dynamics of a simple revolute joint planar manipulator in phase space. When an actuator is added to the system, the response is no longer similar to that of a planar revolute joint manipulator as the joint impedance will usually cause some restriction of motion that is proportional to the angle, velocity or acceleration of the joint. A typical example of this is shown in the figure below, where a simple three link manipulator is modeled with and without joint impedance. One can see that in the system shown as Figure 1.1, each joint responds to torque in a simple Newtonian manner. For the system shown in Figure 1.2 one example of joint impedance is modelled, which takes the form of a spring and a damper at each joint. This is often what you would see on a system actuated by a pneumatic actuator, but in the general case, each joint has a term $T = f(\theta,\omega)$, which dictates the non-linear joint impedance torque that restricts motion. This can be generally modeled as a non-linear spring/damper on each joint. In the case of something like a geared electric motor, you can have a much more complex joint impedance term that can significantly affect the model dynamics [4].

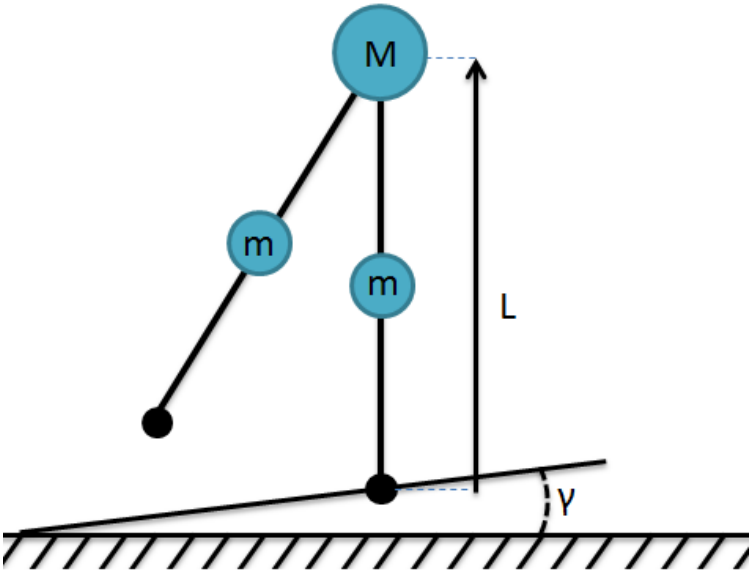

Figure 1.1: Fully Passive Walker – without Knees and without Joint Impedance

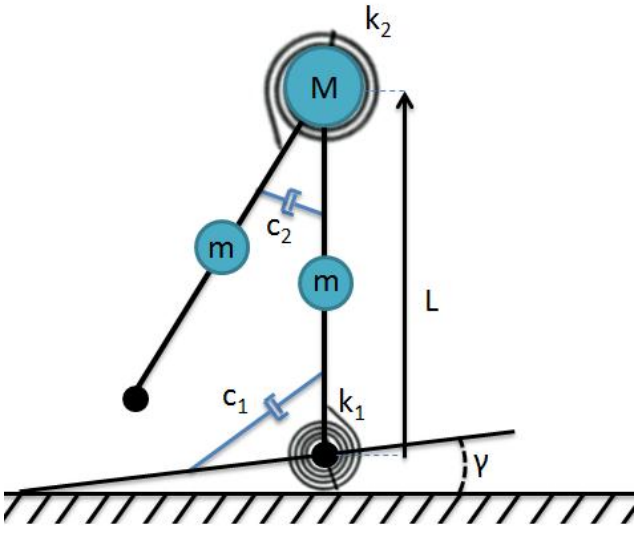

Figure 1.2: Fully Passive Walker – without Knees and with Joint Impedance

Up until recently, in the field of passive dynamics, the main research focus has been towards understanding the effect of actuators on a system. This is generally based around including the actuator dynamics in the control of a biped. This leads to countless examples (notable ones in [5] [6] [7]) where bipedal walkers are built that have full actuation (i.e. the

system has every degree of freedom actuated) or walkers that are under-actuated but with a trajectory planning based control system for the overall walker. These walkers all fundamentally have one drawback: the efficiency of the actuated walkers is substantially lower in practice than what can be achieved with a purely passive walker. An example of this can be seen when we consider the purely passive walker in [1], where the total cost of transport for the walker can be computed as:

$$C_t = \frac{P_{Input}}{mgv}$$

This cost of transport is a non-dimensional measure of the total energy efficiency of a process that transports mass. In a traditional walker, it can be seen that the power input to the system is only due to gravitational energy, so if the walker is on a constant slope the net cost of transport is equal to $sin(\gamma)$, where γ is the ramp angle in radians. Now when we look at one of the most notable efficient active-passive walkers in [3], we see that the mechanical cost of transport (C_{mt}) is 0.055, from $sin(\gamma)$, and the added electrical cost of transport is (C_{et}) is ~ 0.2. These figures are for a walker which is under-actuated and uses a passive knee. This results in a net C_t ~ 0.255, which is substantially higher than the purely passive biped from [1], that can operate on a low ramp angle of 2.29˚ with similar mass and has a C_t = 0.04, which is six times less. Now although it's easy to say that the system itself is mechanically efficient and that the electrical portion has less efficiency compared to the system in [1], a more accurate statement would be: the systems are not fundamentally the same and therefore the effect of the actuation on the mechanical efficiency is difficult to measure. This is mainly because the effect of the actuation impedance changes the system dynamics from the baseline unactuated walkers that are frequently studied. When comparing the presence of natural dynamics to an unactuated system, it becomes difficult to understand where the actuation is providing efficient walking energy and which portion of the walking gait is done via passive dynamics. This makes it incredibly difficult to study the nature of the passive dynamics and what effect the system parameters have on the passive dynamics as they interact with the actuation, which is one of the key research foci in the field of passive/active dynamics.

1.3 Current Research Approaches

Based on the difficulty of actuating a mainly passive system, without affecting the dynamics, the primary focus of current literature is clear: finding a method to decouple joint dynamics from the actuation dynamics.

1.3.1 Series Elastic Actuation

One key approach taken in literature is to use what are known as “elastic actuators”. A very simple version of this type of actuator is known as a Series Elastic Actuator (SEA). The fundamentals of SEA use are covered in [8], where a simple scheme is proposed to couple a physical actuator with an elastic element. A typically chosen combination for an SEA is a DC motor with a spring box or torsional spring. In terms of passive bipeds, several notable bipeds use this type of SEA to great effect [9] [10] [11].When an SEA is added to the system, the joint dynamics become more predictable as the elastic element of the actuator masks the actuator joint impedance, since the spring elastic force of the SEA is the primary force acting on the joint. When the actuation torque is applied to this, the spring tension is varied, which means that the actuation can be modeled as a variable rate spring, which allows for a system model with predictable dynamics. The main downside to this is that the passive dynamic model presented in [1] is no longer directly comparable if a spring is added at each joint, and the efficiency of the walker then becomes a property of the actuation method and control scheme as well as any desirable passive dynamics the new system model would have. As an example [12] is a biped that uses SEA to provide energy into the system, but without the actuators, the biped cannot walk on its own. This indicates that the natural dynamics of the system cannot provide enough energy to produce a walking motion on their own, and therefore are directly comparable to the dynamics in [1].

A common argument for SEA based approaches is that the dynamics of a system need not adhere to the guidelines in [1] in order to benefit from passive dynamics. Although this is a valid statement, the simple counter argument comes from the research presented in [1]. Although all systems with no joint impedance exhibit passive dynamics, the benefit to a bipedal walker is that portion of the passive dynamics that produce joint torque favourable to a passive walking

gait. In a system that doesn't follow the form posed in [1], the insight provided by the thorough quantitative analysis done on passive walking bipeds cannot be applied in a simple manner. Without this insight into what the passive efficiency of the system is and insight into how the energy in the system behaves naturally, it becomes very difficult to draw conclusions about additional actuation of the system and its effect on passive dynamics. As an example of this, we could take a simple case of an actuated walker on a ramp of 2.29˚. In the case of the passive system in [1] it is known that the dynamics of the system can be set with certain mass parameters to produce a stable walking gait with C_t = 0.04 when started with specific initial conditions. If actuation is then added to the system but using SEA, and the walker is no longer capable of walking passively, then a successful active walking gait at 2.29˚ has a $C_t = 0.04 + C_{mt} + C_{et}$, where C_{mt} and C_{et} come from the resulting gait parameters and the energy usage of the actuation. In this situation the abovementioned problem occurs, namely that the two cases (the passive and active) no longer are directly comparable. This means that while the original system used C_t = 0.04 from gravitational energy to produce a walking gait, it is not possible to determine how much of the energy input in the new system is coming from the gravitational contributions and how much comes from the actuator. All that is known is that in the combined case of $C_t = 0.04 + C_{mt} + C_{et}$, a walking gait is produced. This results in a very weak understanding of the effects of the actuation on the passive dynamics of the model, because it is very difficult to decouple the passive/active efficiencies.

One particular subset of SEA actuation is the use of a pneumatic actuator, which by nature acts as an SEA. One of the main differences in the implementation of a pneumatic actuator is that the normal use of this actuator is in line with the legs of the actuator (described as an axial SEA) vs. the use of a motor driven SEA at a rotational joint of the walker. An example of a biped that uses this is given in [13], which uses McKibben muscles to provide actuation energy into the walker. Another example is shown in [14], where FESTO PMA muscles are used in a tandem pair to actuate the joint with a comprehensive muscle model to characterize joint impedance. This has also led to developments in fully actuated bipeds using several pneumatic air muscles for actuation such as the biped developed in [15] and Lucy, a fully actuated pneumatic muscle biped [16]. Ultimately, these bipeds present controllable joints and relatively predictable joint

dynamics, but have the same fundamental problem as motor based SEA: with the actuation disabled, none of the referenced walkers have the capability to walk passively.

1.3.2 Inertial or Pulsed Energy Input

From the previous section, we see that there is a substantial challenge to most approaches that use SEA: the un-actuated form of the walker no longer describes a well-documented passive walking biped. One approach that can be taken to completely circumvent this problem is to design a walker that uses a pulsed actuation method that injects energy into a passive system and then allows the system to control and shape the energy into usable motion via its passive response. If this pulsing motion is of a discontinuous type (i.e. the actuation can be removed from the system dynamics), then the dynamics of the original system in [1] can be preserved. The concept behind this type of actuation is that the discontinuous coupling of the actuator to the system substantially reduces the effect of the joint impedance on the system. If the actuation can be nearly instantaneous, then the effect of the joint impedance change can be largely ignored. In contrast to previously discussed approaches, this also optimizes the passive dynamics of the system to provide the best walking capability and also allows for actuation to potentially enhance the basin of attraction (BOA) or the quality the walking gait. In [1], such a method is discussed, where the possibility to use a spring actuator is brought up but never developed. Based on these concepts, three main works have been developed [17] [18] [19] that are notable in literature. In [17] an adaptation of [1] is proposed with elastic actuation at the hip and a discontinuous actuation at the toe. This produces a simple system with energy injection through an impulsive toe-lift, which still has predominantly passive dynamics. In [18] a theoretically implemented adaptation of [17] is presented, where the concept of a passive toe-lift biped is discussed/modelled, to show that impulsive actuation (if applied at the toes of a biped) is viable. In [19], a different approach is taken, where a clutched SEA actuator is used so that the actuation can be decoupled from a system. In this case however, the actuation is not applied to a passive walker system, but still introduces the concepts involved.

Another approach that can be taken to solve these problems is through the use of a momentum wheel actuator. These types of actuators use a flywheel at the hip of the walker of substantial mass that is spun up or down using a specified angular acceleration. When the

angular acceleration change is substantial, the reaction force can be sent into the stance leg, or if a motor connection is used, it can be sent into the swing leg. An example of this is shown in [20], where a theoretical implementation of a momentum wheel actuator is implemented. Another example of this (but applied to a simple inverted pendulum system) is [21]. From [20] we can see that this approach tends to require near zero actuator inertia, due to the highly discontinuous nature of the control output requirements for a reaction wheel. This is fundamentally known as an issue with impact based passive walkers, as the dynamics of the system require large and abrupt changes in angular velocity to correct for the dynamics of the system, as shown in [22] and [23]. This is the rationale for approaches such as [24], where the requirement for a non-linear control for mimicking passivity in a biped system is analytically shown. One of other limitations of this approach is that the implementation of such an actuator is extremely difficult on a walking system, due to the need for a hip shaft that not only pivots and floats but has near zero friction.

1.3.3 Overview of Different Approaches

The natural evolution of these approaches is to go towards what is presented in [24], where a model is proposed that is capable of having adaptive, non-trajectory planned dynamics, in a walker that is “pushed” towards a desirable limit cycle type response via actuation. Although the combination of the actuation method in [19] and the control method in [24] would create a rather efficient walker that is actuated yet primarily relies on passive dynamics, the level of overhead and complexity is very large and is not something that is trivial to implement on the vast majority of systems. It also becomes very complex to compare the resulting system to the original system in [1]. This is because the energy efficiency has decreased and it can be seen that the walking gait is not as efficient as what was originally presented, however the dynamics of the system are vastly different and the versatility is substantially improved.

1.4 Previous Work at the University of Manitoba

In the field of passive dynamics, a substantial basin of knowledge has been developed at the non-linear dynamics laboratory at the University of Manitoba under the guidance of Dr. Christine Wu. Initially, the research focus was based on experimental walkers, starting with a

bipedal walker developed that used wooden legs and a pair of knees. The dynamics of this walker were studied experimentally as detailed in [25]. The work was then developed into a more comprehensive physical walker constructed using aluminum legs and a simple knee mechanism [26]. These two walkers both had round feet and work was done to compare the results to [1] [2], and it was found the walkers constructed in the lab used very similar gait patterns and had a similar structure to many commonly studied passive walkers. The analysis of the gait patterns produced by these walkers was measured in [27] [28] [29] and it was shown in all three cases that the behaviour of the walkers constructed in the lab and the techniques used to test them were capable of producing highly accurate bipedal walkers.

Once a solid experimental background was established, a significant amount of analytical and simulation work was completed in the lab based on and developed from the experimental side. A fully modelled 2 link walker, with frictional modeling for the ground interaction, was developed and validated in [30] and a thorough analysis of the stability of 2 link walkers was conducted in [31] based on a non-impact contact model. Models were also developed to study the effect of compliant ankle joints in a walker model [32] with a conceptual design for an elastic actuator being presented in [33]. Models for impact dynamics and foot constraint conditions in bipedal walkers was also studied in [34] and [35], applied specifically to the heel and knee impact events in a walker model. The latest research is based on passive/active bipedal walkers, with a proposed model in [36] that utilizes a hip actuator. Finally one of the most recent works in the laboratory has been to develop a comprehensive model based on gait events for kneed bipedal walkers with compliant ankles and flat feet [37]. This work is focused on incorporating actuation into the hip of the walker, and was experimentally validated via a SEA based walker with a torsional spring based hip actuator.

Between both the computational and experimental work done in the non-linear dynamics lab, there is a significant pool of knowledge to draw upon for a bipedal walker design. In the case of this thesis, the work presented primarily draws from the work done in [30] [36] [34], with the goal of strengthening the fundamental knowledge of passive dynamics at the lab by exploring active/passive bipedal walking using a simple model and experimental setup.

1.5 Overview and Thesis Approach

From the previous section, it is clear that there is a gap in current published research in terms of developing a passive walker that uses actuation of an impulsive or discontinuous nature, and can achieve a motion that: is similar to that of [1], is less complex to implement than [24], and is less complex from an actuation perspective as what is presented in [19]. To this effect, the research presented in this research aims to introduce a novel energy injection method into an otherwise passive system, the end result of which is a selectively actuated system that primarily operates on passive dynamics. To achieve this, three main research goals are set:

1. create a simulated passive walker that is capable of being accurately modelled, and have the versatility to walk on a variety of fixed ramp angles;
2. create an experimental setup that can be validated against the simulated walker model;
3. fit the experimental walker with an actuation system that uses an impulsive and discontinuous actuator to supply energy into the system; and
4. explore the performance of the actuation system to gain insight into active/passive hybrid systems.

Since the approach taken is one which is relatively novel, the main aim for the research is to gain insight instead of producing a viable alternative to present actuation methods. Based on this, many of the design decisions are directed towards producing a wide range of results and focus on the physical/simulation model interaction, instead of looking at simple optimized cases. In order to do this, the first step requires an in-depth understanding of what a passive model is, for a walking system, and the construction of a computational backbone for the project as detailed next.

Chapter 2

Mathematical Model

2.1 Introduction

In order to explore how to selectively actuate a passive system, the very first step is to come up with a model and an experimental walker that behave similarly. Unlike a simple investigation into passive walking, the addition of actuators and tuning results in a fairly large number of trials required to explore an active/passive system. Now although this is possible with a simple walker on its own, a validate-able computational model corresponding to a physical system allows for quick investigation of a broad number of actuation types and also allows for simple iterative tuning of parameters. In order to do this, the first step is to pick a system model with desirable passive dynamics. In terms of passive walkers, a variety of models are available, including bipedal walkers with knees [1], without knees [2], and other walking models (ballistic, quadruped, etc…) . The simplest of these systems that retains a strong analog to human walking is a bipedal walker with or without knees. In terms of bipedal walkers, the three main considerations are: the dimensionality of the walker (planar vs. 3d), the inclusion of a knee to the walker, and the foot shape of the walker. Looking at the main goals of the research, it's clear that the selection of a "simple model" is ideal as the goal of the study is not to analyze the most realistic model of human walking, but merely provide a simulacrum for bipedal locomotion as a medium to study active/passive actuation. This idea leads to a serious complication, since there is the need to develop an experimental setup and do limited

parametric study, as the definition of a “simple” model must then take into account what is simple in terms of an experimental walker as well as what is simple in terms of a simulation model. This leads to an aspect of design, where each aspect of the model can be considered from all viewpoints to create a model that is best suited to achieve the research goals, as discussed next.

When thinking of a passive walking model, one of the concerns with the type of feet chosen is the difficulty created in accurately modeling the feet of the walker. In a simple case (point feet), the only forces capable of being transmitted by the feet are point loads, and with careful material selection, the constraint at the foot of the walker can be considered as a simple holonomic constraint. When the weight of the walker is applied to the point of the foot, a frictional force is created that prevents the foot from moving. With a sufficiently sharp point the foot has the capability to pivot bi-axially around the point of contact. This means that contact model is relatively simple and any errors can be accounted for via tuning of the pre/post impact velocities of the model. When using round feet, this problem becomes much more complex, as the constraint becomes non-holonomic, with the frictional force and the mass center location determining the constraint conditions. Although this can be modeled using a friction and contact model, this makes the walker gait computation incredibly complex [38]. The other complication is that the equations of motion of the walker are also influenced by this constraint as the rotation of the leg causes a shift in the location of the mass center of the walker. This means that the precision of the contact model is very important, which further complicates modeling. On the other hand, a thorough qualitative and quantitative parameterized design guide is given in [1] for walkers of this type. In terms of a flat-foot walker, the addition of an additional joint also creates a substantially more complex walking model, with relatively unknown passive dynamics. If the joint is instead treated as a *slave joint* in that the foot is flat on the ground at all times and the ankle has zero impedance, then the walker is fundamentally a point foot walker with extensions to the feet, and can be modeled via a point foot model.

In terms of the dimensionality of the walker (i.e. 2d vs. 3d), there are compelling research arguments for each case. From a modeling perspective, the 2D walker moves only in a planar

motion (looking perpendicular to the axis of rotation of the joints of the walker) and any and all lateral motion is cancelled out internally on the walker. This poses some interesting challenges physically, as described in [1], but provides a drastic decrease in model complexity as the angle of each joint can be described by a single principle angle instead of two. Comparatively, a 3D walker is more complex in that there is a yaw motion present in the walker (hip motion in all three dimensions), which makes the model substantially more complicated. In the case of emulating human bipedal locomotion, it is obvious that a 3D model would provide substantially better representation. If has however been shown that the walking gaits in even the simplest 2D models are sufficiently analogous to human walking gaits to provide a basis for study of bipedal locomotion [1] [2]. One major benefit of the 2D walkers, from an actuation perspective, is that that the actuation of a hip joint on a planar walker requires a simple actuator since the joint only has one DOF. The actuation is also relatively simple, since the joint torque is always perpendicular to the direction of forward walking motion. This makes actuator design much easier than a 3d walker, where the joint torque at the hip is multidimensional and the 3D actuation torque has to be accounted for during the walking gait.

In terms of knee joints, the first point to consider is the primary function of the knee in a passive walker; it is present simply to provide foot clearance during the swing phase to prevent *toe-scuffing*. By allowing the knee to bend, the leg can naturally shift the tip of the swing leg foot (considered as the toe regardless of layout) at the point when the walker has both its legs at an equal absolute angle to the horizontal. This action is also coupled with a mechanism to prevent hyperextension, such that the leg can support weight without buckling and the walker ends the stride with a straight leg. This usually takes the form of having a knee that can lock (so that the stance leg can take the compressive load of the walker weight) and selectively unlock as the knee swings. This poses a large challenge both experimentally and from a theoretical standpoint as the ability to selectively lock a joint during motion, in a predictable manner, is not a trivial problem from either perspective. From the mechanical side, this is usually achieved by using an offset foot contact point (*foot offset*), which places a locking torque on the knee when the foot is under load (i.e. on the stance leg) and places a non-holonomic constraint on the swing leg knee joint. This means that bending of the knee is permitted in one direction, but the

knee is constrained at the point of hyper-extension [1] beyond the locking point (full extension). From a computational perspective, this is far from a trivial solution as the addition of a second non-holonomic constraint to the system requires an impact model or other state transition model between the locked and unlocked phases of the swing as well an additional knee lock constraint used during simulation of the leg post knee lock. Another complication is that the use of this type of knee lock requires that the walker model is of the round/flat foot type, which in itself poses a computational challenge. An alternative to this is to use a point foot walker with an active knee lock. This means the constraint in the model is holonomic, and is accompanied by a state transition (a loss of 1 degree of freedom) at the point of knee lock. This poses a challenge experimentally, as an active knee lock system is not trivial to construct and requires careful tuning to manage the dynamics of the knee lock impact, and must be tunable to match a basic impact model.

If no knee joints are present, the walking model becomes substantially simpler and is still considered as a simulacrum of human locomotion [2]. From a modeling perspective, this approach also substantially decreases the complexity and also the computational burden when simulating gaits. From an experimental side this approach does pose one main difficulty: unless a system is made to allow for foot clearance, the walker must walk on a surface that has relief for the swing leg, in order to prevent toe-scuffing. The solutions to this are normally twofold: an active retraction system for the swing leg which allows the walker to walk on a flat surface without scuffing, or stepping stones that the walker walks across to elevate the contact point of the walker above the ground and allow foot clearance.

2.2 Proposed Mathematical Model

Between the considerations in the previous section, it’s clear that there are a large variety of configurations of walkers to base a model on. Since the goal of the study was to focus on the actuation, it is desirable from a simulation perspective to choose a simple walking model that is capable of describing a wide range of walking machines. To this effect, the model that was chosen is of a planar walker with point feet and selectively lockable knees. The advantage to this model is that it describes bipeds that are relatively simple to theoretically analyze, and can

encompass bipeds that have knees (if the selective knee locking is used) as well as bipeds that do not have knees (if the knees are permanently locked). Shown below is the basis for this model, in Figure 2.1.

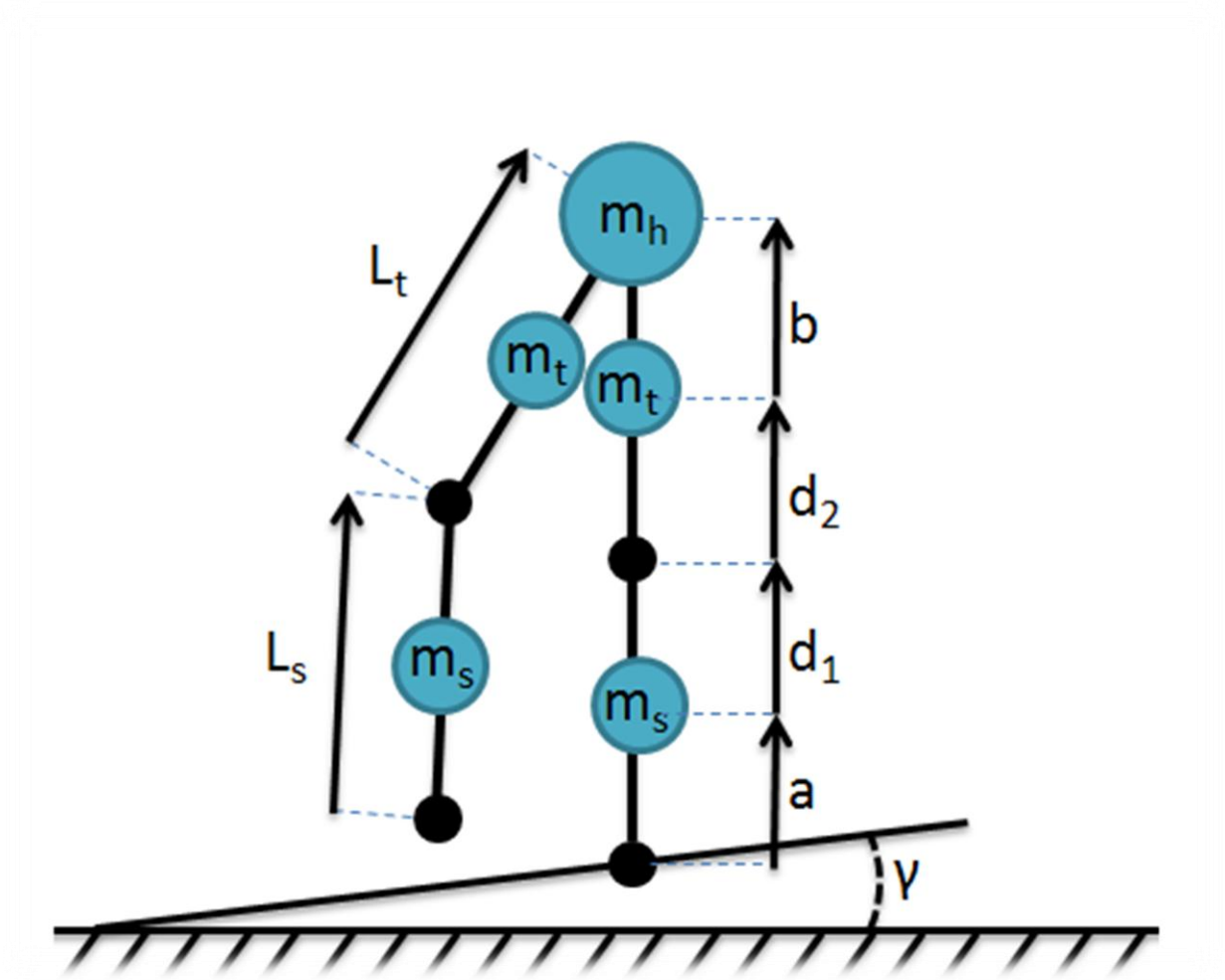

Figure 2.1: Passive walker model with knees (K-Walker)

From the figure above it can be seen that model *K-Walker* is a simple three link planar manipulator with a shank of length L_s and a thigh of length L_t as components of a swing leg of length L and a stance leg of equal length. The connections are all treated as revolute pin joints, with a holonomic constraint for the swing foot and ground connection. In order to study the dynamics, the links of the walker are treated as rigid and lumped mass, with a point mass located at some distance away from each pivot point on each link. When the legs of this arrangement are locked we see that we end up with a simple 2 legged walker with no knees. In

this case it would make sense to reduce the number of leg masses to 1 per leg. The model without knees, *NK-Walker*, is illustrated in Figure 2.2.

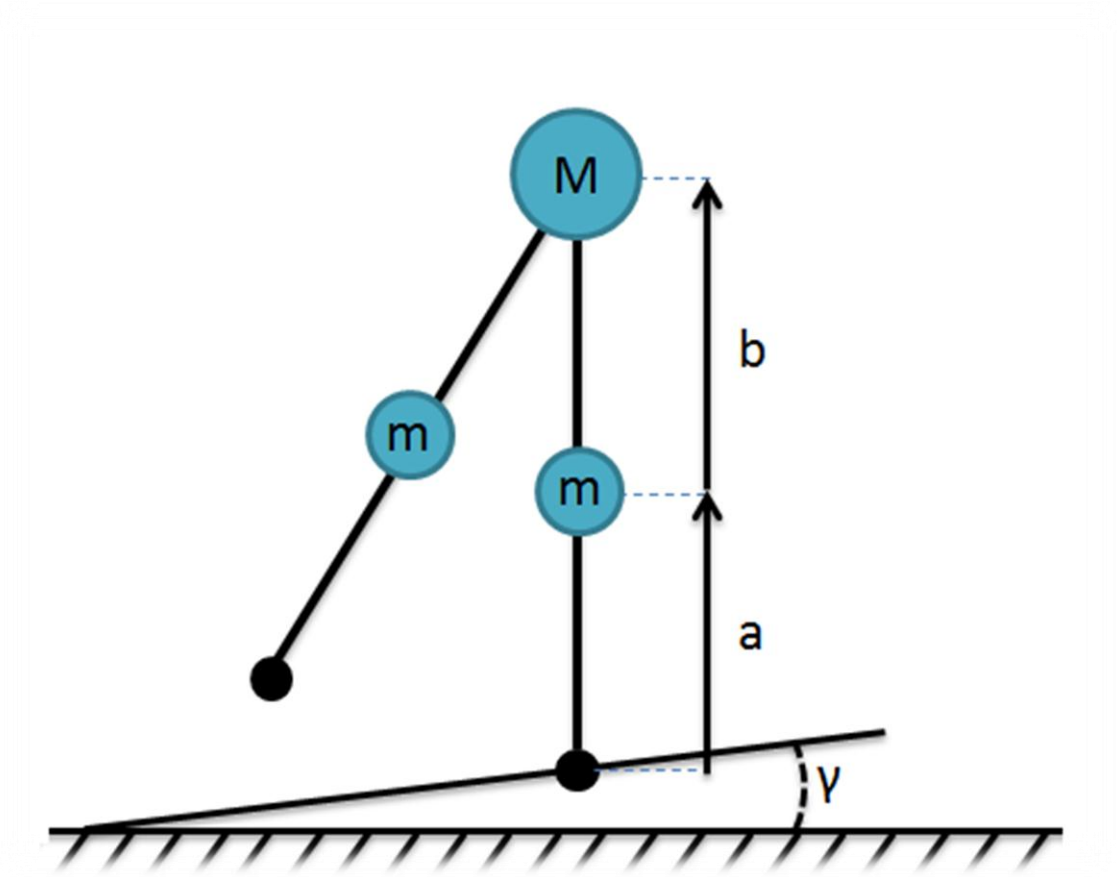

Figure 2.2: Passive walker model without knees (NK-Walker)

Based on these two model descriptions, we see that we have a general description of a model that will meet all of the original research goals, and is capable of describing a wide range of walking machines, as discussed in the previous section. With the desired model in mind, the next step is to come up with a mathematical description of its dynamics.

2.2.1 Models for Continuous Dynamics

In the simplest case of a two-legged non-kneed biped, the walking gait is divided into 3 discrete actions: heel off, swing phase, and heel strike. During the swing phase, the dynamics of the system are merely those of a 2 link rigid planar manipulator. However, during the heel off and heel strike events, there exists a nearly discrete impact in the walker model which must be

simulated. In order to do this, the simplest approach is to use numerical integration to solve the equations of motion of the manipulator during the swing phase, and use a discrete impact event to model the interactions at the heel strike event. Based on Lagrange's Equations, we end up with the following system of equations for the K-Walker in its 3 link phases:

When the knees are unlocked, dynamics are given by: $\boldsymbol{M}_a(\boldsymbol{\theta})\ddot{\boldsymbol{\theta}} + \boldsymbol{M}_b(\boldsymbol{\theta}, \dot{\boldsymbol{\theta}})\dot{\boldsymbol{\theta}} + \boldsymbol{M}_c(\boldsymbol{\theta}) = 0$

$$\boldsymbol{M}_a(\boldsymbol{\theta}) = \begin{bmatrix} M_{a11} & M_{a12} & M_{a13} \\ M_{a21} & M_{a22} & M_{a23} \\ M_{a31} & M_{a32} & M_{a33} \end{bmatrix}$$

$$\boldsymbol{M}_b(\boldsymbol{\theta}, \dot{\boldsymbol{\theta}}) = \begin{bmatrix} M_{b11} & M_{b12} & M_{b13} \\ M_{b21} & M_{b22} & M_{b23} \\ M_{b31} & M_{b32} & M_{b33} \end{bmatrix}$$

$$\boldsymbol{M}_c(\boldsymbol{\theta}) = \begin{bmatrix} M_{c11} \\ M_{c21} \\ M_{c31} \end{bmatrix}$$

$M_{a11} = m_s(a^2 + L^2) + m_t((l_s + d_2)^2 + L^2) + m_H L^2$
$M_{a12} = -c_{(1-2)}(m_t b + m_s l_t)L$
$M_{a13} = -c_{(1-3)}(m_s d_1)L$
$M_{a22} = m_t b^2 + m_s(l_t)^2$
$M_{a23} = c_{(2-3)}(m_s l_t d_1)$
$M_{a33} = m_s d_1^2$

$M_{b12} = -\dot{\theta}_2[m_t b + m_s l_t]Ls_{(1-2)}$, $M_{b21} = -M_{b12}(\dot{\theta}_1)\dot{\theta}_2^{-1}$
$M_{b13} = -\dot{\theta}_3[m_s L d_1]s_{(1-3)}$, $M_{b31} = -M_{b13}(\dot{\theta}_1)\dot{\theta}_3^{-1}$
$M_{b23} = -\dot{\theta}_3[m_s l_t d_1]s_{(2-3)}$, $M_{b32} = -M_{b23}(\dot{\theta}_2)\dot{\theta}_3^{-1}$
$M_{b33} = M_{b22} = M_{b11} = 0$

$M_{c11} = -g[m_s(a + L) + m_t(L + d_2 + l_s) + m_H L]s_1$
$M_{c21} = g[m_t b + m_s l_t]s_2$
$M_{c31} = g[m_s d_1]s_3$

Once the knee lock event occurs in the K-Walker model, the dynamics are then modified to the equations of motion of a 2 link manipulator. It can be noted that the dynamics can be

mathematically rearranged to represent the case of the NK-Walker by setting: $d_1 = d_2 = 0$, and $m_s = m_t = \frac{1}{2}m$. In this case, we end up with a model defined by Figure 2.2, in the previous section. The dynamics for the general case are listed below:

When the knees are locked, dynamics are given by: $\boldsymbol{M}_a(\boldsymbol{\theta})\ddot{\boldsymbol{\theta}} + \boldsymbol{M}_b(\boldsymbol{\theta}, \dot{\boldsymbol{\theta}})\dot{\boldsymbol{\theta}} + \boldsymbol{M}_c(\boldsymbol{\theta}) = 0$

$$\boldsymbol{M}_a(\boldsymbol{\theta}) = \begin{bmatrix} M_{a11} & M_{a12} \\ M_{a21} & M_{a22} \end{bmatrix}$$

$$\boldsymbol{M}_b(\boldsymbol{\theta}, \dot{\boldsymbol{\theta}}) = \begin{bmatrix} M_{b11} & M_{b12} \\ M_{b21} & M_{b22} \end{bmatrix}$$

$$\boldsymbol{M}_c(\boldsymbol{\theta}) = \begin{bmatrix} M_{c11} \\ M_{c21} \end{bmatrix}$$

$M_{a11} = m_s(a^2 + L^2) + m_t((d_2 + l_s)^2 + L^2) + m_H L^2$
$M_{a12} = c_{(1-2)}[m_s L(b + d_1 + d_2) + m_t Lb]$
$M_{a22} = m_t b^2 + m_s(d_1 + l_t)^2$

$M_{b12} = -\dot{\theta}_2[m_t Lb + m_s L(d_1 + l_t)]s_{(1-2)}$
$M_{b21} = \dot{\theta}_1[m_t Lb + m_s L(d_1 + l_t)]s_{(1-2)}$
$M_{b11} = M_{b22} = 0$

$M_{c11} = -g[m_s(a + L) + m_t(d_2 + l_s + L) + m_H L]s_{(1-\gamma)}$
$M_{c21} = g[m_t b + m_s(d_1 + l_t)]s_{(2-\gamma)}$

Since the system of equations describing the system is non-linear and coupled, a closed form solution is not available. Hence an alternative approach must be taken to solve the system dynamics: namely computing the trajectories of the system via numerical integration. While this gives a reasonably accurate approximation of the system dynamics, the insight into the system's topology is curbed by the issue that a large portion of the system dynamics is hidden. This is because the numerical integration approach only provides solution trajectories evolved from specific initial conditions, with no higher order dynamical insight into the system behavior. One large advantage of this approach, however, is that the solution concept for both NK-

Walkers and K-Walkers would be identical, and the overall model would cover the continuous dynamics of both models, based on different knee lock conditions. With this in mind, we can simulate a passive walker of either configuration through the swing phase by describing an initial condition of the set:

$$\left[\overrightarrow{\theta_i}, \overrightarrow{\omega_i}\right], where\ \theta_i, \omega_i \in \mathbb{R}$$

Once the dynamics reach one of the two major gait events described earlier, namely the knee-lock or heel-strike events, the model reaches a point where the dynamics must account for these new gait events. This can be done via a contact or impact based model as discussed next.

2.2.2 Models for Impact Events

In the case of the heel-strike event, the walking motion will continue forward as weight is transferred from the stance leg to the swing leg, and if the walking gait is successful there will be a repeatable limit cycle gait. Numerous studies have looked at the effect of this type of motion transition and the best way to study it. A particularly interesting method is highlighted in [38] where a passive walker is implemented that uses a friction model (LuGre) to describe the complex interactions between the stance/swing feet and the ground. When such a complex model is considered one of the main challenges that arises is that the analysis of the system becomes excessively complex. This, in turn, causes tuning of the system parameters to match an experimental setup (required for validation of the model) to become a much more involved process than with a simpler model. In terms of the knee lock collision, there is a potential for even more complex behavior as the walker can have compliance and play in the joints that would then have to be accurately modeled or compensated for via extensive model parameter tuning. Between these aspects it's clear that any work that can be saved at this stage in the model will allow for substantially simpler validation and a simpler model overall.

In the case of a simple point foot walker, the actual behaviour of the system is much simpler and therefore easier to model in a different manner. In the event of a heel strike, the physical

walker has a rigid point foot impacting on a hard substrate in a nearly inelastic manner. In the event of a knee lock, the walker (using a knee lock system based on a latch or solenoid) has a nearly inelastic knee lock, resulting in a loss of 1 degree of freedom in the system. Both of these events can be considered as inelastic collisions as long as little to no elasticity is present at the ground and knee of the walker, and can be modelled simply as such. Since the experimental walker can also be built to match the theoretical system, it is relatively straightforward to physically ensure the walker has tolerable inelastic collision behavior in both of these events.

For the heel strike case, the NK-Walker or K-Walker geometry can be used and an inelastic collision can be considered about the pre-impact swing foot. Considering that the impact foot has the only external force on the system at the point of impact, the angular momentum is conserved about this point before and after impact, leading to a simple state transition matrix that can be used to describe the pre-impact and post-impact velocities. In the case of the NK-walker, the pre-impact walker and post impact walker are both 2 link systems, but the angular numbering convention of the leg angles are reversed after collision (as the stance and swing foot swap) for convenience of modelling. In the case of the K-walker, the pre-impact walker is a 2 link system, and the post impact walker is a 3 link system (as the knee unlocks). In order to solve for this extra degree of freedom, a constraint is used such that the shank and thigh of the swing leg have post collision angular velocities that are equal, since they are locked during the event. This means that the walker is treated the same in the K-Walker and NK-Walker cases during heelstrike. To this effect, the state transition matrix is given by: $\dot{\boldsymbol{\theta}}_+ = (\boldsymbol{Q_a})^{-1}\boldsymbol{Q}_b\dot{\boldsymbol{\theta}}_-$

$$\boldsymbol{Q}_a = \begin{bmatrix} Q_{a11} & Q_{a12} \\ Q_{a21} & Q_{a22} \end{bmatrix}$$

$$\boldsymbol{Q}_b = \begin{bmatrix} Q_{b11} & Q_{b12} \\ Q_{b21} & Q_{b22} \end{bmatrix}$$

$Q_{b11} = m_s a(l_t + d_1) + m_t b(l_s + d_2) - (m_h L + 2m_t(l_s + d_2) + m_s a)L\alpha$
$Q_{b12} = m_s a(l_t + d_1) + m_t b(l_s + d_2)$
$Q_{b21} = m_s a(l_t + d_1) + m_t b(l_s + d_2)$
$Q_{b22} = 0$

$Q_{a11} = (m_s(l_t + d_1) + m_t b)L\alpha - L^2(m_h + m_s + m_t) - m_s(a)^2 - m_t(l_s + d_2)^2$

$Q_{a12} = (m_s(l_t + d_1) + m_t b)L\alpha - m_s(l_t + d_1)^2 - m_t(b)^2$
$Q_{a21} = (m_s(l_t + d_1) + m_t b)L\alpha$
$Q_{a22} = -m_s(l_t + d_1)^2 - m_t(b)^2$

$\alpha = \cos(\theta_1 - \theta_2)$
$(\theta_1)_+ = (\theta_2)_-$
$(\theta_2)_+ = (\theta_3)_+ = (\theta_1)_-$

In the special case of the K-Walker system, the additional impact event is the knee lock event, where the leg is prevented from hyper extension and the system converts from 3-link manipulator to a 2-link manipulator. In this case, an impact is exerted at the knee. This causes an internal force at the knee, which means that angular momentum conservation can only hold for the stance leg about its foot and for the swing leg about the hip. Using the third condition that the leg angles before/after impact are equal, a state transition matrix can be formed as:

Knee Lock Dynamics given by: $\dot{\boldsymbol{\theta}}_+ = (\boldsymbol{Q_a})^{-1}\boldsymbol{Q}_b\dot{\boldsymbol{\theta}}_-$

$$\boldsymbol{Q}_a = \begin{bmatrix} Q_{a11} & Q_{a12} \\ Q_{a21} & Q_{a22} \end{bmatrix}$$

$$\boldsymbol{Q}_b = \begin{bmatrix} Q_{b11} & Q_{b12} & Q_{b13} \\ Q_{b21} & Q_{b22} & Q_{b23} \end{bmatrix}$$

$Q_{b11} = L\alpha(m_s l_t + m_t b) + L\beta m_s d_1 - L^2(m_h + m_s + m_t) - m_s(a)^2 - m_t(l_s + d_2)^2$
$Q_{b12} = L\alpha(m_s l_t + m_t b) - m_s d_1 l_t \varphi - m_s(l_t)^2 - m_t(b)^2$
$Q_{b13} = -L\beta m_s d_1 + m_s d_1 l_t \varphi - m_s(d_1)^2$
$Q_{b21} = -L\alpha(m_s l_t + m_t b) - L\beta m_s d_1$
$Q_{b22} = m_s d_1 l_t \varphi + m_s(l_t)^2 + m_t(b)^2$
$Q_{b23} = m_s d_1 l_t \varphi + m_s(d_1)^2$

$Q_{a11} = (m_s(l_t + d_1) + m_t b)L\alpha - L^2(m_h + m_s + m_t) - m_s(a)^2 - m_t(l_s + d_2)^2$
$Q_{a12} = (m_s(l_t + d_1) + m_t b)L\alpha - m_s(l_t + d_1)^2 - m_t(b)^2$
$Q_{a21} = (m_s(l_t + d_1) + m_t b)L\alpha$
$Q_{a22} = -m_s(l_t + d_1)^2 - m_t(b)^2$

$\alpha = \cos(\theta_1 - \theta_2), \beta = \cos(\theta_1 - \theta_2), \varphi = \cos(\theta_2 - \theta_3)$

For both of the discrete events, an impact surface and an error function are created to describe the proximity of the system state to the impact point. For the heelstrike case, the impact surface is taken as:

$$S_1 = \{h \in \mathbb{R}^2 \colon F(h) = \cos(\theta_1 + \gamma) - \cos(\theta_2 + \gamma) = 0\}$$

In the case of the knee lock, the impact condition is taken as the point where the swing leg thigh and shank angles are equal. This is described by the surface:

$$S_2 = \{h \in \mathbb{R}^2 \colon G(h) = \theta_2 - \theta_3 = 0\}$$

In a typical walking gait, the impact matrix for both of these events is non-singular; therefore an error function can be used to interrupt the numerical integration when either of the impact conditions is reached. The actual impact point is then calculated by cubic interpolation between the highest tolerance numerically computed pre/post impact states. At this point, there are now two different sets of continuous dynamics: one set of equations of motion describes a 2 link walker and one describes 3 link walker. There are also two separate discrete events: one describes the heel strike event of a 2/3 link walker and one describes the knee lock event of a 3 link walker. In order to simulate the walkers, a set of scripts were written using MATLAB that utilize an ODE45 based solver to numerically integrate the dynamic equations with simple state transition functions to handle the discrete events. The end result is a stride function as described in [1], but describing a simple point foot walker with or without knees.

2.2.3 Overview of Proposed Model

The end goal of this phase of research was to produce a model that described a walker that is predominantly passive, and we see that the goal has been satisfied as the walker model described in this section can simulate the passive dynamics of the walkers similar to those in [1] and [2] and is similar to the models proposed in [39] and [40]. From this, it can be concluded

that the passive dynamics of the chosen model are already well known as it is predominantly analogous to countless passive models in literature and is capable of simulating a large variety of them with some modifications. Based on the proposed model, the next step is to investigate the performance of the model, which can be done using the baseline geometry presented in [39].

2.3 Baseline Simulation Results with Proposed Model

With the proposed model thoroughly described in the previous section, the first issue worth noting is that the system that is being studied does not have a closed form solution. This means that the kinematics of the system are only observable (i.e. topological dynamics cannot be analytically determined) and any study is normally only from looking at individual trajectories. The downside to this approach is that there is little to no insight into how any type of actuation would affect the stability of the system short of testing a wide variety of actuation cases and having the model tuned and validated to match an experimentally developed walker.

The restriction this places on the research is that the walker model must be well understood and developed prior to considering an actuation scheme, as the model can only provide representative results for the specific mass/inertial parameters chosen for the passive walking system. With this in mind, we can do some preliminary theoretical testing of the walking model, to help characterize the system behaviour. A series of Matlab scripts were created to iterate the stride function of the walker, which is the complex non-linear discrete mapping ***f*** which includes the continuous and discrete dynamics of the walking gait and is of the form:

$$\left[\overrightarrow{\theta_\iota}, \overrightarrow{\omega_\iota}\right]_{n+1} = f\left(\left[\overrightarrow{\theta_\iota}, \overrightarrow{\omega_\iota}\right]_n\right)$$

Where: $\overrightarrow{\theta_\iota}, \overrightarrow{\omega_\iota} \in \mathbb{R}$

In the case of the NK-Walker, the stride function is a mapping that takes initial conditions at the start of the stride, namely the starting angles/velocities of the limbs, and maps them to the post heel strike angles and velocities. Through the mapping, the initial conditions are first simulated via the continuous mechanics of the NK-Walker model and a script is used to check

for the only impact event of the walker: heel strike. When the heelstrike event takes place, an internal discrete mapping is used based on the momentum conservation state transition matrix to map to post heelstrike velocities and angles, which is the output of the stride function.

In the case of the K-Walker, the stride function is a mapping that takes initial conditions at the start of the stride, but treats the walker as a two link walker initially. This is due to the legs being locked immediately before heel strike, leading to the same initial conditions for both the shank and thigh of the swing leg. The function computes the 3 link kinematic model of the K walker, looking for the transitional gait event created by the knee lock condition of the walker. Once a knee lock is detected, the model uses the internal discrete mapping of the knee lock state transition matrix to map the pre/post impact velocities of the event. Then the K walker is simulated as a locked knee walker via the 2 link kinematic model, until the next transitional gait event: the heel strike. For the heel strike event, the state transition matrix maps the pre/post impact velocities for the swing/stance legs, which is the output of the stride function.

Both of these functions have complex internal dynamics, as the mapping is a discretized version of a very complex system, therefore analysis of the stride function directly is not feasible. One of the inherent limitations to this type of study is also that there is no way (without higher order dynamics or a closed form solution to the system) to modify the system parameters and easily acquire the new initial conditions that would produce a walking gait. Thankfully, in the case of the walking models selected, we note that there exist stable periodic gaits in literature for the specific conditions described in [1]. We note that any initial condition set mapped by the stride function that is within the basin of attraction of a stable periodic gait for a walking model will be a period 1 fixed point of the stride function mapping ***f***. We also note that gaits can exist that are *n- cycle* fixed points, which are multiple step gaits. In the case of a stable period 1 gait, we note that a fixed point is of the form:

$$\left[\overrightarrow{\theta_\iota}, \overrightarrow{\omega_\iota}\right]^* = f\left(\left[\overrightarrow{\theta_\iota}, \overrightarrow{\omega_\iota}\right]^*\right)$$

Where: $\overrightarrow{\theta_\iota}, \overrightarrow{\omega_\iota} \in \mathbb{R}$

In the general case, however, we can describe all period gaits by the *n-cycle* fixed points:

$$\left[\overrightarrow{\theta_\iota}, \overrightarrow{\omega_\iota}\right]^* = f^n\left(\left[\overrightarrow{\theta_\iota}, \overrightarrow{\omega_\iota}\right]^*\right)$$

Where: $\overrightarrow{\theta_\iota}, \overrightarrow{\omega_\iota} \in \mathbb{R}$, $m = 1,2$, $n \in \mathbb{R}$

The downside to this system is that there are an excessive number of parameters that can be varied in the mapping ***f***, based on the various physical parameters of the walker, and for each of these variations there is a narrow basin of attraction in each dimension of state space that can produce stable periodic gaits. As described in [1], there exists methods of quantitatively characterising these parameters, but the time involved is beyond the scope of this research. Without the data from a parametric study, the approach that is left is simple: take a known walking geometry with known initial conditions and iterate it while changing parameters to a more ideal baseline. The initial baseline is taken from [39] for the NK-Walker and the model parameters are taken as: *a = 0.5, b = 0.5, m = 1, M = 2.* When iterating the walker, we note from [1] that the masses of the walker can be scaled without affecting the gait, but the mass ratio M/m is a fundamental parameter of the gaits. We also note that the leg length and mass center location must also be changed based on the chosen walker geometry.

If parametric study is required, a method that can be used to great effect is the iterative parameter scaling method. This method is a type of iteration that utilizes the structural stability of the fixed point of the walking gait and allows for parametric variations. To use this approach, one walker parameter (such as *b*, *L*, etc..) is defined as a parameter *C* where $C \in [C_1, C_2]$, with all other parameters held fixed. With the starting value as C_1 and the terminal value of C_2, we also define a disturbance ε such that $\varepsilon \in \mathbb{R}$ where ε is a sufficiently small value. An iterative loop is set up, as shown:

Define $C = C_1 + \varepsilon$, *iterate* $f\left(\left[\overrightarrow{\theta_\iota}, \overrightarrow{\omega_\iota}\right]^*, C\right)$ *until:*

$$\left[\overrightarrow{\theta_\iota}, \overrightarrow{\omega_\iota}\right]^* = f\left(\left[\overrightarrow{\theta_\iota}, \overrightarrow{\omega_\iota}\right]^*, C\right)$$

Where: $\overrightarrow{\theta_\iota}, \overrightarrow{\omega_\iota} \in \mathbb{R}$

Redefine C as $C + \varepsilon$, *repeat process until* $C = C_2$

It should be noted that this approach is not guaranteed to work in all cases, but for most walker geometries it was tested with a reasonable success rate as long as *ε* is sufficiently small

and the geometry defined by C + ε can produce a stable n-cycle walking gait.

Since the experimental walker geometry is unknown, a stride function was tested with the baseline geometry and actuator impulses $L(\omega) = 0$, the output of which is shown in Figure 2.3, and a BOA for the gait in Figure 2.4. We can see that a stable limit cycle gait of period 1 develops for the model for the initial conditions $\overrightarrow{\theta_m} = [0.2191, 0.3252]$, which matches the results in [39].

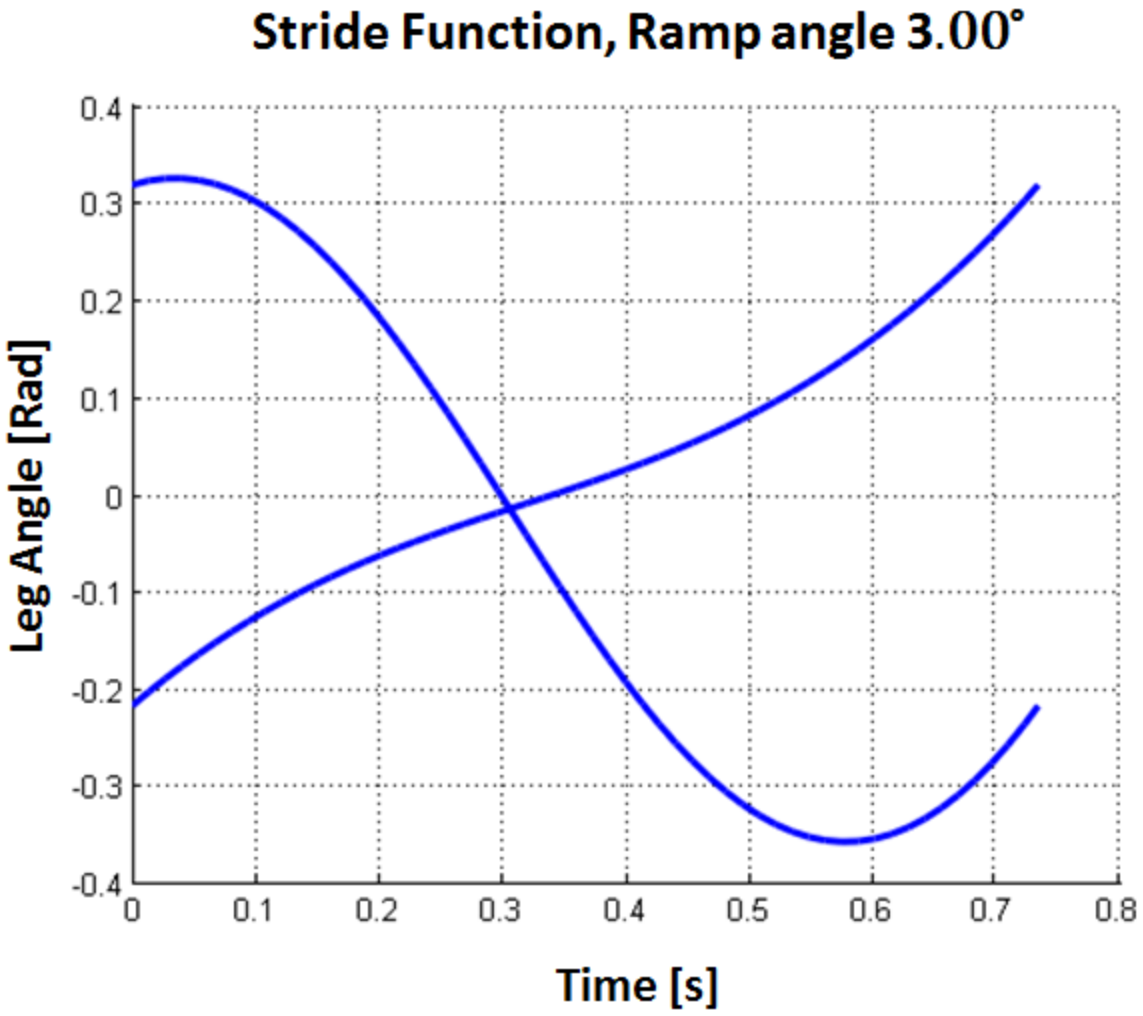

Figure 2.3: Stride Function of baseline walker at 3.00˚ ramp angle

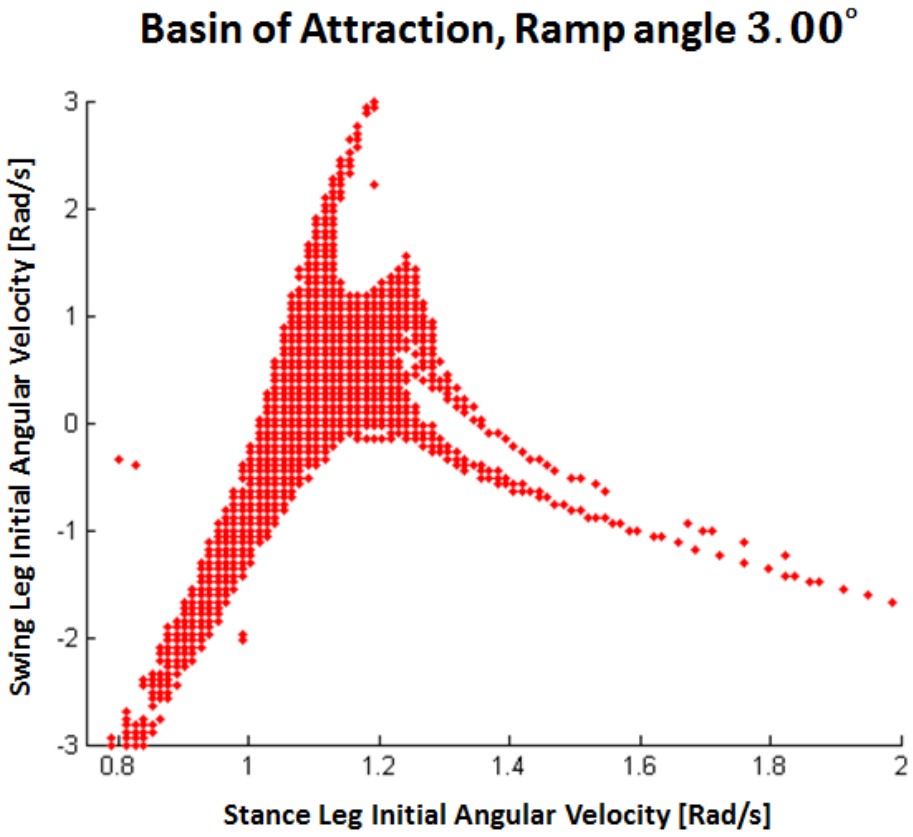

Figure 2.4: BOA of Baseline Walker at 3.00° Ramp Angle

From the BOA and phase portrait shown above, we note that the expected results for the geometry selected match the results in [31] and [39], where the same shape of phase portrait and basin of attraction are present for a very similar geometry. Noting the work in [2] we can also see that the results are in line with what is expected with a round foot passive walker, indicating that the model is also similar in behaviour to a round foot passive biped of similar structure. When the value of the fixed point is considered, we can also see that it accurately captures the results of study done using the exact same walker geometry [39]. The angle changed is then changed slightly to 2.86°, and the leg length scaled to 14.5" leg length (the height of the last passive walker from the lab discussed in [29]) using the iterative parameter scaling technique, as discussed earlier in this section. Based on these new parameters, a new gait for the walker is described in Figure 2.5 and Figure 2.6, with the phase portrait describing the state space trajectories of the walker and the stride function describing the angles with

respect to the time domain.

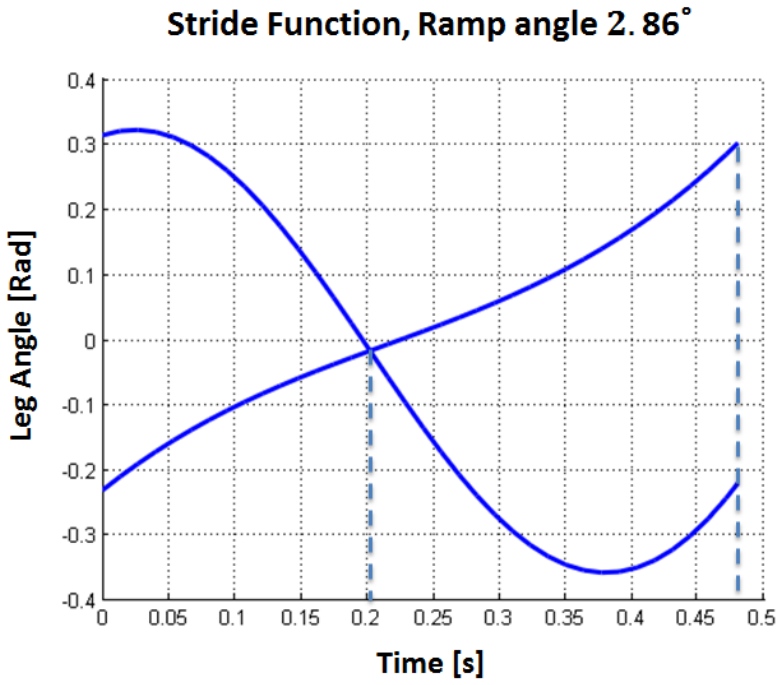

Figure 2.5: Location of the EA Crossing Point for an Archetypal Gait

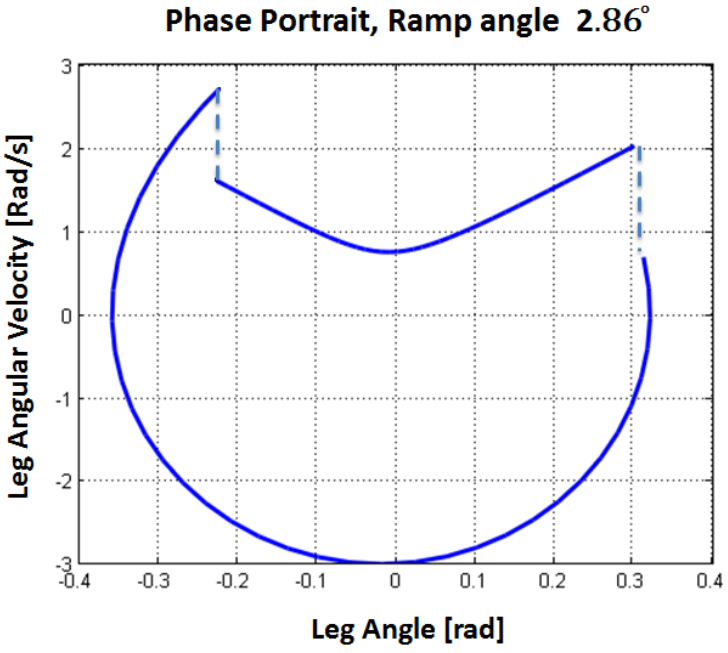

Figure 2.6: Phase portrait of a benchmark NK-Walker at 2.86˚ ramp angle.

In this gait, we note that there are two key points in an archetypal NK-Walker gait cycle: the heelstrike point, and the EA crossing point. Both of these points are recurring gait points, which occur once per gait cycle for any given stable gait of the NK-Walker. If the angle of the gait is parametrically varied, we note that these points remain approximately in the same location, as shown in Figure 2.7 below.

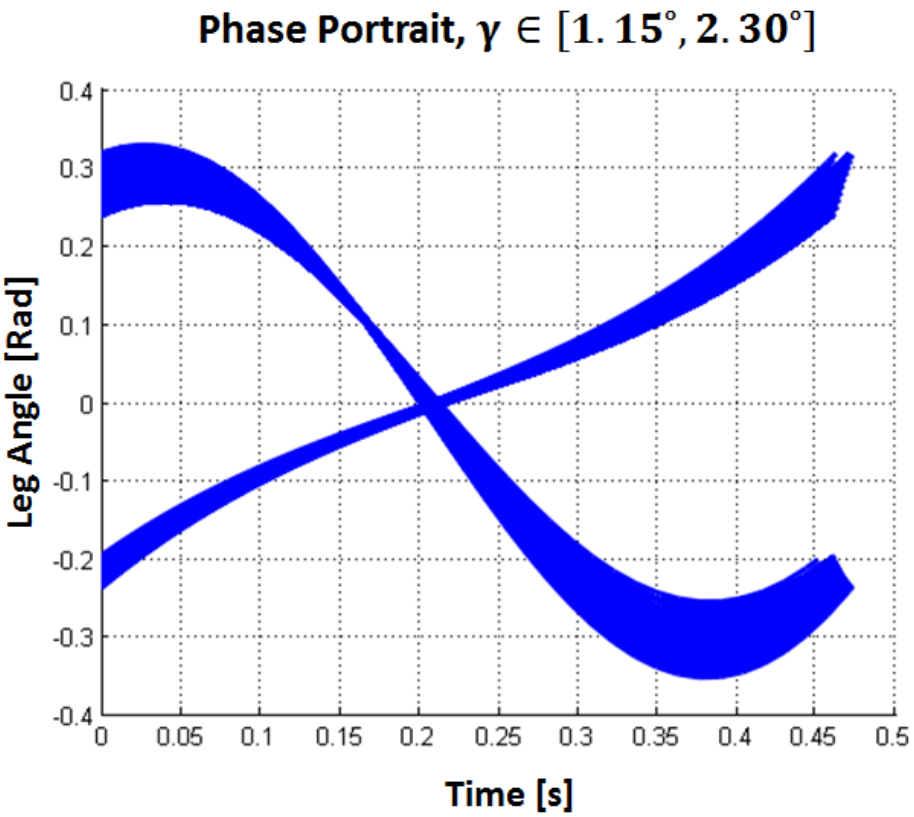

Figure 2.7: Stride Functions for Various Stable Walker Gaits

One important behaviour that can be observed when generating the various stride functions in Figure 2.7 is that the gait patterns exhibit a predictable behaviour when the target gait is either higher or lower than the initial conditions. In the case of low ramp angle gaits situations, there is a tendency to diverge inwards i.e. the limit cycle magnitude tends to zero. In the case of high ramp angle gaits, there is a tendency to diverge outwards, i.e. the limit cycle magnitude tends to move away from zero. This behaviour can be seen clearly in the plots in Figure 2.8 and Figure 2.9 respectively.

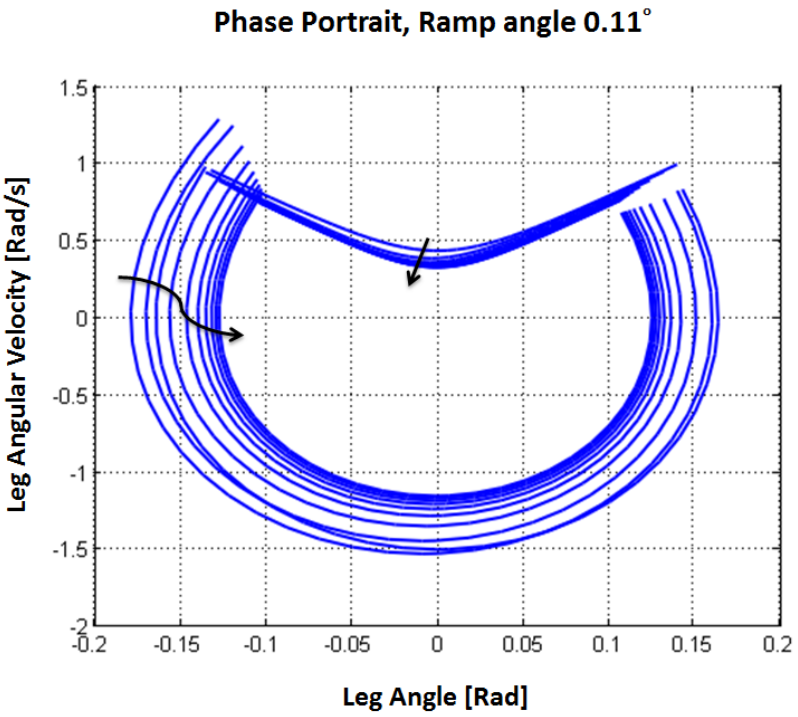

Figure 2.8: Low ramp angle gait divergence

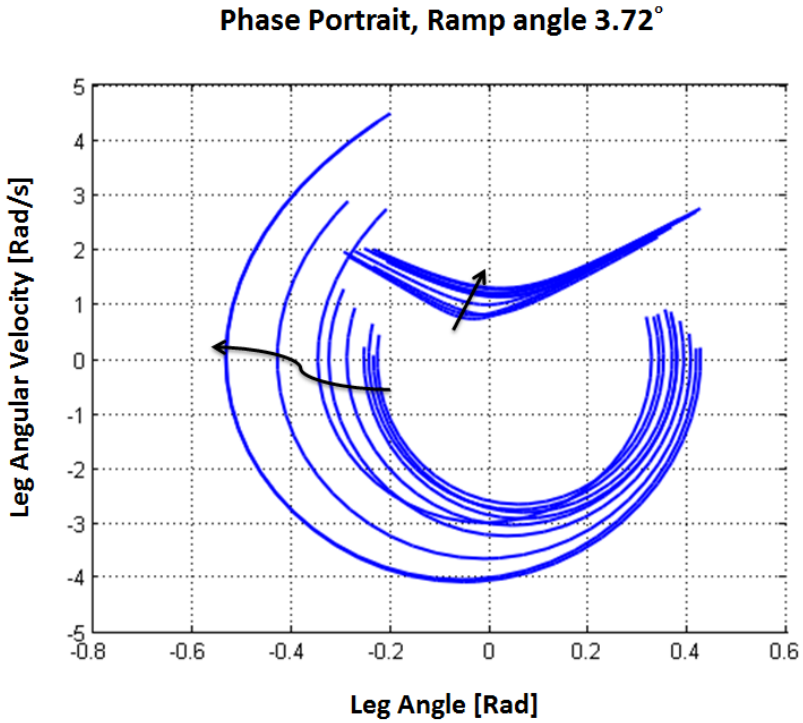

Figure 2.9: High ramp angle gait divergence

Since the proposed model is clearly capable of producing a wide range of results, the next step is to discuss the results and determine the best way to implement an actuation system into the existing passive model.

2.4 Adding Actuation to the Proposed Model

The first step to solving the problems posed by varying actuation approaches is to look at the model itself and understand how it is that the passive motion in the model is perpetuated from one stride to the next. It can be seen from Figure 2.6 that the walking gait in the NK-Walker is composed of two continuous motions where energy in injected into the system and this energy is then regulated by a set of impact events. The smooth motions are shown above as the solid lines in the phase portrait, with the impacts (occurring at a single angle) being the vertical dashed lines. The key to the walking motion is that the impact events control the distribution of angular momentum between the two legs and allow for the swing leg to transfer energy to the stance leg. We note that neither leg has an angular velocity of zero before or after the impact point, as both legs share the energy of the walking gait and transfer it between each other. We can also see that the net angular velocity of the swing leg tends to be higher than the angular velocity of the stance leg and therefore the angular kinetic energy (as the legs are symmetric) is also higher.

A fundamental aspect of the walker is that the system falls into a regulated rhythm of energy balance given a certain level of energy injection and the behavior of the system during the impacts. In the simple case of the NK-Walker, large ramp angles affect this regulation substantially, as the energy going into the walker is too high and the regulation is not capable of effectively controlling the gait energy. This would be akin to the case of putting a ball on a slope, where the energy injection is not bounded by the system and the ball increases in speed continually. In the case of a passive walker, this result causes the walker to fall outside its operating range and ceases to produce a stable gait. As the ramp angles become smaller and smaller, the energy injection is not sufficient during the transfer event to correct the walkers leg velocities back to their initial conditions. An example of this is shown below from NK-Walker

simulation where low ramp angle phase portrait trajectories are shown in Figure 2.8 and high ramp angle phase portrait trajectories are shown in Figure 2.9. We see that in either case, the energy injection is either too high or too low, causing the system to not be able to converge to a stable walking gait.

Another way to consider this is the case where heelstrike event does not occur. In this case, any gait cycle could theoretically be a limit cycle if an event existed that translated the pre-impact states to the initial conditions of that specific stride. It is known that in an inelastic collision based walking model, the governing dynamics of the impact events are based on the conservation of angular momentum of the legs. This means that we can base an actuation event on the same principle as the impact events, and have it coincide with the impact that occurs at the heel strike event. The result of this can be called a *MTGE* or *modified transitional gait event*, which is an event that affects the passive dynamics of the system (but modifying the effect of the impact events, or creating new ones) but does not change the continuous dynamics of the system. Looking at the previous diagram we see that in the case where the walker is at a low ramp angle, a *MTGE* could be used to correct the terminal conditions of the walker to the starting conditions via an increase in the energy of the system. Since this requires both a change in initial and terminal angles as well as angular velocities, the effect of this event on the continuous dynamics must also result in a favorable outcome, as a *MTGE* as described can only change the angular velocities for a given set of leg angles. This concept, at its heart, is the principle of what is proposed in this research as a hybrid passive/active dynamic walker.

2.4.1 Simple MTGE Concept

In the case of the walking model proposed in section 2.2, the two main impact events of the walker can both be treated as *MTGE*'s if actuation can inject angular momentum into the system but otherwise does not affect the dynamics of the system. Since these events take the form of inelastic collisions, a simple approach would be to use an actuator that uses ballistic actuation, capable of providing a controllable joint torque that occurs over a very short period of time and with a controllable rate of angular momentum change on the joint. This can be modelled as actuation that takes the form of angular impulse at the joint, the simplest example

of which would be a flywheel that can provide selective torque to the joint. With a simple flywheel setup, the angular momentum could be varied via the rotational speed of the flywheel and the inertial properties of the flywheel. If the flywheel could be selectively coupled/de-coupled from the joint, then the actuation could also be varied. In the event that this coupling/decoupling could produce an inelastic collision, then the end result could be combined with one of the existing discrete events in the gait to create what was referred to earlier as an *MTGE*.

In the case of the walking model described in Section 2.2, the addition of such an actuator to the model would be as simple as providing a fixed increase in the angular momentum about the actuated joint during the existing gait event. In order to do this, the form taken by an *MTGE* is expressed as:

$$\dot{\boldsymbol{\theta}}_+ = [\,(\boldsymbol{Q}_a)^{-1}\boldsymbol{Q}_b + L(\omega)]\dot{\boldsymbol{\theta}}_-$$

This results in a simple expression of the actuation of the system via the function L with parameter ω. In the case of the flywheel, the momentum is given by:

$$L(\omega) = \omega \sum_{i=0}^{n} I_i$$

Where I_i is the index inertia of each portion of the actuator about the hip axis

When parameter ω is zero (the limiting case of zero angular velocity for a flywheel) the total momentum is zero and the energy injection is zero. We see that for both *MTGE's* in the K-Walker and the one *MTGE* in the NK-Walker, this would result in no change to the original system model proposed in Section 2.2. This is because the addition of zero angular momentum will cause the impact event that the MTGE is based on to proceed as it would passively since the angular momentum is conserved about the stance foot just as it is in the existing impact equation. When ω > 0, a positive injection of angular momentum is present at the joint, and in the case where ω < 0, a negative injection of angular momentum is present at the joint. Since both discrete events can have this energy injection and all 3 joints (in case the K-Walker, or 2 in the case of the NK-Walker) can have this type of energy injection, there would be up to 5

different energy injection positions in a standard gait cycle that qualify as simple *MTGE's*. These points can be seen on the figure below of an archetypal stride function for an K walker (which has the most potential MTGE points:

- Stance foot torque at A
- Swing foot torque at A
- Hip torque at A
- Knee torque at B
- Hip torque at B
- Stance foot torque at B

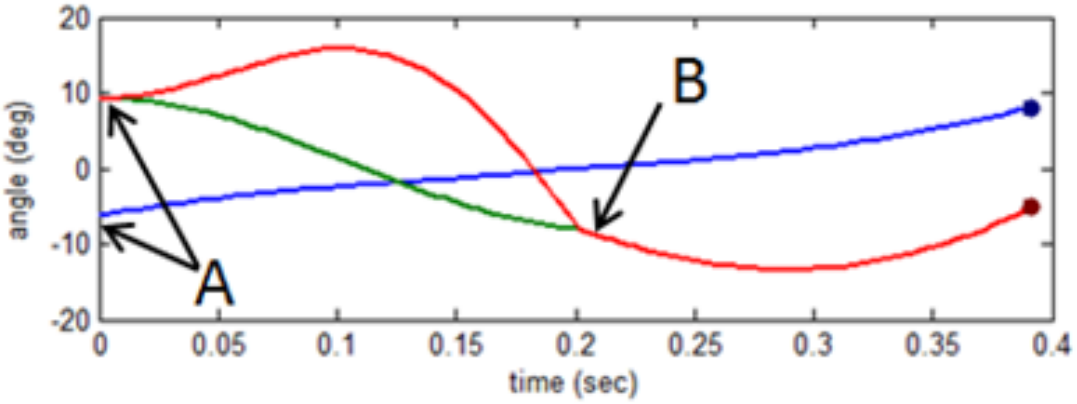

Figure 2.10: MTGE points for a general K-Walker model

An important note for the NK-Walker is that all of the events at B disappear if describing *MTGE's* as defined earlier in this section. In every other case, the result of actuation torque simply modifies an existing impact event through the injection of additional angular momentum at different points. At each of these points there exist two distinct actuation possibilities, one where the momentum is added constructively with the motion of the walker, and one where it is added to counter the motion of the walker. A measure of this can be called the *polarity* of the actuation, which is fundamentally linked to the direction of each ω_i at the point of actuation, but is a net quantity combining all of the effects of the direction of each ω_i. In essence, the injection of different ω_i at a joint not only affects the magnitude of the actuation event, but also the net effect of the *MTGE* on the stride.

2.4.2 Complex MTGE Concept

Another interesting concept that is developed when pursuing this actuation method is the capability to provide actuation at times where the model is not undergoing an existing gait event. Instead of piggyback actuation at a time when there is an impulse event, an *MTGE* could also occur during one of the continuous dynamic phases of the gait. The inspiration for this concept comes from the original development of the passive walking knee. In a passive walker with knees, one of the fundamental purposes of the knee is to prevent toe scuffing when both legs are at an equal angle. The locking action of knee provides an additional impact event where an impulsive collision is used to provide regulation to the passive walking gait and the energy injection into the system. The effect of this action provides additional stability to the walking gait [1] [2], which leads to the fundamental question: can the addition of new impulsive events in the gait cycle also produce similar results? In what can be called a complex *MTGE*, we can pick any repeatable point in the gait cycle and create an artificial *MTGE* by injecting energy impulsively, similar to the knee lock event on the K-Walker model.

In order to create a complex *MTGE*, the first step is to understand a concept known a repeatable gait point. In a walking gait, there are many different points that could be chosen as a complex MTGE point, but the complication is that these points may not always recur in a given gait if the event is time based, or tied to a specific state, as the gait will change in period and step length as the ramp angle is changed [1]. An example of this is shown in Figure 2.7, where we see the stride function of the various limit cycle gaits of a passive NK walker, as the ramp angle is changed.

The complication that arises out of this is simple: it is difficult to find a dynamic landmark in a walking gait. By definition, a dynamic landmark would be a point that occurs in all stable gait cycles and is a function of both leg angle states. Examples of this from a typical gait K/NK-Walker would be the heelstrike or knee lock points. One simple point that does this to some extent however, is the *Equal Angle* point of the stride, which is the point where the absolute leg angles are the same (as measured from the horizontal). On any recurring gait, this point takes place at the crossing point of the legs due to simple geometry. This point does not necessarily

occur at the middle of the stride (with respect to the time domain), as shown in the Figure 2.5. We see that the equal angle crossing varies in the time-domain of a gait, but the points are all still roughly around the half-way point in the stride (in the time domain).

When the actuation is done at this equal angle crossing point, the only potential actuators that should be used are of the hip actuation type or the foot actuator type, regardless of if the walker is of the NK or K configuration. This is because, In the case of the K walker, although knee actuation is possible, actuation at the EA point could cause the shank to swing forward too quickly. This would cause foot-scuffing which is a very undesirable effect on the gait, so to avoid foot contact, the actuation would have to be carefully tuned.

When looking at theoretically described actuation concepts, one simple question that is often asked is: are these actuation events feasible in experiments or are these events something that can't be implemented on a physical walker? In the case of the hip and knee actuation, the simple clutched flywheel example given earlier in this section would suffice as a real world application, although the physical construction of such a device would prove to be challenging as discussed later in this research. In the case of the toe/foot actuation, a simple method is described in [17] where ballistic foot actuation is used, however the impulse provided by this actuation does not produce an ankle torque, therefore changes to the actuation model used in this research would be required. An alternative method of providing foot actuation would be via a walker with low-mass flat-feet, actuated via a ballistic or a clutched flywheel approach. This would likely manifest itself as a pair of flat feet that follow the ground pivot point and have no ankle impedance. These feet would be capable of being clutched in and actuated with respect to the shank of the leg. From a mathematical perspective, this would represent a point foot walker (as the foot cannot take any load when unclutched) with the potential to provide positive/negative ankle torque. In a simple experimental case, it would be logical to choose only one or two of the potential actuation types since the goal of the research is to understand the effect of the actuation on the system, and each of these cases are analogous in the study of *MTGE*'s.

2.4.3 Integration of MTGE's into Proposed Passive Model

Overall, between the simple *MTGE's* and the one complex *MTGE* discussed, there are 2 potential actuation points for the simple NK-Walker model using a simple inertial actuator that can be used for an initial study of *MTGE* actuation. This increases up to 3 potential points in a K-Walker model when similar actuation is used. It is clear that the only time the knee actuation can realistically be used is on the K-Walker, right before the knee lock event. Comparing this to the other two types of actuation, it's clear that a simple actuation study should be focused on one of the other two types of actuations (hip actuators and toe actuation) in order to maximize the potential to study the system.

In the case of simple *MTGE*'s, all that is required to implement them in both models is a correction to the state transition matrix from the impact events to reflect the additional angular momentum being injected. For the case of a complex *MTGE*, another terminal gait event is added with a state transition matrix determined by the type of actuator used and the position of the system pre/post actuation. For both walkers, an actuator at the hip that is active at heel strike was implemented in the model, with parameter $L(\omega)$ being the magnitude of angular moment injected at the hip during heel strike. In the case of the NK walker, a complex *MTGE* was also added, where the transitional condition is the equal angle crossing point, and a hip actuator is modeled as injecting momentum $L(\omega)$ at the hip. In the K walker case, an additional hip actuation was also considered at the knee lock case with magnitude $L(\omega)$.

2.5 Overview of Mathematical Modeling

Overall, it's clear that the passive walker model presented in this section is capable of emulating a broad range of walking machines and is perfectly suited for the goals set out for this research. This is however not without a major drawback, in that the model parameters are suited to a baseline walker that is 1m tall and has a total weight of 4kg. From the work in [1] we see that the leg masses can be scaled, meaning that any walker with a leg length of 1m using point feet and no knees can be emulated using this model, however the baseline walking gait

requires a mass ratio M/m = 2. When either the leg length, mass location, or mass ratio are changed, the dynamics of the walker will change drastically, therefore any further research into the walker model requires a finalized geometry. Ideally, the baseline case represents a functional example of stable walker geometry, but from an experimental view this is not ideal as it might not be possible to construct a physical model to meet the baseline parameters when an actuation system is added. Since one of the research goals is to produce a walker geometry that can produce stable walking gaits while actuated/unactuated without any changes to the walker, care must be taken to ensure that the theoretical and experimental walker models match closely. This means that the next step towards studying the model is to design/build the experimental setup of the walker and finalize the mass properties of the walker, before doing further analysis.

Chapter 3

Experimental Setup

Since an all-inclusive passive model was proposed in the previous section, the typical step forward would be to perform a comprehensive simulation study using the baseline geometry. Following this, an experimental walker could be built to match the model parameters. In any walking model however, one of the key issues is that the basin of attraction of the walker is rather narrow and fundamentally varies when the mass parameters of the walker are modified. If the walker mass parameters are varied substantially from the baseline parameters, the basin of attraction shrinks rapidly. In an extreme case, a change in mass parameters can result in the disappearance of the gait cycle. In the case of an actuated model, this is typically a large stepping stone that must be overcome, as the physical implementation of a walker often changes the model substantially from the ideal baseline. The mass and inertia added by actuators and their joint connections are not simple to account with a simple walker model. In the case of a passive walker, even a robust walker produces results that are difficult to reproduce and require a high degree of precision in the construction of the walker itself [1]. To this end, the goal of this section is to construct a walker that uses the baseline geometry as a design guideline with constant interplay between the walking model and the experimental walker to ensure that in the end, the experimental walker is accurately characterized in the walking model. To start this process, we can begin by looking at the various mass parameters and focus on selecting ideal values that are physically viable to design the experimental setup around.

3.1 Mass Parameter Selection

In the case of the NK-Walker model, the physical design of such a walker can be done in a large variety of ways; one of the most basic methods is to build a simple planar walker out of planks of aluminum, some form of foot at one end, and a pivoting hip at the other. The problem with this approach, and one of the fundamental stumbling blocks of experimental walker design, is that simple mechanical solutions can often complicate the walker model. In the case of a walker leg, one can treat it as a simple pendulum or inverted pendulum (depending on which leg is swinging). Just like a simple pendulum, the walker can have a point mass placed somewhere on the leg, which affects how the leg behaves. The leg acts as a pendulum of length *a* (in the NK model) when the leg is the stance leg, and acts as a pendulum of length *b* (suspended from a moving point) when the leg is the swing leg. In the case of large a plank aluminum leg, the problem is that there is a large amount of inertia in the leg that is not accounted for. In the case of a leg of length *L* with a uniformly distributed weight m_L, there exists methods to model the leg as a simple pendulum if held from either end (using the principle of a physical pendulum), however the effective length of the leg in the model would then be the summation of the two simple pendulums. This would result in a model which accurately describes a single link system, but when the second link is added, it causes the model to not be able to correctly describe the system. To solve this problem, a traditional approach is to try and model the walker with variable mass on the legs to get a more complex description of the inertial properties of the leg.

An alternative approach that is being used in this research is to view the analytical-simulation paradigm from a different perspective, and change the physical system to match the model. In the case of many systems of engineering relevance, this is not a possibility, because the physical system of interest is one that already exists in the physical world and cannot be changed without trivializing the research. In the case of a passive dynamic walker, however, the system is based on a mathematical concept, namely a behavior that exhibits itself in systems of a certain topological structure that have similar kinematics. This is often a mistaken fact, as many researchers view a passive walker as a simulation of human walking, which is not strictly

true. In the case of human and other bipedal locomotion, there is generally always a mechanism to provide energy into the walking gait, which means that nearly all walking motions in nature are a mixture of passive and active dynamics. With a passive walker, the main goal is to study the passive side of this type of motion, via dynamical systems that can be designed to have bipedal walking gaits when specific initial conditions are used. To this effect, we can take the numerical model, one with massless links and point masses, and try to build a physical walker that has similar properties. In a physical sense, this is not entirely possible as the legs of the walker will always have some mass, but by minimizing the differences between the physical walker and the model as much as possible there exists the possibility to match the two without changing the model proposed in section 3.

From the baseline geometry, we see that the walker should have a M/m ratio of about 2, but the actual masses can be of any value, without changing the model behaviour. The leg length, however, determines the stride length of the walker as well as the step period [40] and therefore it is important to settle on a desired leg length. For a physical test walker, an appropriate leg length (from previous work in the field) is between ~200mm-400mm, as the weight of the walker starts to become very large with longer leg lengths and it is also very difficult to work with long leg walkers on a test ramp. A midrange value of ~300mm was chosen as a design goal, with the requirement design feature to allow for small adjustment up and down in terms of leg length.

With the leg length set, the next parameter to decide on is the mass of the leg. In the model, the walker masses (as described earlier) allow each leg to act as linked simple pendulums. This means that each leg can be kinematically described by three fundamental properties, the inertia of each leg I_o, the mass centre location x_m, and the radius of gyration r_g. In terms of the model, each of these properties is easy to determine:

$$x_m = \frac{2b}{\left(M/m\right) + 2}$$

$$I_O = mb^2$$

$$r_g = \frac{b}{\sqrt{(M/m) + 1}}$$

Between these parameters and the M/m ratio of the leg, there is a full description of the leg mass in the model as well as the physical walker. From the baseline geometry, the M/m value of 2 produces a reasonable basin of attraction, and higher mass ratios have been shown to be favourable via preliminary analysis, therefore the design goal is set at $M/m > 2.0$.

The last parameter to be selected was *b*, the location of the leg mass relative to the hip. To select an ideal value for this parameter, a small-scale parametric study was done for mass ratios between: $1.5 < M/m < 5.0$ .The result of this study showed that $b \sim 0.5L$ is a reasonable value for *b* that produced a large basin of attraction at nearly all mass ratios chosen.

With these initial design goals set, the next aspect of the experimental walker is the design of the actuator. Since the actuator mass/inertia must be hidden in the walker frame (for it to be modeled accurately) it is of great importance to have an initial design of the actuator based around the target mass properties of the walker, and also to evaluate the types of actuation that can be successfully done on the walker for an initial study.

3.2 Actuator Design

From the discussions in the previous sections, the baseline for the experimental walker was selected as: a four legged planar walker that has point foot legs with *L~300mm*, $b \sim 0.5L$, and M/m > 2. To produce a physical walker, the first issue that came up was the design of the actuation system. In the proposed hybrid active/passive model, one of the key aspects is that the unactuated walker has the same mass properties as the actuated one (no removal of actuators for passive walking) and that the dynamics of the actuator when disengaged are included in the joint motion. This presents a series of technical problems that were solved during the design of the walker, namely:

1. The actuation system must be composed of elements that can be reasonably modelled with a point mass walker model.
2. The actuator dynamics must be known when disengaged and have little to no effect on the aforementioned kinematic properties of the leg.
3. The actuator must be able to provide a reasonable amount of angular momentum compared to the nominal angular momentum (pre-collision) at the joint, in order to actuate the walker to a reasonable degree.

In order to minimize the first issue, the goal would be to place the actuators such that they are in line with the axis of rotation of the joints. Small/slender actuators would permit the actuator to be primarily equivalent to a point mass (in the planar view) as long as the actuator has a sufficiently small diameter. In the case of a linear actuator, there would have to be some sort of linkage converting the actuation motion to rotary motion, which makes it very difficult to produce a small size actuator. This means that the most reasonable choice would be to go for a rotary actuator that acts directly on the joint of the walker. Since it was determined in section 2 that the simplest actuation case would be the hip only actuator, the simplest design concept is to place an actuator directly on the hip axis. This would affect the mass properties of the walker because: additional mass from the actuator M_A at the hip that would have to be accounted for by the mass M in the model and an additional inertia about the hip (I_o) from the diameter of the actuator which would have to be accounted for in the model by increased mass m. In terms of the type of actuator, 3 main types were considered: electric, hydraulic and pneumatic. Due to the very small rest time ($\tau \sim 0.3s\text{-}0.9s$ from the baseline geometry), a hydraulic actuator can be ruled out due to feasibility and ease of actuation. Another concern would be the effect of additional high pressure lines coming out of the walker, which is a significant concern in both the pneumatic and hydraulic cases, but largely minimal in the electric actuation option. Based on these simple issues, the most logical decision was to use an electric motor at the hip to provide electric rotary actuation, with careful design of the wiring to the actuator to ensure that there is no joint impedance added by the power lines to the walker.

Since the theoretically desired actuator response is discontinuous and impulsive, the next

problem is to determine how to physically achieve discontinuous (or near discontinuous) response. There are a wide variety of methods that can be used to provide impulsive actuation including: using an impact hammer type mechanism, using a high impulse rotary actuator, using a high torque actuator geared for abrupt actuation, and finally using a clutch between the actuator and the walker. In the case of an impact hammer type mechanism, one of the issues is that the actuator response must be quick enough to overcome the lag in the system (time between activation of the actuator and timing the "kick" from the impact hammer). This type of lag is very difficult to mechanically tune into the system, and would vary with actuation force/speed, creating the potential for a large amount of tuning required to match the actuator response to the impact model. In terms of high impulse actuators and high torque geared actuators, it can be seen easily that both suffer from the same problem: namely, relatively high actuator impedance. This is because any option with a relatively high actuation potential either uses a strong magnetic motor drive system or a gearbox, both of which result in significant joint impedance on a light frame walker. In the case of a high torque rotary actuator, concepts such as a harmonic drive based actuator were considered in order to minimize this, but the dynamics imposed on the joint by the actuator when unpowered (being driven) are amplified by the gearbox substantially, so ultimately the joint impedance is still high. This leads to the most reasonable option, where a clutch is used to decouple and recouple the actuator from the walker. In the case of a clutch, abrupt engagement of the clutch results in a fixed amount of inertia being added to the joint based on the components of the clutch that spin with the hip shaft and the speed at which they are spinning. When the clutch is disabled, the actuator dynamics are completely decoupled from the joint, and when engaged, the actuator and the joint are forced to match angular velocities. The issue with a system like this occurs when the actuator is coupled to the joint. If the actuator has internal dynamics that affect the joint dynamics, the portion of actuation where the clutch engages results in a portion of the walking gait where joint impedance must be considered. One way around this is to reduce the clutched time to a near instant impact event, and also to use a low torque high speed actuator with a flywheel to build up inertia and minimize the joint impedance when engaged.

Considering an actuator of this form, the first challenge is to design a physical

implementation of this concept that is feasible. The first issue is to select a motor type, for the energy injection part of the actuator. Although a wide variety of motor types are available, the simplest type to use would be a simple brushed DC motor with low mechanical impedance. By using a high rpm low torque motor, the impedance is minimized, which allows the effect of the motor dynamics (when connected to the walker) to be minimized. For the time response, we can look at the rest time for the baseline walker ($\tau \sim 0.3s\text{-}0.9s$) and note that even in the event of a single MTGE, the actuator must be able to achieve full speed in under 0.3s, in order to actuate once per cycle. If multiple MTGE's are used, this rest time decreases as well. We note that in a very simple case (no loss), the torque for a typical brushed PMDC motor is given by the first equation below, where T_0 is the stall torque and K_t is the torque slope. The angular acceleration of the actuator is given by the second relation, where $\alpha(t)$ is the acceleration of the actuator and I_A is the net inertia of the actuator about the hip axis. The last equation is the solution to the linear ODE of the hip actuator response ω as a function of time:

$$T(\omega) = T_0 - K_t\omega$$

$$\alpha(t) = \dot{\omega}(t) = \frac{T_0 - K_t\omega(t)}{I_A}$$

$$\omega(t) = \frac{T_0}{K_t}\left(1 - e^{-t\,\tau^{-1}}\right),\ \tau = \frac{I_A}{K_t}$$

From these equations, we can see that there is a simple method to select an actuator once the walker has already been constructed. Firstly, the design values for the walker must be chosen, and the rest time for the chosen passive geometry must be determined. The target motor characteristics can then be easily found.

The next step is to address the clutch itself, and to find a suitable design to actuate the walker leg. From simple mechanics, we can see that the walker needs to be able to actuate the swing leg, however there would be an internal reaction force via the motor frame which must be countered. In the case where the walker is in single support (i.e. immediately after heel-strike, or at any point before the next heel strike), we see that the stance leg is fixed with

respect to the ground. The actuator must therefore be mounted in such a way that the reaction torque is reacted by the stance leg, while the impulse is provided to the swing leg. After several design iterations, the final layout was chosen to be a simple configuration using a floating hip shaft (B) with inertial weights (C/D), a pair of axially mounted motors (E), and a set of clutches (A) that have a dog engagement system to the inner legs and are pinned to the hip shaft. The letters 'A through E' are labelled in the diagram in Figure 3.1.

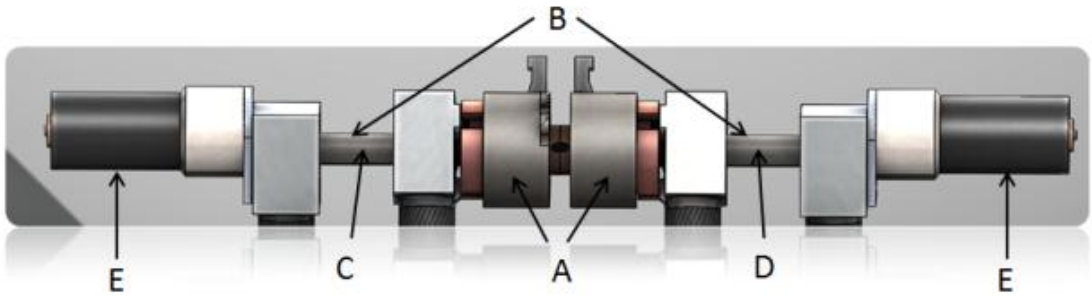

Figure 3.1: Component View of Hipshaft Actuator

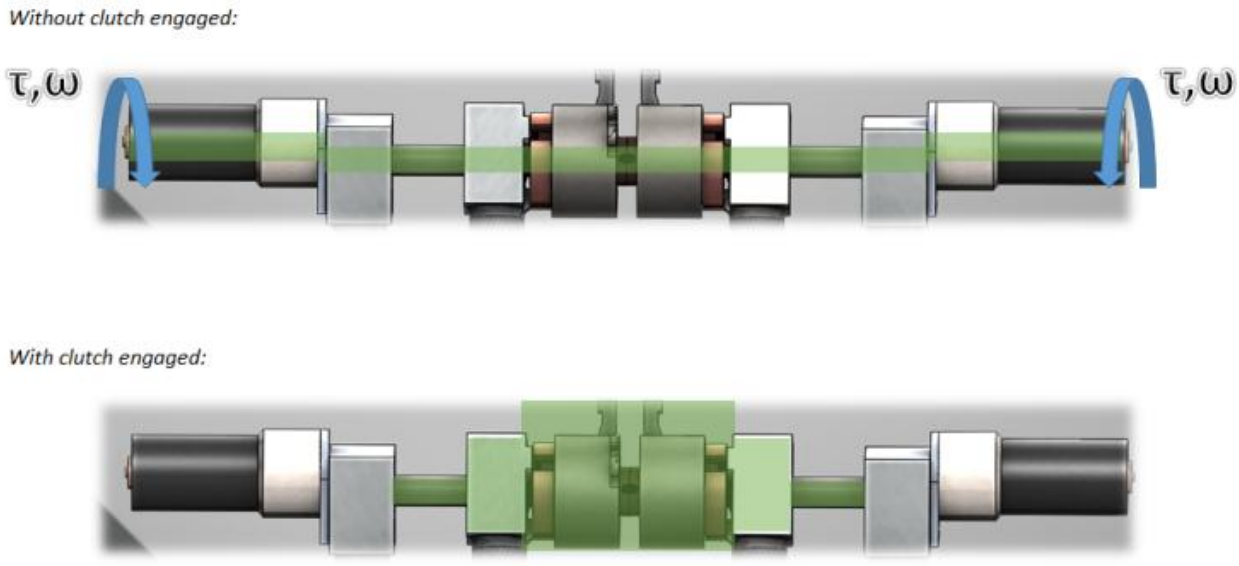

Figure 3.2: Clutched Actuation Mechanism

When the motors spin up the hip shaft, the reaction torque is applied to the fixed leg about the hip axis (which doesn't affect the walking dynamics of that leg). When the hipshaft reaches

its peak actuation speed at $t \sim 3\tau$, the clutches can engage and the motor can disengage. This adds the angular momentum of the: hipshaft, the clutch assembly, the inertial weights, and the motor rotating assembly to the swing legs. These are noted as the sum of all of the rotational inertia in the actuator assembly about the hip, to the inner legs of the walker in the equation below. If the rotation of this assembly is the same direction as the motion of the swing legs then the *polarity* of the actuation (as discussed in section 3) is positive, which causes the energy to be injected into the system in the direction of motion. If the rotation is reverse, then the polarity is negative and energy is injected into the system to counter the motion of the swing legs. The net momentum injection into the system, if ω reaches the value of $\omega(\tau)$ is:

$$L(\omega) = \frac{T_0}{K_t} \sum_{i=0}^{n} I_i$$

With the actuation system designed in concept, the next step is to set up the structure of the walker, and finalize the physical design for the walker so that an actuator can be selected.

3.3 Walker Design

One of the primary goals of the experimental physical walker is to establish a physical geometry that is nearly identical to the NK walker model. As discussed earlier in this section, this means matching the three main dynamic parameters of the NK walker model, namely the radius of gyration (r_g), the inertia about the hip (I_O) and the mass centre location (x_m). Since the walker model was designed in 3D cad software (a combination of NX and Solidworks) the main mass properties for the designs were extracted from the mass properties of each element of the design, with careful physical measurement of all fabricated and purchased components. This allowed different design concepts to be evaluated based on how close the walker was to the NK walker geometry. Since the NK walker is a point mass, as shown earlier, all of the parameters are linked mathematically since the walker has point masses and massless links. In the case of the real walker, all three of the parameters can be individually varied, which poses a rather large design challenge. Ideally, the leg component of the physical walker would be nearly massless, so the inertia would come only from the thigh mass. This means that increasing thigh

mass and hip mass at the same time result in the same mass centre location but increasing inertia. In this same example on the physical walker, the issue is to get the large hip mass to be small enough in diameter to not create a significant inertial contribution to the walker. This leads to a design with a very wide structure that is difficult to experimentally handle. If this is ignored and the hip mass ends up adding inertia to the legs, the only way to account for it is to model mass *m* as larger than it actually is, or change parameter *b*, both of which drastically affect the model. It is also incredibly important to balance these effects between the four legs of the walker (since it is a planar biped) so that the physical properties of each leg are not only similar to the model, but are identical to each other. To accomplish this, a hollow 6061-T6 light alloy tube is used for each leg with 7075-T6 light alloy hard anodized point feet and FORTAL HR light alloy hip components. This design was optimized via structural analysis to be as light as possible, to minimize the non-modelable inertia and mass of the walker frame.

Figure 3.3: Bare Experimental Walker Frame

The end result is shown above, without any inertial weights on the frame. The net walker structure has the following parameters: 0.669kg weight (without a hipshaft), 74.8 kg•cm^2 of inertia, leg length *L* of 350mm, and center of mass location of 38mm (down from the hip of the

walker). This correlates to a walker model with 0.247kg of leg mass and 0.8kg of hip mass with a *b = 0.5L*, and L = 350mm, which is very reasonable for just the frame of the walker. Very little leg mass was required to balance the inertia. In order to mask the mass properties of the walker, large weights were added at length *b* from the hip location of the walker (effectively increasing mass *m*). In order to mask the weight of the walker frame, a large magnitude was chosen for the leg weight. As a baseline, a weight of 1.26kg was chosen, split between the outer legs. With just this mass added, the new properties of each pair of legs of the walker were: I_0 = 500.22 kg-cm^2 and x_m = 0.45L. Compared to the model, this setup has the same properties as a walker with *m = 1.63kg, b = 0.5L, L =350mm,* and *M = 0.17kg*. This result is very reasonable, as there is variation in the leg mass of the model to account for the weight of the frame of the walker, and the inertia of the foot assembly, and *M* is now very close to the hip weight of the walker. In order to then push up the mass ratio, additional mass was added to the hip of the walker, via a hipshaft, inertial weights, and a pair of counterweights (which would eventually be replaced with motors) to bring the net hip mass up. The total hip weight added was ~5.6kg, resulting in a total hip weight of 5.8kg in the physical walker. At this point, small changes were made in the geometry of the walker, including adding additional weight to the walker legs until the final parameters were set as shown in Table **3**.**1**.

Table 3.1: Experimental properties of the walker vs. model parameters

Model	Physical Walker
m = 1.63kg	*m ≈1.50kg*
M = 5.825kg	*M ≈ 5.99kg*
M + 2m = 9.09kg	*M + 2m = 8.99kg*
L = 0.368m	*L = 0.368m*
b = 0.5L	*b ≈ 0.5L*
M/m = 3.57	*M/m ≈ 3.99*
I_O *= 552.75 kg-cm^2*	I_O *= 550 kg-cm^2*
x_m*= 6.61cm*	x_m*= 6.09cm*
r_g *=7.80*	r_g*= 7.82cm*

For the actuation, a set of Pittman PMDC motors were used with a peak joint torque T_0 of 288 N-cm, and a torque slope of -8.49x10^{-3} Nm-s K_t. The net inertia of the actuator assembly I_a is: 5.82x10^{-5} kg-m^2. Based on the equations derived earlier in this section, this results in an actuation time constant of $\tau \sim 7ms$, which is more than acceptable to actuate any of the observed walking gaits. From these parameters, the peak angular momentum that can be injected $L(w) = 0.0125$ kg-m^2/s, at t = τ. If the time between steps is substantially higher, one can assume that $\omega \rightarrow \omega_t = 339$ rad/s, which results in an energy injection $L(w_t) = 0.0197$ kg-m^2/s. Both of these figures are easily achieved with $\tau \sim 7m$, therefore the upper value of $L(w_t)$ will be used as a peak actuation force. It is worth noting that w_t varies in a somewhat linear manner (as tested) by applying varying voltages to the motors for speeds in the range of $0.5\omega_t$ to ω_t. This means that a net actuation force can be varied somewhat linearly between the approximate range: 0.01 kg-m^2/s $< L(\omega) <$ 0.02 kg-m^2/s, with the potential to drop L(ω) lower than 0.01 with some difficulty using careful voltage/speed regulation. For the clutch setup, a pair of Reel EC25L's were used for either direction (four clutches in total) providing a net forwards/backwards torque of 566 N-cm, and an engagement time of τ_e < 15ms. Combining this engagement time with the previous time constant of actuation, the end result is a bi-directional actuator capable of providing up to 0.02 kg-m^2/s with a positive or negative actuation *polarity* within time ~ $3\tau + \tau_e = 36ms$. This means that all of the tested benchmark gaits can be actuated well within the bounds of a stride, such that continuous actuation of a gait is allowable including more complex MTGE's.

With the baseline mass parameters set, the full physical walker was constructed and weighted with the pair of Pittman PMDC motors and REEL clutches described above. A view of the physical walker is shown in Figure 3.4, with all of the major components attached to the walker and accounted for via the walker model as well. With some careful weighting of the existing components of the walker, the actuator setup was added on with no change to the mass parameters from Table 3.1.

Figure 3.4: Experimental Walker Model

With the main portion of the physical design complete, the next step is to test and tune the actuation system of the walker. Since the actuation system is not well tested in literature, an important part of this testing is to ensure that the actuator behaves as predicted, to ensure that the active/passive walker model is correct.

3.4 Experimental Results

In order to test the actuation, a simple setup was used to validate the dynamics of the actuator against the theoretical behaviour. The angular momentum input to the system was set

to a desired level and the mass/inertial properties of the system were modified slightly. This was achieved by removing components of the leg to make the system behave more like a simple pendulum. The walker was then held by the fixed portion of the hipshaft (the motor housings), and the natural frequency f_0 of the system was measured. With the walker legs stationary, energy was injected into the system at the EA actuation point continually, with the same magnitude of *L(w)*. The EA point was chosen as its easily repeatable and always the point of peak swing velocity for all amplitudes of oscillation. The frequency of the new oscillations was then measured for values of *w* from near zero to near w_t. For this experiment, the mass was varied on the leg such that the f_0 = 1.25 Hz, and the experimentally measured natural frequency for each actuation speed is measured and plotted below. Theoretically it is expected that there is no variation of f_0 with actuation speed ω.

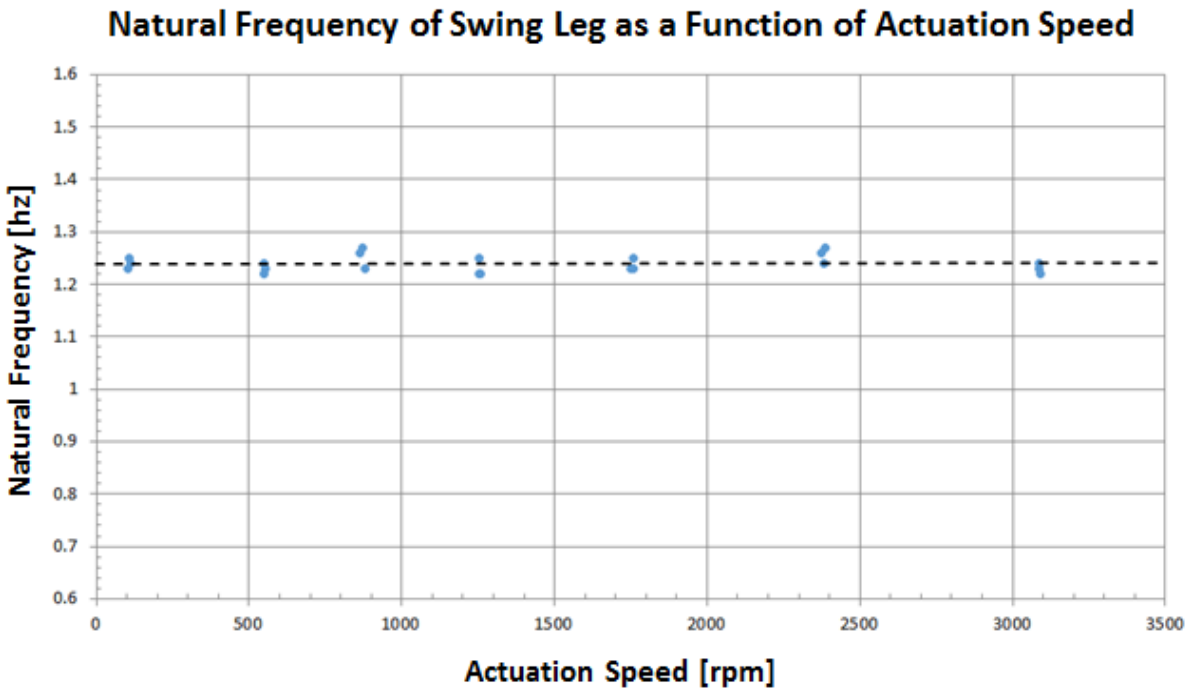

Figure 3.5: Swing Frequency of Walker Leg under Varying Actuation Impulse

As predicted by the actuation model, the injection of angular momentum into the system via the clutched setup resulted in the walker reaching peak amplitudes that varied according to the energy input into the system. The time it took to reach the peak amplitude also decreased

as the energy injection increased. It is however notable that the natural frequency of the system did not change, and it stayed relatively constant at an average value of f_0 = 1.24 Hz as measured by the best bit line through the data points measured. The data points were measured by allowing the leg to reach peak amplitude and timing the distance between actuation points, which were triggered with an optical sensor set to go at the equal angle crossing point of the legs. The clutch actuation was done using a pair of arc suppressors and a fast action relay fed by a switch-mode high current supply. The net triggering/disengage time for the clutch with this arrangement was estimated via manufacturing specs to be < *20ms*, which results in a modified net actuation time constant of $\tau < 41ms$ This result indicates that the effect of the actuation is not to change the dynamics of system it's actuating, but to inject energy into the system via an increase in angular momentum. If the dynamics of the actuator were to come into play the natural frequency of the system would be likely vary due dynamics of the actuator.

With the actuation testing complete, the final stage of the preliminary testing of the physical walker is to get the walker to produce a stable gait and measure the key gait parameters: the stride length and the time per step. This gives the rate of advancement (speed) of the walker, as well as two values to compare in the model to determine how close the theoretical model is to the physical walker. Although this normally just involves finding an angled surface to launch the walker on, the complication that arises when using an NK-Walker is the issue of foot scuffing. With a traditional K-Walker model, the purpose of the knee is to provide foot clearance at the EA point of the gait, such that the toe is lifted due to a bend in the knee when the swing leg passes the stride leg. If this does not occur, when the walker reaches the equal angle point the tip swing leg and the stance leg feet both share the exact same vertical position at the equal EA point. The walker will scuff the swing leg foot on the ground upsetting balance. One simple solution to this is to use "Lift Pads", which are small platforms that elevate the points of contact of the walker with respect to the ramp surface. These pads are thin risers that are placed at every point where a stance leg is expected to pivot on, i.e. when the outer legs are the stance legs, the first set of pads would be under the outer feet and a pair of pads for the inner feet would be spaced away by the stride length L_S of the walker.

These pads require a fairly accurate knowledge of the fixed point stance angle $\theta_S = [\theta_1 + \theta_2]_{terminal}$ of the gait so that they can be spaced apart by the stride length $L_S = 2Lsin\left(\frac{\theta_S}{2}\right)$. This is complicated by the need for these pads to be as narrow as possible and have minimal height. The complication that arises if the pads are too tall is that the walker can abruptly fall off the pads causing a large upset in balance. The complication from having them too long (in the direction of travel) is that the actual stride length of the walker can vary slightly from the pad spacing. If the length is different than the spacing, after a few steps the contact points of the walker on the steps will shift forwards or backwards from the centreline which means the walker will eventually fall off the steps or scuff on them due to the gap for clearance not being in the right location relative to the stride. In order to implement these lift pads, a ramp was built which has 3" long hardwood pads of 3/8" height that are nailed down to the ramp surface underneath. A shim based angle adjustment setup to allow for ramp angles from γ = 0 – 10 degrees was implemented. Pre-set shims were used to increase angles by 1 degree increments, with a digital inclinometer fixed to the ramp to set the angle accurately to any intermediate point using a series of finer shims. The designed ramp therefore allows for a variable ramp angle γ in ~0.05˚ increments as well as variable stride length L_S, if the pads are moved and reattached in new positions. Safety rails were also installed on the side of the ramp to allow the walker to rest on the motors in the event of the walking gait failing (to catch the walker from falling). The height of these rails was very carefully set as the vertical location of the walker hip deviates by a maximum of $y_h = 2Lsin^2(\frac{\theta_S}{4})$ once per stride. The height was set such that a peak stride of 40˚ was allowable before the walker hits the rails, so that a wide variety of potential walking gaits is possible, but the walker is still protected from falling any substantial height.

With the ramp set to an initial ramp angle of $\gamma = 0.05rad$ and the lift pads set in place with double stick tape, several trial runs were made to get the walker to produce a stable gait pattern with the end result being a passive walking gait with the Gait parameters shown in Table **3.2**.

Table 3.2: Measured Gait Parameters of the Experimental Walker

Parameter	Value
Stride Length	L_S =8.0" (average) ± 0.1"
Step Period	τ_s = 0.492s ± 0.041s
Walking Velocity	*v = 0.413 m/s*
Froude Number	Fr = 0.222

The ramp arrangement is shown below, with the physically constructed walker shown in mid stride, and the lift pads, guide rails and weighting system clearly shown.

Figure 3.6: Walker Test Ramp

This gait cycle was reasonably repeatable with a launch success rate of ~20%, and when the motors were turned on for the actuator (but no clutch engagement) the walker was still able to achieve the same walking gait. This indicates that that model for the actuator when disabled that was described in section 2.2 was accurate, resulting in an experimental setup that is largely analogous to the proposed passive walker model.

3.5 Experimental Setup Overview

Since the walker was shown to be able to produce a stable walking gait, the instinctive thought is to proceed experimentally to dynamically characterize the actuation. This is not a very reasonable option, however, since it took weeks of work to grasp the basic dynamics of the walker, be able to produce a limit cycle gait, and measure the gait. This highlights one of the main advantages the simulation approach has over the experimental one: changes can be made rapidly and the effect of small changes can be documented. Between these difficulties and the limited time scope of the walker project, it was decided that the dynamic characterization of the hybrid active/passive portion of the walker would be via simulation first. This means that the actuation on the experimental walker was characterized via simulation. After some insight is provided into the dynamics, specific actuation points can be selected and experimentally tested.

Chapter 4

Active/Passive Simulation Results

In this section, the simulation results from the model proposed in Section 2.2 will be discussed, scaled to the parameters of the experimental setup listed in 3.3. The baseline simulation results are shown first to validate the proposed model. Following that, three cases of actuation are implemented and tested via simulation: simple MTGE energy injection at heel strike, complex MTGE energy injection at the EA point, and a combined case. These cases are tested at low and high ramp angles to characterize the response of the system to varying levels and types of actuation. To start this process, first the experimental setup results (passive) will be validated.

4.1 Validation of Passive Experimental Setup

With both the experimental setup and the fully functioning simulation model for the system complete, the next step in the research is to link the two such that they both are representative of the same walker geometry. This means that the model parameters must be matched to the parameters of the experimental setup. In all research involving passive dynamics walkers, this is a challenging process as the system is not structurally stable in the region surrounding the period 1 cycle walking gait fixed point. This means the fixed point as well as the Basin of Attraction (BOA) both shift rapidly as model parameters are changed, and for many physical arrangements of the walker the fixed point of the gait cycle disappears completely. An example of where this would happen is shown in chapters 2 and 3, where the physical geometry of the walker was changed multiple times in order to present a physically realizable walker. Small

changes were also made as the walker was constructed and the actuation system was built. If this was done without any regards to the established guidelines set out in section 3, there would have been a large possibility that the system would not produce a walking gait. By keeping track of the model parameters required to represent the physical system, we end up with the following parameter set for the simulation model vs. the original baseline geometry explored in Section 2:

Table 4.1: Comparison of Baseline and Experimentally Derived Model Properties

Model	Baseline Geometry
$m = 1.63kg$	$m = 1\ kg$
$M = 5.825kg$	$M = 2\ kg$
$M + 2m = 9.09kg$	$M + 2m = 4\ kg$
$L = 0.368m$	$L = 1m$
$b = 0.5L$	$b = 0.5L$
$M/m = 3.57$	$M/m = 2$
$I_O = 552.75\ kg\text{-}cm^2$	$I_O = 2500\ kg\text{-}cm^2$
$x_m = 6.61cm$	$x_m = 25\ cm$
$r_g = 7.80$	$r_g = 25\ cm$

The chosen parameters are fairly far from the baseline geometry, and do not have a known walking gait fixed point but they are representative of a physical walker that produces a walking gait, so it is known that a simulation gait for this walker must exist. Each parametric change will result in a change to the walking dynamics, and therefore must be accounted for independently. For example, the increase in leg length will end up changing the walking gait, as the stride length and step period both change with leg length. The Mass parameter *b* also affects the stability of the walker, but it still remains unchanged with respect to *L* compared to the baseline geometry. The mass ratio has also increased by a factor of 1.8, which also affects the gait of the walker. To accomplish the parameter matching task, the iterative parameter scaling technique from section 2.3 will be used. Each parameter from Table **4.1** was scaled, with an example of the Leg length scaling being shown in Figure 4.1.

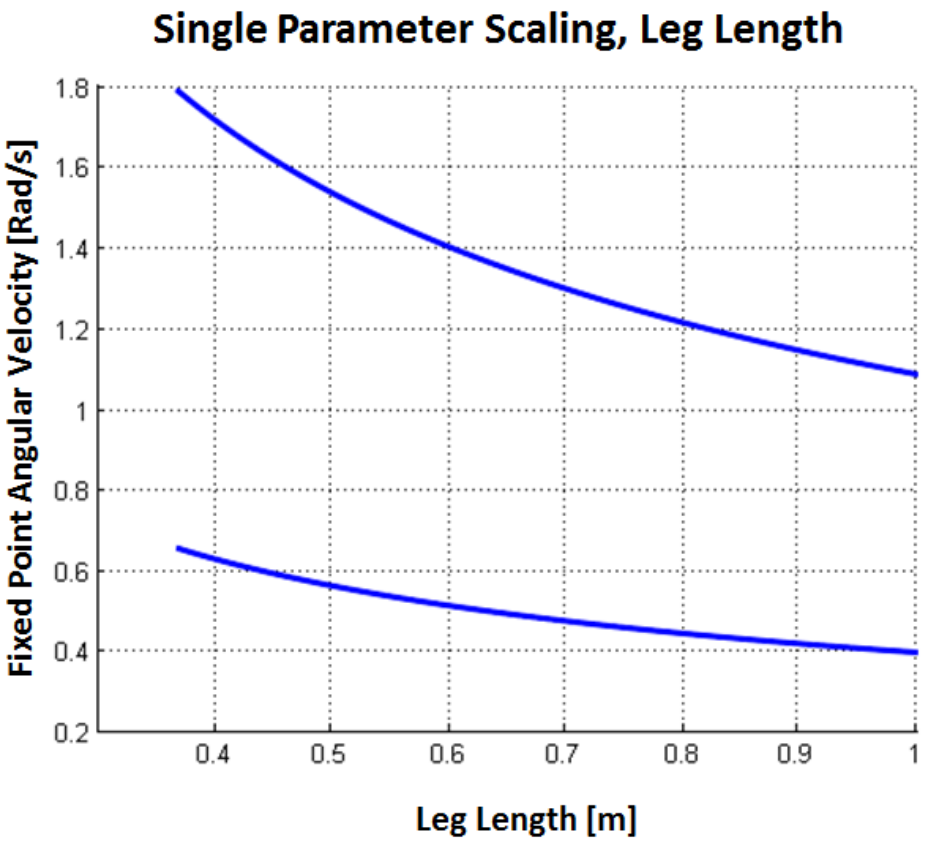

Figure 4.1: Walker Fixed Points as a Function of Leg Length

After short iteration process both the leg length and mass ratio were modified from the baseline parameters to account for changes in the experimental setup. Since the leg lengths *b* and *a* remained the same (with respect to L), they did not need to be scaled. The individual mass values can also be scaled without changing the gait, as long as the mass ratio is the same, so the experimentally derived mass values were input into the model directly with the experimental walker's mass ratio. With the updated parameters, we end up with a stride function and a basin of attraction for a stable walking gait as shown in Figure 4.2 and Figure 4.3, with a benchmark ramp angle of γ = 0.05 rad. We note that the step period of the stride changes considerably (compared to Figure 2.5), but the basic stride function of the walker remains visually similar to the results in [1] [38] [39]. This is reasonable, because a shorter stride length is shown to have shorter step periods in [1] and [2]. It is also expected that the simulation setup can produce a stable walking gait considering the experimental setup was able to produce a stable walking gait using the same parameters.

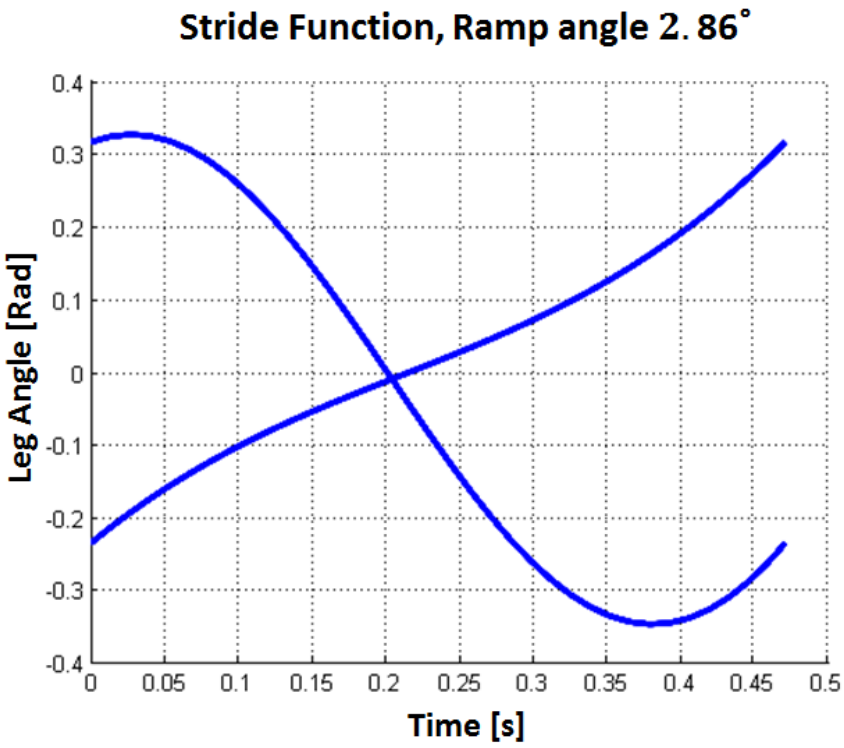

Figure 4.2: Stride Function, Using Experimentally Derived Mass Properties

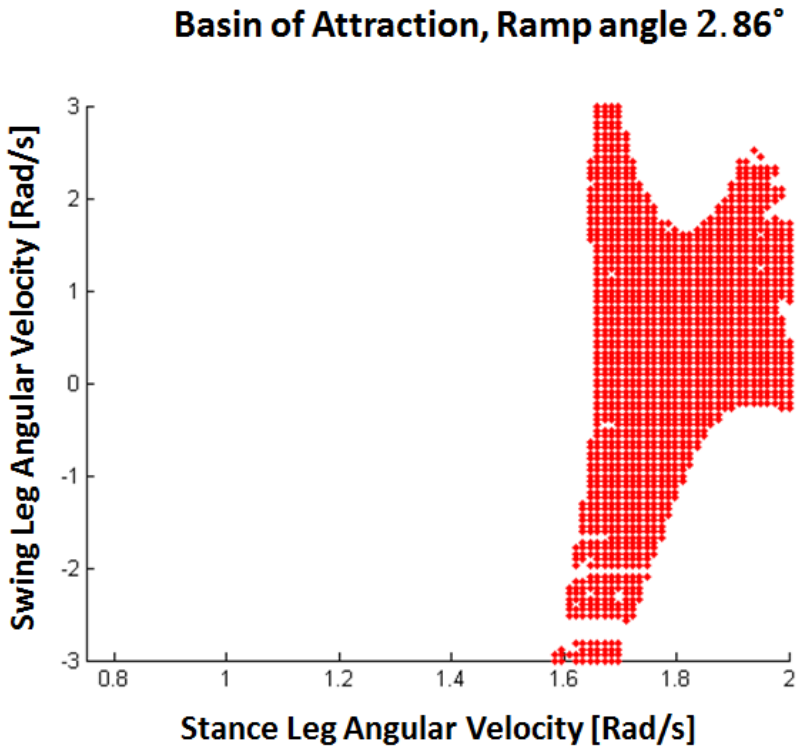

Figure 4.3: Basin of Attraction, Using Experimentally Derived Mass Properties

These outputs show that for the experimental NK-Walker with a moderate ramp angle (2.86˚), there is a small yet physically attainable period-1 gait cycle with a basin of attraction characteristic of a typical passive walker [39]. For selected geometry we find that the peak stride length is 7.99”, with a step period of 0.474s, and the following fixed point:

$$[\overrightarrow{\theta_i}, \overrightarrow{\omega_i}]^* = \begin{bmatrix} -0.2460 & 1.7523 \\ 0.3460 & ' 0.6316 \end{bmatrix}$$

From the result above, we see that the walker model has been successfully scaled to the parameters of the experimental setup. From this fixed point with high ϵ iteration using the iterative parameter scaling technique in section 2.3, a fixed point was also found at 2.29˚, as shown in the table below. To compare these to experimental results, the walker was first tested in simulation, then the walker was walked ∼5 steps with the experimental setup. The values of stride length L_s and step period τ_s were compared as shown:

Table 4.2: Gait Parameters Comparison for Experimental and Simulation Models

Angle *γ*	Model	Physical Walker
2.86˚	*L_s = 7.99”, τ_s =0.474s*	*L_s = 8.0”± 0.1”, τ_s =0.492s ± 0.041s*
2.29˚	*L_s = 7.44”, τ_s =0.470s*	*L_s = 7.6” ± 0.1”, τ_s =0.451s ± 0.041s*

Comparing these values, it’s clear that the walker model has a strong correlation to the experimental setup with both the absolute value of the step length and step period being very close for the same ramp angle. It should be noted that the chosen geometry (from the model) exhibits a variation of stride length with ramp angle, which is documented well in [2] and in [30]. The error of measurement is small enough on the experimentally measured stride length to agree with this trend. In terms of step period, there is no trend noted in the simulation results, and the experimental results (factoring in the error measurement) also agree with this. Overall, these results would indicate that the walker model in its passive form can provide a valid approximation for the performance of the experimental walker, which allows for iterative optimization and testing of the model. Since the model has been validated, the next step is to explore the passive side of the walker in the simulation domain to gain an understanding of its

dynamics prior to actuation. To start this process, a small parametric study is done on the walker, such that multiple gaits can be easily studied.

4.2 Parametric Study of Proposed Model

When the walker was tested in Section 3, it became abundantly clear that the work involved in establishing a stable walking gait, with little quantitative knowledge of the walker's passive dynamics, becomes a daunting task. The need to accurately set the lift pads and match the initial conditions of the walker make it nearly impossible to get the walker to produce a stable gait without repeated runs and video analysis of the walker as the gait fails. With a good parameter matched simulation model, many of the variables of the walking gait are removed (in the simulation domain) and it becomes much simpler to investigate the walker's behaviour at different ramp angles. This means that it is possible to characterize several stable gait cycles in the simulation domain, then go back to the experimental walker and set a *launch target* (of a specific set of initial conditions, stride length, and ramp angle) in order to make the walker physically produce a stable walking gait. If the values of the fixed point were not available, launching the walker becomes very difficult as there are four parameters that can be varied: the stance angle θ_S , stance leg initial angular velocity $\dot{\theta}_1$, swing leg initial angular velocity $\dot{\theta}_2$, and the ramp angle γ.

When looking at the basin of attraction of the walker, it is clear that these four parameters span an oddly shaped and rather complex basin of attraction where: $\theta_S = f(\dot{\theta}_1,\dot{\theta}_2,\gamma)$. When launching the walker, there is uncertainty in $\dot{\theta}_1$ and $\dot{\theta}_2$ as there is no simple way to control the angular velocities of the links when launching, so this makes it very tough to produce a stable gait for a walker without a known set of initial conditions. If the conditions are known however, the value of γ can be carefully set to match the model, and the value of θ_S can be controlled via markings on the walking surface to give a visual guide for the launching stride length. This only leaves the angular velocities to adjust, which can be subtly adjusted over a large number of launches to identify the correct technique required to hit the fixed point velocities when releasing the walker. This type of launch target is especially important in the case of the NK-

Walker, as the walker requires lift-off pads to be placed such that toe scuffing does not occur at the *equal angle* point of the gait. These pads require a fairly accurate knowledge of the fixed point stance angle θ_S of the gait so that they can be spaced apart by the stride length L_S. In order to assist with launching the walker, the next step is to then produce curves of fixed points such that a variety of ramp angles can be tested with all of the launch target values known. The curves for $[\overrightarrow{\theta_i}, \overrightarrow{\omega_i}]^*$ as a function of Y are listed in Figure 4.4 and Figure 4.5 respectively.

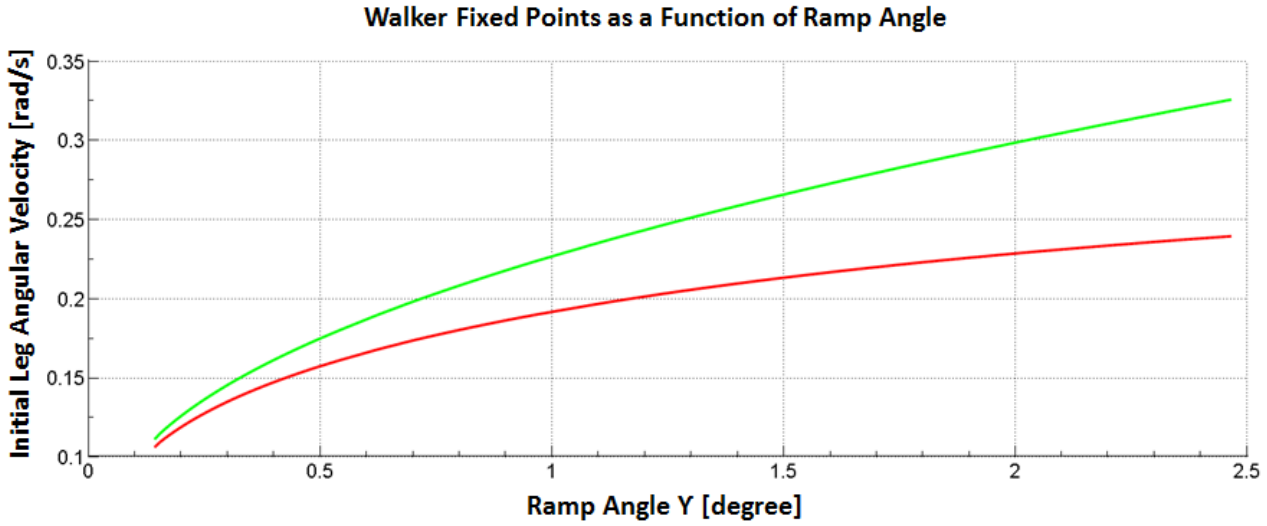

Figure 4.4: Fixed Point Leg Angles as a Function of Ramp Angle

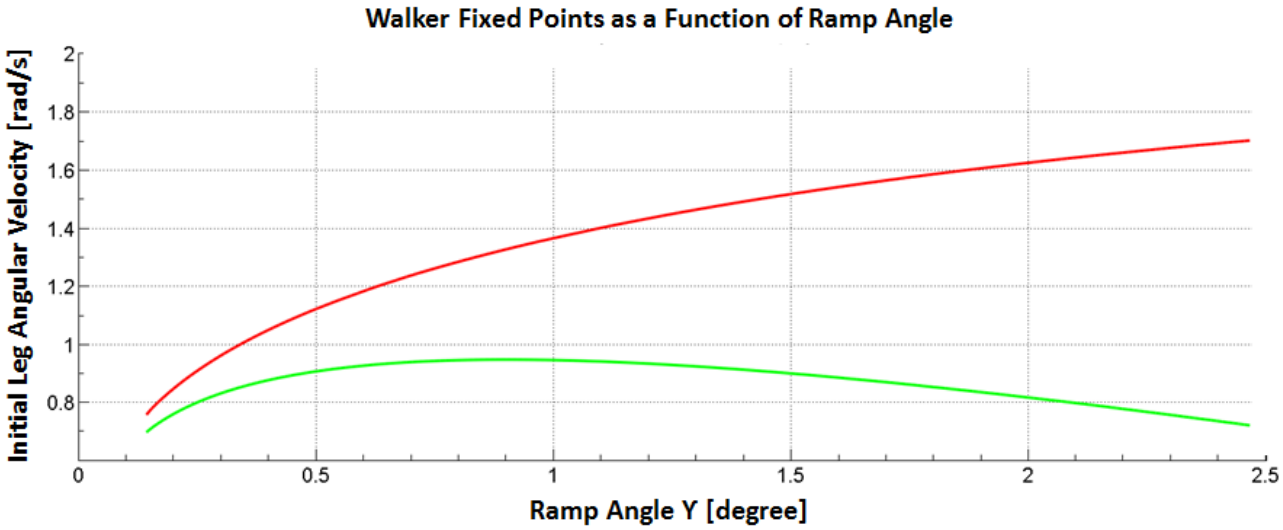

Figure 4.5: Fixed Point Leg Angular Velocities as a Function of Ramp Angle

From these curves, we see that the fixed points for θ_1 and θ_2 decrease somewhat linearly from about 1 degree to 2.5 degrees with a sharp taper off after that. This means that the stance angle θ_S (the sum of the two curves) also decreases linearly. With the passive dynamics of the system reasonable characterized, the next step is to introduce some level of actuation into the model to study the effects of varying levels and cases of MTGE based actuation.

4.3 Actuation Case Studies

With the basics of the passive portion of the model covered, and the model parameters scaled to match an experimental setup, the last step in the model is to test the actuation portion of the model to see how the walker behaves. Since the model bears a strong correlation to the physical walker, the actuation behaves in a predictable way (as tested in section 3), and does not add significant joint impedance to the system. This means that simulation testing is a reasonable approach to use to explore the actuation dynamics. In the theoretical model, the difficulty in "launching" the walker is not present as there is no disturbance built into the initial conditions of the walker, i.e. if the basin of attraction for the walking gait fixed point collapsed into a single point, the theoretical model would still be able to produce a walking gait. In the case of actuation and studying the behaviour of the actuated system, the key point is that the trends do not necessarily have to be physically achievable via the current experimental setup to be valuable, as the goal of the study is to provide insight into the behaviour of a system. With this in mind, the first step is to try a single actuation at the heelstrike event via a simple MTGE, as this is the simplest way to actuate the walker.

For actuation system, there are two basic positive outcomes that could arise from energy injection: the gait of the walker changes in terms of speed/stride/period, or the basin of attraction changes. If the basin of attraction of the walker increases, the result is desirable as it indicates that the energy from the actuation system is making the system more stable and therefore easier to launch/implement. This would drastically affect the efficiency, as the size of the basin of attraction is not included in the non-dimensional cost of transport C_t, however the energy input into the system affects this value negatively. It the case of a modified gait, the cost of transport is affected both positively and negatively in combination with the increase in

energy use, so there is a chance to keep the walker at the same or comparable efficiency as a purely passive system. To test this, the simplest method is to select an angle with a known set of fixed points where the walker produces a reasonably large basin of attraction but is on the lower end of the feasible walking angles. In this case, 2.29˚ (0.04 rad) is a good angle to start with. For this angle, the C_t = 0.040 and the fixed point is given by:

$$\left[\overrightarrow{\theta_i}, \overrightarrow{\omega_i}\right]^* = \begin{bmatrix} -0.2348 & 1.6733 \\ 0.3148 & ' 0.7595 \end{bmatrix}$$

In order to test actuation, *L(ω)* was linearly increased from 0.00 in increments of 0.001 *kg-m^2/s* and using the same scheme for iteration as the parameter scaling approach followed earlier in this section.

4.3.1 Simple MTGE Testing, Stance Point Impulse

To do an initial study of MTGE actuation, a simple actuation procedure was tested where only stance point actuation was used. Since the goal was to increase the energy in the system, only positive polarity actuation was tested. It was found that 0 < *L(ω) < 0.05 kg-m^2/s* produced walking gaits with reasonable basins of attraction, and any impulse beyond ~0.05 *kg-m^2/s* resulted in large reductions in the basin of attraction size. The BOA's for two extremes of actuation, at 0.00 *kg-m^2/s* and at 0.05 *kg-m^2/s,* are shown in Figure 4.6 and Figure 4.7 respectively. These figures were generated using a mesh of initial conditions and testing if they produced a limit cycle gait. Any red point is one that belongs to the BOA of the stable walking gait. Comparing the change in fixed points, we note little stance angle variation:

$$\left[\overrightarrow{\theta_i}\right]^*_{L(\omega)=0.00} = \begin{bmatrix} -0.2348 \\ 0.3148 \end{bmatrix}$$

$$\left[\overrightarrow{\theta_i}\right]^*_{L(\omega)=0.025} = \begin{bmatrix} -0.2352 \\ 0.3152 \end{bmatrix}$$

$$\left[\overrightarrow{\theta_i}\right]^*_{L(\omega)=0.05} = \begin{bmatrix} -0.2369 \\ 0.3169 \end{bmatrix}$$

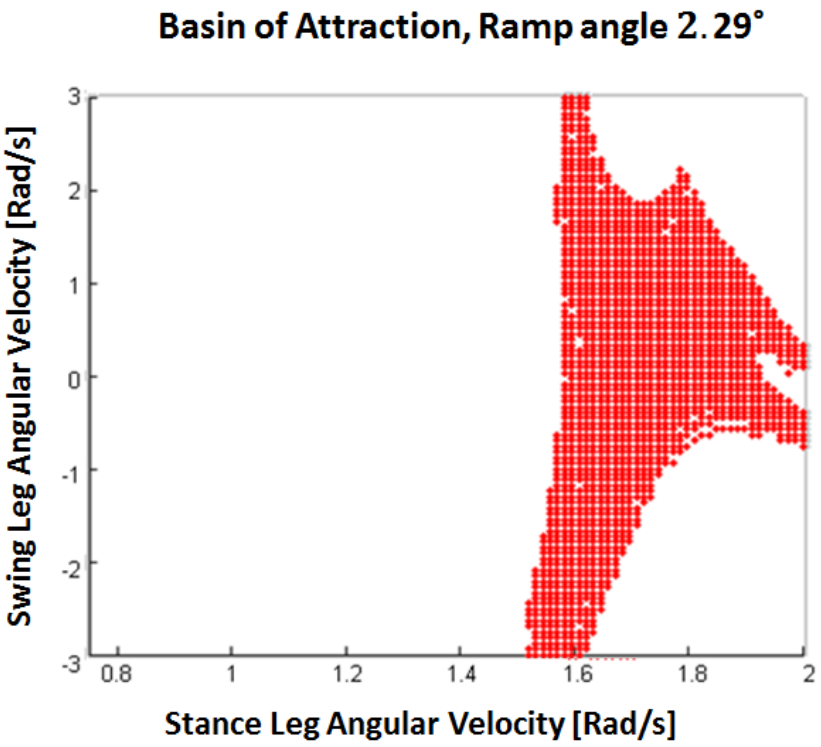

Figure 4.6: BOA at 2.29˚, Stance Impulse, L(ω)=0.00 kg-m^2/s

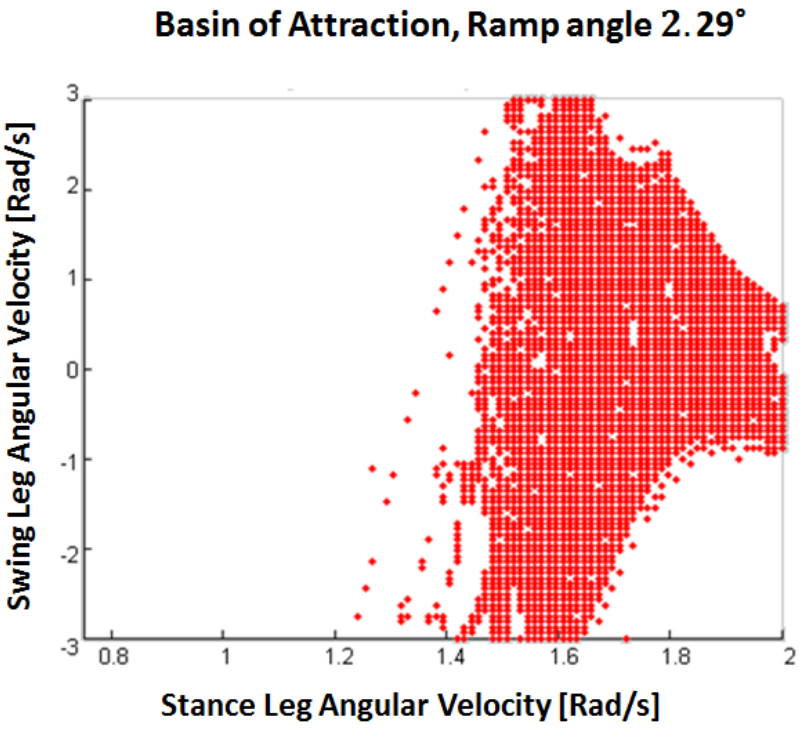

Figure 4.7: BOA at 2.29˚, Stance Impulse, L(ω)=0.05 kg-m^2/s

From the fixed point values, it's noted that the stance angle θ_S does in fact increase but only by a relatively small amount (~1%). When comparing the step period, it is also found that the period stays relatively fixed at ~0.45-0.47s with a variation of 4.5% between the unactuated and fully actuated cases at steady state walking fixed point. In terms of the basin of attraction, however the change is rather pronounced, where a large number of IC's are now included in the basin of attraction, which would otherwise not produce a stable gait. This has two effects, one is that the system has a larger stability region; the other is that the robustness of the system has increased in terms of handling disturbances in the angular velocities. This may seem like a trivial gain, but in the case of a physical walker, the stride to stride interaction with the ground has a significant amount of variability. This means that even if the walker is launched perfectly, the small imperfections in the ground and variations in ramp angle can cause the gait to swing outside of the stability region relatively easily. In order to mitigate this when designing the experimental walker, a large push was made to create a very solid impact event to minimize this variation. This results in high loads throughout the walker and very sharp point feet which limits the real world application of the walker substantially, as the walker requires minor surface penetration in order to keep the feet from moving. This is often not possible in real world use, but is used simply to provide a stable test platform. With a more robust system, more compliance could be added to the system in order to make the walker easier to launch and able to produce more versatile gaits. The negative side to an increase in BOA size is that the system efficiency will have clearly dropped (as discussed later in this section) due to additional energy being injected into the system with negligible changes in the walking gait.

One point worth noting from the above plots is that the experimental walker is unable to provide actuation higher than the peak value of $L(\omega) < 0.02$ kg-m^2/s, so although the model can predict the results at higher magnitudes, the feasible level is less than half of that. Shown in Figure 4.8 is the more realistic actuation level of $L(\omega) = 0.025$ kg-m^2/s, which is attainable with the addition of some small inertial weights on the walker.

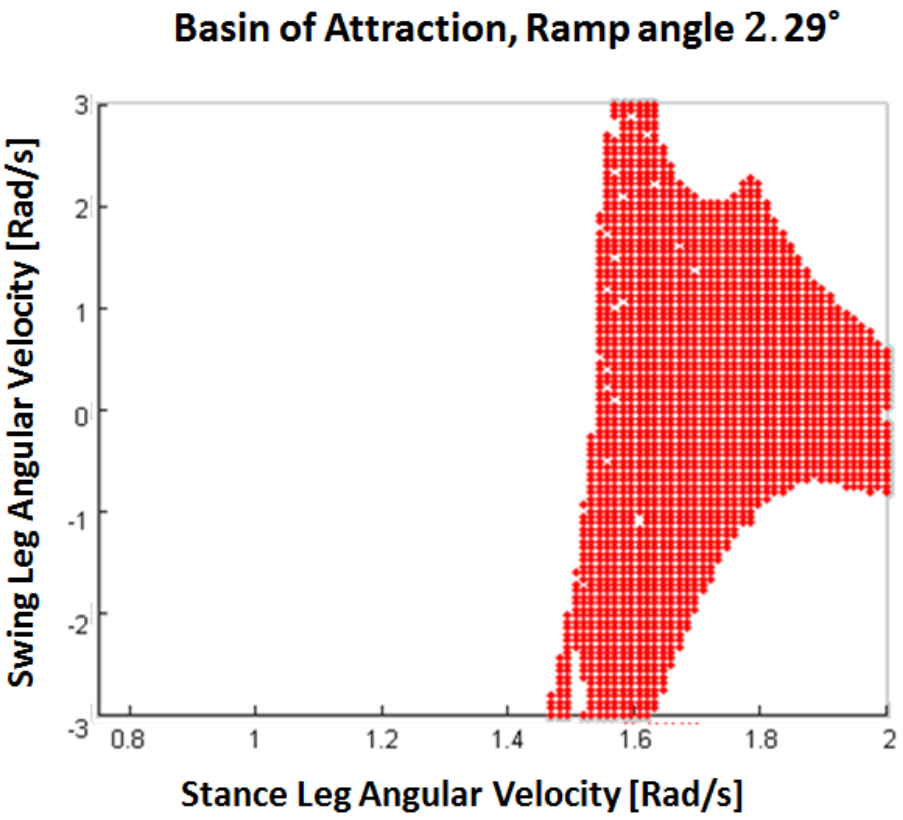

Figure 4.8: BOA at 2.29˚, Stance Impulse, L(ω)=0.025 kg-m^2/s

Although the BOA at *L(ω) = 0.025 kg-m^2/s,* is not as large as the BOA for *L(ω) = 0.05 kg-m^2/s,* the result still shows a measurable improvement over the unactuated case. Next, the penalty on the non-dimensional cost of transport of these cases can be calculated. We note that each one carries the following cost:

$$L(\omega) = I_a \frac{T_0}{K_t}$$

$$E_{Input} = \frac{1}{2} I_A \omega_t^2 = \frac{I_A}{2} \left(\frac{T_0}{K_t}\right)^2$$

$$C_{et} = \frac{E_{Input}}{m_s g L_s} = \frac{I_A \left(\frac{T_0}{K_t}\right)^2}{4Lsin\left(\frac{\theta_S}{2}\right)(m+2M)g}$$

$$C_{mt} = \frac{m_s g L_s sin(\gamma)}{m_s g L_s} = sin(\gamma)$$

$$\therefore\ C_t = C_{et} + C_{mt} = \ sin(\gamma) + \frac{I_A \left(\frac{T_0}{K_t}\right)^2}{2L_s(m+2M)g}$$

From these equations it's noted that the fully passive system at $\gamma = 0.04\ rad$ has a C_t = 0.040. Using the value of $L(\omega) = 0.025\ kg\text{-}m^2/s$ and $\omega_t = 339\ rad/s$ from section 4, we find that I_a would need to be increased by 7.6% to $I_a = 7.37 \times 10^{-5}\ kg\text{-}m^2$. This means $E_{Input} = 4.23J$. Therefore $C_{et} = 0.237$ and $C_t = 0.278$. Now although this figure seems substantially higher than the passive walker alone, some of the most notable active/passive walkers have a $C_t > 0.25$ as discussed in section 1. The case chosen in this example is also the case where the actuation system is least efficient i.e. the stride length is not changing measurably and the energy injection is only providing an increased basin of attraction. From these results, we can see that a K walker with a simple MTGE actuation at the heelstrike event, at a moderate ramp angle where there is sufficient energy in the walker, can accept $L(\omega) < 0.05\ kg\text{-}m^2/s$, of actuation. The result of this is to measurably increase the basin of attraction with $0.04 < C_t < 0.44$.

One very important note from this section, however, comes from the definition of the $L(\omega)$ actuation efficiency. From the previous equations, it can be seen that the magnitude of $L(\omega)$ is proportional to ω and I_A, so for any given value of $L(\omega)$, a much larger value of I_A can be used to reduce the value of ω_t required during actuation. However, when looking at the energy term, we note that the proportionality changes to ω^2. As a case study of this, the $L(\omega) = 0.025\ kg\text{-}m^2/s$ case can be used as an example. If I_A is increased by 12 fold to $8.844 \times 10^{-4}\ kg\text{-}m^2$, then ω_t = 28.25 rad/s. This in turn decreases the value of E_{Input} to only 1.01J, which is a decrease from before of 74%. This means for a 15 fold increase in I_A, C_{et} drops by 74% down to 0.0612, which leads to a C_t of 0.101. This value is substantially lower than most notable active-passive walkers in literature, again in the worst case in terms of efficiency of this specific walker.

To evaluate the feasibility of such a change in inertia, one could simply look at the idea of using annular weights on the hip. With the hipshaft of the walker being 6.35 mm in radius (r_1) and with 25.4mm of length L_W on either side of the walker (between the legs), we see that a pair of annular tungsten weights ($\rho \approx 19{,}250\ kg\text{-}m^3$) would have the following inertia:

$$I_w = \rho \pi L_W (r_2{}^4 - r_1{}^4)$$

If this is solved for the 15 fold increase of inertia from before, we find that weights of approximately 24.02mm diameter are required, which adds a total floating mass of 0.31 kg to the walker. In terms of the time constant of actuation τ, it increases to 104ms, which is still a very reasonable value of τ for a gait with a period of ~0.47s; especially considering ω does not have to reach ω_t with the increased inertia. In terms of the physical model, although it would be relatively simple to add on inertial weights, one of the goals of the original design was to have the walker compatible with a wide range of gaits initially to test the design. The principle of the proposed hybrid model is that the difference between a large inertia low velocity actuator and a small inertia high velocity actuator can easily be modelled, so a change in these properties does not drastically affect the model or its validation. So with that said, although the possibility exists to lower the physical C_t, the physical walker actuation properties will be left as is to continue exploring gait parameters with the potential for future optimization for specific gaits.

4.3.2 Complex MTGE Testing, Equal Angle Point Impulse

With the equal angle case explored extensively at a single angle, the next step is to explore the addition of a complex MTGE at the equal angle point in the gait. Since this was already setup in the previous sections as a part of the model, it becomes simple to test various magnitudes of it. Since the study on the simple MTGE case used the ramp angle γ = 0.04rad, the same angle can be used for the complex MTGE case. In the same way as in the previous case, the first thing to do is to use the single parameter modification iteration approach to figure out an upper bound to the magnitude of a positive polarity *L(ω)* complex MTGE at the equal angle point. With the simple MTGE even disabled, it was found that only $L(\omega) < 0.01\ kg\text{-}m^2/s$ of angular momentum could be added before the basin of attraction became so small that physical walking would have been unfeasible. The BOA plots of these cases are shown in Figure 4.9 & Figure 4.10 respectively, with the fixed points of the gaits shown immediately following Figure 4.9 & Figure 4.10.

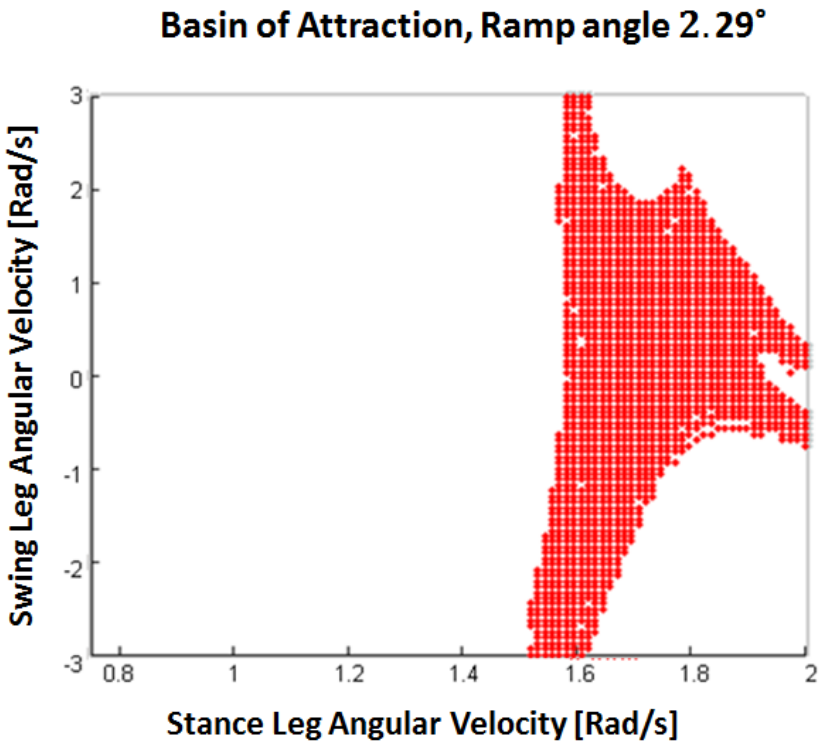

Figure 4.9: BOA at 2.29˚, EA Impulse, L(ω)=0.00 kg-m^2/s

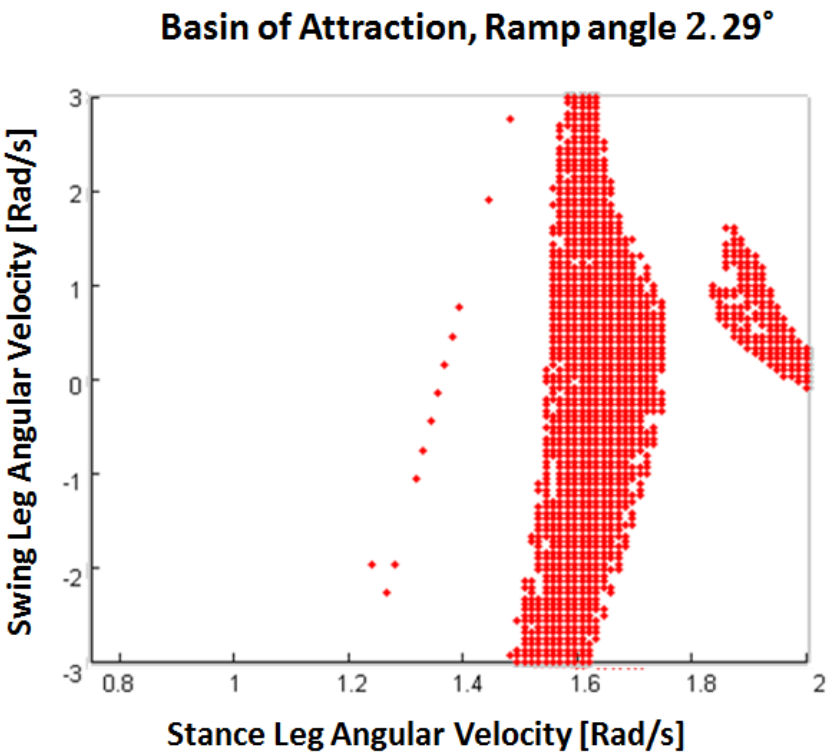

Figure 4.10: BOA at 2.29˚, EA Impulse, L(ω)=0.01 kg-m^2/s

$$\left[\overrightarrow{\theta_i}\right]^*_{L(\omega)=0.00} = \begin{bmatrix} -0.2348 \\ 0.3148 \end{bmatrix}$$

$$\left[\overrightarrow{\theta_i}\right]^*_{L(\omega)=0.01} = \begin{bmatrix} -0.2383 \\ 0.3183 \end{bmatrix}$$

$$\left[\overrightarrow{\theta_i}\right]^*_{L(\omega)=0.02} = \begin{bmatrix} -0.2316 \\ 0.3116 \end{bmatrix}$$

From these plots it's clear that the complex MTGE produces substantially poorer results than the simple MTGE taking place at the heel strike. We see that the behaviour of the walker is similar in terms of stride length (small, largely insignificant increase) and step period (more or less the same) for *L(ω) < 0.01 kg-m^2*. Above that point we see the stride length decreases and there was a notable reduction in BOA that resulted in a walking gait fixed point that would not be physically realizable. It was also noted that most of the gait cycles for *L(ω) < 0.01 kg-m2* had a 2 cycle periodic form, which is not a desirable quality in the walker. An example of this is shown in Figure 4.10, where the split BOA represents two different fixed points for the same gait cycle that alternate from step to step. In general we note that the effect of injecting energy via the EA impulse is to decrease the BOA substantially and increase the stride length marginally. Since the energy input and efficiency calculations are identical to the previous analysis, the C_{et} can be stated as 0.0034, and C_t can be stated as 0.043 in the case of *L(ω) = 0.01 kg-m^2,* with a semi optimized I_A = 8.844x10^{-4} *kg-m^2* and *ω_t= 11.31 rad/s*.

Based on the comparison of results of the simple MTGE vs the complex MTGE shown above, it's very clear that the complex MTGE does not actuate the system effectively, nor does it produce a positive result on the system. This is likely because the injection of energy at mid stride alone causes a jump in energy at a point in the walking gait where it has diminished stability, disrupting the passive dynamics of the walker. This is, as noted in section 3, one of the fundamental drawbacks of this actuation method, as there is no way to determine exactly why the actuation at that point alone is not effective without more information about the system dynamics.

With the two basic cases tested, a simple option exists for a third test case: to combine the two types of actuation and see if a positive result can be gained by injecting energy at both points. This is a fundamentally different actuation type than either point alone as the walker

would have a higher energy when crossing the equal angle point due to the simple MTGE, which could result in substantially different actuation effects.

4.3.3 Combined MTGE Testing, Stance and EA Impulse

Since the EA impulse case was shown to produce poorer results, the concept of the third test case is to combine case 1 and 2, and have two points of energy injection into the walker. In general this concept could be evolved to include multiple complex MTGE's so this test is just an example of the most basic form of a multi MTGE injection system. To have the results directly comparable to the previous cases, the same ramp angle as the previous cases (γ = 0.04rad) will be used, and two separate MTGE's were defined, with an independent value of $L(\omega)$ for each. For the simple MTGE at heel-strike, $L(\omega)$ would be held at the peak value of $L(\omega) = 0.05\ kg\text{-}m^2$ from the previous case. This means that the most energy possible is injected into the walker at heel strike. For the complex MTGE, the value of $L(\omega)$ was increased from zero actuation up to the maximum that the walker model would take while still producing a stable walking gait. It was found that $L(\omega) < 0.01\ kg\text{-}m^2$ produced stable gaits, but with $L(\omega) = 0.005\ kg\text{-}m^2$ producing the best results from the $\Delta L(\omega) =$ 0.0025 spaced grid of values tested. Although further optimization would be possible by then redoing the study with a grid of values of $L(\omega) < 0.05\ kg\text{-}m^2$ for the stance impulse, the simplest case will be studied as an initial view of the effects of complex/simple MTGE actuation with the potential for future work to expand the scope of the research. The actuation study resulted in the following fixed points, and the respective BOA's shown in Figure 4.11 and Figure 4.12.

$$\left[\overrightarrow{\theta_i}\right]^*_{L(\omega)=0.000} = \begin{bmatrix} -0.2369 \\ 0.3169 \end{bmatrix}$$

$$\left[\overrightarrow{\theta_i}\right]^*_{L(\omega)=0.005} = \begin{bmatrix} -0.2384 \\ 0.3184 \end{bmatrix}$$

$$\left[\overrightarrow{\theta_i}\right]^*_{L(\omega)=0.010} = \begin{bmatrix} -0.2211 \\ 0.3011 \end{bmatrix}$$

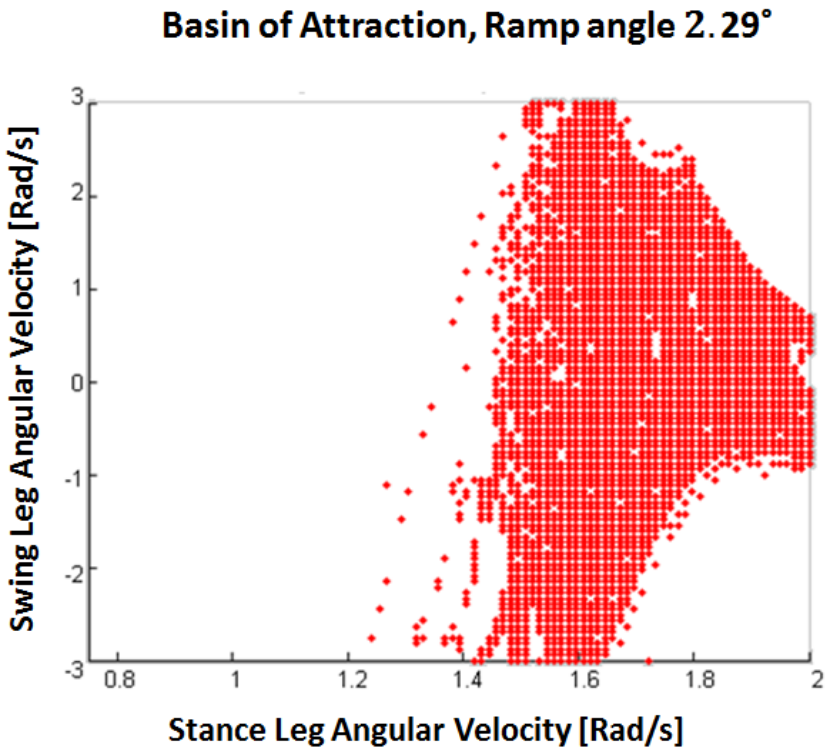

Figure 4.11: BOA at 2.29˚, L(ω) = 0.05 kg-m^2/s (Stance), L(ω) = 0.00 kg-m^2/s (EA)

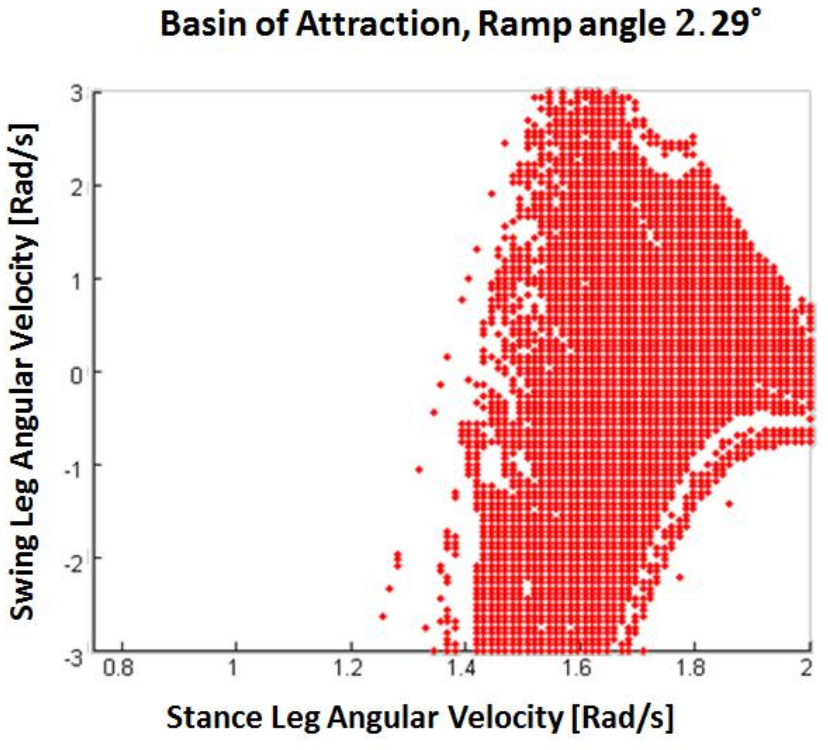

Figure 4.12: BOA at 2.29˚, L(ω) = 0.05 kg-m^2/s (Stance), L(ω) = 0.005 kg-m^2/s (EA)

The results from this case present an unexpected result compared to the previous two studies. Since the simple MTGE case produced positive results, and the complex MTGE case produced negative results, it is logical that the end result would be a combination of those two effects. Since the model behaviour is governed by very complex non-linear dynamics, the actual effect of the combination of the two actuations is much more complex. The end result, as can be seen from the BOA plots above, is that the addition of a complex MTGE at the equal angle crossing point actually increases the BOA of a stable walking gait, again without effecting the stride length or step period significantly.

For the efficiency of this actuation, some small adjustments must be made to previous estimates, as the value of ω decreases for the second MTGE due to less energy being put into the system, considering that I_A cannot be changed mid stride without a more complicated physical system with variable I_A. For the simple MTGE, we take the value of $I_A = 8.844 \times 10^{-4}$ *kg-m*^{2} from previous simple MTGE case, which requires $\omega = 56.28$ *rad/s* in order to get $L(\omega) = 0.05$ *kg-m*^{2} for the first actuation event, and with I_A held constant, we see that $\omega = 5.63$ *rad/s* for $L(\omega) = 0.005$ *kg-m*^{2} in the complex MTGE case. This results in a total E_{Input} of 1.42J, which results in a $C_{et} = 0.086$, and a $C_t = 0.126$, which is still exceptionally low.

Compared to the previous cases, we see that this case carries the highest cost of transport, but as discussed earlier there exists the possibility of optimization in this case. Unfortunately, due to a lack of higher order characterization in the chosen model from a lack of a closed form, the system dynamics become very complex, and in turn the 2 parameter optimization problem becomes much more complex than a simple linear system. In a simple linear system, if the dynamics are known, the effect of one parameter can be studied, and the effect of the second parameter can be studied independently. The results can either be combined via superposition (on some systems) for an accurate characterization. In the case of a highly non-linear system, the complexity in the system dynamic means that each possible combination of parameter values can have a drastically different effect. This means that substantial research can be done on interaction of the two types of MTGE's to find an optimal point in future research. To compare the final actuated result with the initial BOA, both plots are overlaid below, with some of the outlier points removed for clarity.

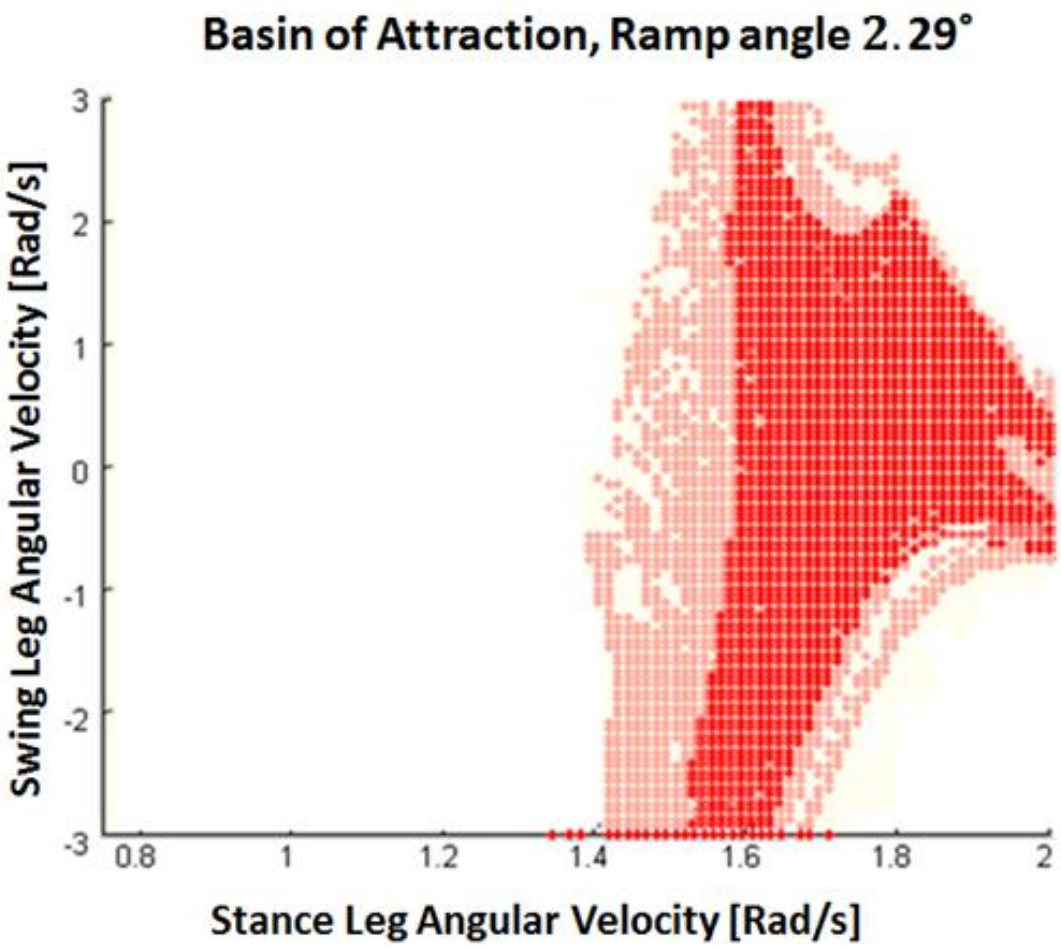

Figure 4.13: BOA at 2.29˚ with Stance and EA impulse vs. Unactuated

From this image we see that there is a 38% increase in the BOA of the actuated system (dark) vs the original system (light) at the peak width point where swing leg initial velocity is ~ 0 rad/s. Considering that the non-dimensional energy cost for this extra robustness/stability is only 2x the walking energy cost, this can be viewed as a very reasonable result, especially considering the passive dynamics of the system are clearly maintained due to the similarity in stride length and step period. One application of this would be to use the actuation method as a control output for a stability control system to assist in launching the walker, but could theoretically be disabled once the walking gait fixed point is reached. This is primarily driven by the benefit that fixed point from the mixed mode actuation is so similar to the fixed point for the un-actuated system that they both lie in overlapping BOA's. This means that a steady state system (that is already converged to the fixed point) can theoretically remain in the overlapping

region and transition from actuated to unactuated without large changes to the system dynamics. This type of "removable actuation" system is one of the main advantages of using an active/passive system, as there is the potential for the system to retain the original dynamics (at a 3 fold efficiency increase) or slightly modified dynamics (at a 3 fold efficiency decrease). Overall, this is a very useful result, because the stride length and step period of this system at the ramp angle of $\gamma = 0.04rad$ are considered to be very reasonable for a passive walker. This also correlates well to one of the favourable simulation outcomes, which is the expansion of the characteristically small BOA of the passive gait.

4.3.4 MTGE Actuation Overview

Between the three cases a wide variety of actuation dynamics have been shown, all at a moderate ramp angle of $\gamma = 0.04rad$. In the case of a simple MTGE, the system responds without a significant change in gait quality, and the overall walking gait character stays roughly the same (Froude Number, Fr $\approx$ 0.231) but with a greatly increased BOA. In the case of a complex MTGE it was found that the gait character did not change much (Fr $\approx$ 0.231), but the BOA area shrank rapidly as energy was injected. In the case of combined actuation, the dynamics of using a stance impulse and an EA impulse with a 10:1 ratio on the magnitude resulted in the dynamics of the system remaining the same (Fr $\approx$ 0.231) but with a substantial increase in BOA ($\sim$38%). For all three cases, the approximate peak energy cost remained under 2x the passive walker energy usage, with an overall C_t of 0.126 for the combined actuation case. With the basics of the MTGE Dynamics worked out at a benchmark angle, the next step is to evaluate the dynamics over a large range of angles to see if the behaviour of the system varies substantially.

4.4 Characterization of Hybrid System Dynamics

The next step in studying the hybrid system is to characterize the behaviour over a large number of ramp angles. Going back to the initial fixed point curve, we can now run an alternate set of curves to the original one to compare actuated/un-actuated cases. The initial curve (solid red) on Figure 4.14 shows the case where no actuation is used. When actuation is added, we have the line shown as the cyan dash-dotted line, where $L(\omega) = 0.01\ kg\text{-}m^2$ is injected at the

equal angle point in a complex MTGE. When further actuation is added, we have the line shown as the dashed blue line, where $L(\omega) = 0.005\ kg\text{-}m^2$ is added at the equal angle point in a complex MTGE and $L(\omega) = 0.025\ kg\text{-}m^2$ is added at heelstrike via a simple MTGE.

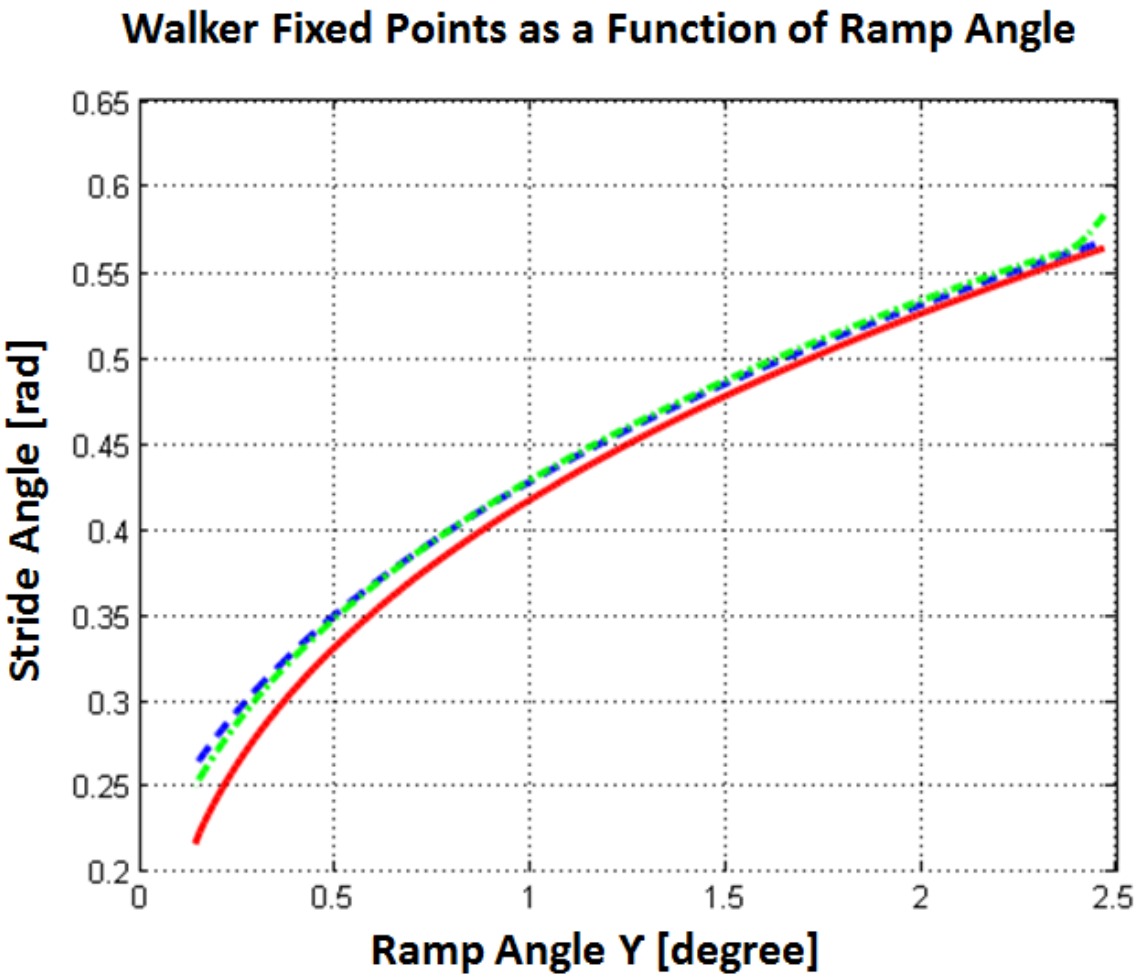

Figure 4.14: Actuated Test Cases, Walker Fixed Point Curves

We see that the behaviour is as expected for higher ramp angles, but as the ramp angles decrease, the divergence between the curves varies substantially, relative to the magnitude of the leg angles. At ramp angles as low as $\gamma = 0.11^{\circ}$, we see that the stride angle of the walker has increased over 29%, which is a substantial increase in stride length on the walker, compared to the < 1% change in the stride length at higher ramp angles. These curves provide initial insight into how the system behaves under actuation given the chosen parameters. At higher ramp angles, where the gait parameters of the walker are nearly ideal, most of the energy from the

actuation (via the simple and complex MTGE investigated) creates an increase in basin of attraction magnitude. At lower ramp angles where the stride length is small (undesirable), the injection of additional energy produces gaits with longer strides, which means that the energy injection is working to add energy directly into the system dynamics. Although this behaviour is very beneficial, one of the large complications resulting from the use of this type of actuation is that there is little to no control on this. From the magnitude of energy injection, one of the many different fixed point curves can be picked, but unless different types of MTGE's are tested there is no way to control how the curve is specifically shaped. The solution to this would be to try and describe the behaviour of the system via higher order dynamics (such as using conventional stability theories), but the mathematical complexity in those approaches is substantially out of scope of this research. Therefore, the simplest approach is to merely study the extreme cases of the actuation (at $\gamma = 0.04$ *Rad and* $\gamma = 0.002$ *Rad)* and draw general conclusions about the behaviour between the two. Since the behaviour at $\gamma = 0.04$ *Rad* is already described in detail above, the next step is to look at the BOA at the $\gamma = 0.002$ *Rad* case and put a figure to the efficiency of the actuation at that ramp angle.

Energy use in the 0.002 rad studies is based on an inertial actuator of $I_A = 8.844 \times 10^{-4}$ *kg-m*^{2}, with three different terminal velocities for the two different cases. For the case with just knee actuation and $L(\omega) =$ 0.01 *kg-m*^{2}, we have $\omega = 11.307$ *rad/s*, resulting in a total energy input to the system of $E_{Input} = 0.056J$. This results in a C_{et} = 0.0069, which causes the total cost of transport to be C_t = 0.0089, which is substantially lower than other active walkers in literature. When the energy input is increased via two separate MTGE's for the second case, we have the total energy injection increased to E = 0.509J. This results in a C_{et} = 0.0600. When coupled with the walker's passive energy requirements, we have C_t = 0.0620. In the case where no actuation is used, we have C_t = 0.002, which is substantially lower than both of the actuated cases. This result shows that the energy injection requires a fair bit of optimization, as the energy costs vary drastically even though the stride length only changes marginally between the two actuated cases.

From these results we see that the actuation system can provide a wide variety of responses from the system and generally be used to improve the system performance. In the

higher ramp angle cases, the walker stride length is already sufficient to produce a reasonable gait, and the energy from actuation is used towards increasing the side of the BOA. In the case of small ramp angles, the stride length is very small, and the 29% increase in stride length via actuation indicates that a large portion of the actuation energy is going directly into the kinematics of the walker.

4.5 Actuation Performance and Limitations

Now that the actuation of the walker has been carefully examined in simulation, the final step is to evaluate the performance of the walker and validate the simulation model. To do this, quite a challenge is presented based on two simple issues: the tolerance for the physical properties of the gait, and the tolerance of hitting the required initial conditions of the gait. At a ramp angle of 0.1˚, the stride length of the walker is only 2.92”, which is substantially smaller than the 7.44” gait that occurs at 2.29˚. At the larger ramp angle, however, the amount of energy injected into the gait is substantially higher as it is a function of:

$$E_{Input} = MgL_s \sin(\gamma)$$

The difference between the energy consumption at the 0.1˚ ramp angle case (0.0114J) and the 2.29˚ ramp angle case (0.711J) is staggering since more than 62 times the energy input is provided at the larger ramp angle. This is mathematically accounted for when considering the cost of transport for both cases as C_t is substantially higher for the larger ramp angle, at 20 times the non-dimensional cost of the 0.1˚ ramp angle case. Based on this, we can see a clear problem when energy loss is considered in the system: the physical system can afford almost no energy loss at a 0.1˚ ramp angle. In the experimental setup, each of the hip bearings has a small amount of friction associated with it, especially when under load, as do the clutches used to disengage the actuator from the walker. Looking at the ball bearings alone, based on the specified frictional loss for the 8 ball bearings supporting the hip shaft, there would be an average loss of 0.0168W of energy per stride. Comparing that to the power coming into the walker in the 0.1˚ ramp angle case (~0.0285W), we see that nearly half of the energy is consumed just by the rolling friction of the bearings. In the 2.29˚ ramp angle case, we see that

the bearing energy consumption is ~1.50W, with the frictional loss accounting for only 1% of the total energy injected into the stride. This means that at low ramp angles producing a passive walking gait itself is rather difficult. This means that the production of a walking gait stable enough that it can be tested with the hybrid active/passive actuation method is nearly impossible.

The next concern is the variation in the initial conditions of the gait. This poses a challenge not only in the low ramp angle cases, but also in the high ramp angle cases. On the passive high ramp angle (2.29˚) walker, we see a region known as the launch target (shown in the figure below), the centroid of which is the easiest set of initial angular velocities to start with. This is because the launch target centroid is approximately very near the fixed point of the walking gait and is the largest region of gaits that converge very quickly to the fixed point gait.

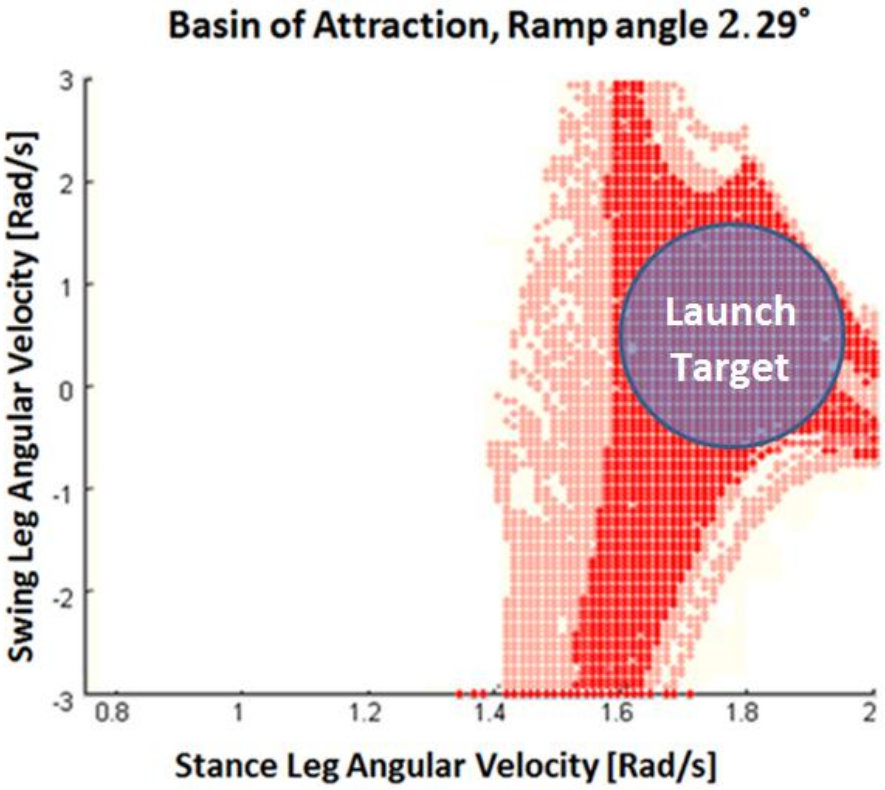

Figure 4.15: Launch Target of Walker, Actuated vs. Unactuated

We note that in order to hit this launch target, the initial conditions must be within the range of 1.5-1.9 rad/s for the stance leg and -1 and 1 rad/s on the swing leg. Of these two targets, the smaller region presented by the stance leg angular velocity is the tougher of the

two to stay within as the tolerance is only 0.4rad/s and both of the values are positive non-zero (as opposed to the simple launch goal of the swing leg angular velocity being 0 rad/s). After a few trial runs with the walker at this angle, the success rate of a walking gait can be seen to be between 10-25% depending on the condition of the lift pads and the condition of the walker (which deteriorates due to falls, scuffs and rounding of the feet). From a study using a simple test setup of an optical encoder and an individual leg from the walker, it was found that the total tolerance for launching with angular velocity of ∼1.0rad/s was somewhere around ±0.3rad/s, with the results improving with practice. What this means is that the results shown for the 2.29˚ case with actuation are very difficult to experimentally reproduce, as the increase in the size of the launch target window (although it increases by 38% at its peak) includes regions on either side of the main BOA where a more complex shape in the BOA exists. This means that although these regions could theoretically increase the basin of attraction, statistically it would be very difficult to measure given the low success rate of launching the walker.

Although both of these issues seem to put the theoretical results in a negative light, the real insight that is gained is the understanding of why a strong link between modelling and simulation is important: being able to see limitations from both the experimental and simulation models and understanding how to work around them. In the case of the first limitation, the energy efficiency of the walker, we can see that a substantially simpler system can be built, compared to the complex experimental prototype in this research, to purely test the actuation at lower ramp angles. The low energy injection levels and energy mean that substantially smaller actuators can be used, and much simpler clutch mechanisms can be utilized to drastically reduce the weight of the walker. Based on the preliminary bearing load calculations, the bearing drag can also be reduced by an order of magnitude by using carbon fibre shank components and a needle bearing setup, which is enough to reduce the bearing drag to only about 5% walker energy use at 0.1˚ ramp angle. Although this was not feasible on a first attempt at making the system, this result gives insight into how to develop the experimental test setup to allow for lower ramp angle walking/actuation. From the launch condition variance, we also note that a key experimental issue with the walker is the ability to

launch the walker with a controlled swing leg angular velocity. This is often overlooked in many passive cases as there are often no ways to subtly improve the stability of the walker. With the potential this research presents, this can be a design consideration for future research. A simple solution to this problem would be to use a launch frame or other jig that releases the walker with set starting velocities/angles such that a wide variety of initial conditions can be tested accurately. Looking at the graph above, we note that if swing leg angular velocity (initial) is kept at ~0 rad/s, an entire range of initial conditions can be tested for the stance leg: from 1.59 rad/s – 2.0 rad/s in the case of the unactuated walker and 1.42 rad/s-2.0 rad/s in the case for the actuated walker. We note that as long as the tolerance of the launching can be done with 0.05 rad/s or finer (±0.5rpm), then the increase in BOA could actually be measured and used as a simple form of validation for the overall system. In the case of the system as it is however, the complications that arise from the actuation performance mean that an alternate approach must be used to validate the system model.

4.6 Discussion of Experimental Testing with Actuation

Due to the technical issues presented by the wide number of actuation potentials, overall actuation testing of the experimental system was done via smaller tests. The first test is to check the walking model passively against the walker itself. This test was done near the start of section 3.5 , to show that the final walker was able to produce a gait with approximately step period and stride length as predicted by the model (with a peak error of 4% on the stride length)

The next step was to show that the actuators were providing energy input into the system in a measureable and controllable manner, and that the natural dynamics of the system were not affected. This was tested in section 3.4 with a simple check involving the natural frequency of the system. By energizing the system with different levels of energy injection the actuator impedance was measured by checking that the natural frequency of the system remained unchanged as it was actuated. The actuation impulse was also checked against the amplitude of oscillation to verify that the energy input into the system was as predicted. With these two validation tests, we can conclude that the walker behaves as modelled, passively, and that the actuator behaves as modelled.

This leads to a final test, which can be done for the overall system, by testing the extreme cases of actuation. We note from the 2.29˚ ramp angle case study that the walker can only accept a certain amount of energy in the form of hip actuation before the stability region drastically shrinks and the stable 1-Cycle walking gait disappears. From the case study, it was found that the limiting value for actuation was at $L(\omega) > 0.01\ kg\text{-}m^2$ applied as an actuation impulse, where the stability region of the walker diminished significantly and a two cycle gait was produced. Since the basin of attraction for this gait is so small and the stride length is not the same as the standard gait, we can use this as a simple test. If $L(\omega) > 0.01\ kg\text{-}m^2$ is applied to the system, we would expect that the walker would not be able to walk, which would mean that the effect of the actuation on the model has a close parallel with the physical system. To test this, the walker was held at a ramp angle of 2.29˚, and $L(\omega) = 0.00, 0.005$ *and* 0.011 were applied at the equal angle point of the stride. In order to measure the magnitude of $L(\omega)$ input, the system was placed at rest on a test stand and the motor was given time to reach full speed at different voltages, using an optical encoder to measure output from the motor. With both motors at near full voltage (22.9V) and using no modifications to the inertial weight of the walker it was found that and $L(\omega) = 0.011\ kg\text{-}m^2$ was achievable. By reducing the voltage to (15.15V) it was found that $L(\omega) = 0.005\ kg\text{-}m^2$ was deliverable, with no changes to the inertial weight. With the motors disabled, the setup could also test the no actuation case. With these three cases in mind, the walker was placed on the ramp with no changes between each setup. With no angular energy input it was found that the walker would walk ∼20% of the times it was launched without any obvious issues. In the $L(\omega) = 0.005\ kg\text{-}m^2$ case, the walker seemed to have no issue launching, with the same approximate success rate (∼20%) as the unactuated case. In the $L(\omega) = 0.011\ kg\text{-}m^2$, it was found that the walker was unable to produce a walking gait of more than 1-2 steps with an approximate success rate of ∼3% in those cases. The test was also repeated with the voltage applied to the actuator but no clutch engagement in all three cases to test for any possible effect from the motor rpm on the walker. All of the trials unactuated cases ultimately resulted in no noticeable change in the walking behaviour, meaning that the actuator dynamics when unclutched from the walker did not affect the experimental setup at all.

With the three validations complete, it was clear that the walking model that was proposed, even if not capable of being fully validated via testing at lower ramp angles, still shared a strong agreement with the experimental setup, and none of the devised checks produced any abnormality as would be expected if the model and the experimental setup did not correlate strongly. Combined with the existing measurements compared to the passive walking dynamics of the walker, this indicates that the walking model presented can be accurately used to characterize the performance of an active-passive hybrid biped with the proposed actuation system.

4.7 Hybrid Dynamics Summary

From these results, we overall see that the initial investigation into the use of the novel method of MTGE actuation resulted in very surprising and useful results. It was found that the actuation behaves in a way that is very desirable, where gaits that have a higher energy cost are affected by the actuation in a way that produces a larger basin of attraction, and gaits that have a low energy cost are affected by the actuation in a way that produces a longer (more useful) stride. In an optimized case at a ramp angle of 2.29˚, we can increase the basin of attraction at its widest by 38% at the cost of ∼2.15 times the walking energy required passively. In the optimized case at a low ramp angle gait at 0.1˚, we see an increase in stride length of over 29%, at an energy cost of equivalent to a walker travelling on a 3.43˚ incline. From both of these results we see that the overall passive-active model proposed has the potential for very interesting results, and considering that there are only three cases of MTGE's and that only the NK-Walker model was considered. Considering that both of these cases were studied from the simplest real world perspective, there is clearly significant future research potential. Overall the novel actuation method researched in this thesis presents a stark contrast to currently published studies in the field that focus on complex actuation and control.

Chapter 5

Conclusions and Future Work

In this thesis, a novel concept has been presented for a discontinuously actuated planar bipedal walking robot. The idea of the walker was shown to fit in a unique gap in current knowledge and published literature, where a passive system (specifically a passive dynamic walker) is actuated via a momentum based approach that injects energy into an existing passive system. A mathematical model for this was proposed, encompassing almost all of the possible simple planar walking systems that can be iterated and used to study the trajectories for a broad range of walking machines. This model was tested and was parametrically studied to provide design guidelines for an experimental walker. It was then also validated against existing models to show that it accurately characterizes the behaviour of a passive walker. A walker was then built based on these guidelines, which utilizes the novel actuation concept presented in the model, in the form of a clutched hip actuation system using a flywheel system to inject momentum in to the walker in a controlled manner. The experimental test setup was then shown to function as a passive walker, and was tested at a variety of ramp angles, with actuation enabled but no energy injection into the system. The walking model was then modified to match the parameters of this experimental setup via single parameter scaling, and a thorough investigation of three main cases of MTGE based actuation events was considered. Via a three point approach, these results were experimentally validated, and several conclusions were drawn regarding the proposed hybrid actuation system.

5.1 Conclusions

The research presented in this thesis overall serves as a design guide for a class of hybrid

actuated walking machines that are not seen in literature, and is therefore the platform for a signification portion of future work. From this research, several key conclusions can be drawn about the behaviour of a passively actuated biped system.

The first conclusion that can be drawn is regarding the general concept of a hybrid active/passive walker. In current literature, a long standing research focus is on using SEA based approaches or other elastic actuation methods to combat joint impedance and create passive bipeds. In the case of this research, a viable alternative has been presented in the form of discontinuous joint actuation via angular momentum injection. In section 3.2 it is clearly shown that this type of actuation is not only viable to implement on the hip of the walker as detailed in this research, but can also be incorporated in the foot, knee, ankle, and any other joint on a passive biped. The model presented in this thesis has been shown to be compatible with hip, knee and foot actuation, and an experimentally implemented test setup shows an archetypal hip actuator of this class.

The second conclusion that can drawn is regarding the effectiveness of angular momentum injection in a passive/active hybrid walker. From the results in section 3.4, it is very clear that an actuator of the form presented not only behaves as predicted, but is also capable of selectively controllable actuation. The tested system was shown to be able to inject $L(\omega) > 0.011\ kg\text{-}m^2$ into the swing leg of the walker, and was able to do so without disturbing the fundamental frequency of the walker swing leg (as shown in Figure 3.5). This system was also shown to be capable of providing discrete values all the way down to the point of no actuation, which means that the energy injection can be accurately modelled, injected, and controlled reasonably and serves to be a high effective actuator for active/passive hybrid walkers.

The third conclusion that can be drawn is regarding the design of the experimental walker, in regards to passive walkers. In the experimental setup a split approach was used, where the model is a simple lumped mass model that is tuned to match the experimental setup and the experimental setup is designed to emulate a lumped mass model. Via the cooperative tuning and single parameter scaling approaches shown, a passive walker was made that was capable of matching the presented simulation model without any parameter scaling or tuning with an peak error of ~4% on the stride length of the walker. This means that the presented approach

for walker design can fundamentally be extended to all walkers attempting to match a lumped mass model.

The fourth conclusion that can be drawn is regarding the actuation of the biped at high ramp angles. At high ramp angles, the proposed actuation model showed that simple MTGE actuation was able to successfully increase the BOA of the walker by ∼33% alone, and when combined with a complex MTGE event, the net result was an increase in BOA width of ∼38%. This came at a total cost of ∼2.15 times the energy input into the system and a theoretically derived net C_t of approximately 0.126. At high ramp angles, a complex MTGE at the stride function was shown to have negative effects on the walking gait, and was not considered a viable option for actuation. Overall, the high ramp angle cases present positive results, where the existing gait quality is retained, and the energy cost of the actuation is put towards expanding the BOA of the walker and improving the stability region.

The final conclusion that can be drawn is regarding the actuation of the biped at low ramp angles. The walking model was shown to produce stable walking gaits down to ramp angles of 0.1˚. At that angle, it was found that a 29% stride length increase could be realized via simple and complex MTGE injection, with the potential for a significant increase via complex MTGE alone. The peak cost increase resulting in a C_t = 0.060, which is approximately equal to the efficiency of a passive walker on a 3.43˚ degree incline. This varies drastically from the high ramp angle cases and presents an overwhelmingly favourable outcome for the low ramp angle cases.

Overall, the research presented showcases some of the rich research potential in the field of active/passive bipedal actuation, with several notable conclusions that have not been seen in the field of passive walking before. The work is intended as a foundation study in the field, and presents a broad potential for future work, as discussed next.

5.2 Future Work

From the work shown above, it is clear that there is substantial potential for research in the field of hybrid active/passive bipeds of the class presented in this thesis. Since the work is functionally a foundational work in the field, there is a significant amount of future work that can be developed based on the presented research. Since the list of long term future work is

quite substantial, it's much more relevant to focus on strategic work that could be done on a short term plan. In general, the strategic future work can be split up in two ways, development of the actuation system (experimentally) and developing more MTGE actuation concepts.

In terms of developing the experimental setup, the current setup has a relatively low efficiency as it uses a high speed low inertia actuation mechanism. By modifying this to be of the high inertia low speed type, the efficiency can be drastically improved. Another issue is that the weight of the setup is relatively high at ~9kg, which means that the dynamic load on the bearings is high. For the low ramp angle cases a much lighter walker with a lower potential actuation system would be ideal to test walker performance in the $<2.0^{\circ}$ range of ramp angles successfully. Finally, significant work should be done on a launch test platform to accurately launch the walker with a specified set of initial conditions. This would make the validation of the walker a straightforward process and also allow for simple validation (experimentally) of the overall actuation system.

In terms of developing the model, countless MTGE events were covered in the course of this research. In terms of dynamical characterization, only the most significant and simple events were considered, as this research is merely an introductory study in the field. In the short term, the other types of actuation presented (knee, foot) can be considered on walkers of the same class but built of a different configuration (such as a flat foot walker). The model can also be modified to accept multiple smaller MTGE's to test the effectiveness of regular (repeatable) MTGE actuation of a smaller magnitude at multiple points. The concept of polarity could also be tested to see if higher ramp angles than normal could be viable via a negative polarity energy injection.

Overall the list of future work for this research is diverse, as the overall work presented is a platform, and is a paradigm shift compared to the current research focus on SEA actuators in the field of hybrid passive bipeds.

Bibliography

[1] T. McGeer, "Passive walking with knees," *Proc. of 1990 International Conference on Robotics and Automation,* pp. 1640-1645, 1990.

[2] T. McGeer, "Passive Dynamic Walking," *Int. J. Robot. Res,* vol. 9, pp. 68-82, 1990.

[3] S. Collins, A. Ruina, R. Tedrake and M. Wisse, "Efficient bipedal robots based on passive-dynamic walkers," *Science,* vol. 307, pp. 1082-1085, 2005.

[4] Y. Sun, Energy Efficient Stabililty Control of a Biped Based on the Concept of Lyapunov Exponents, Winnipeg: Ph.D Thesis, University of Manitoba, 2013.

[5] S. H. Collins and A. Ruina, "A Bipedal Walking Robot with Efficient and Human-Like Gait," in *IEEE International Conference on Robotics and Automation*, Barcelona, Spain, 2005.

[6] R. Tedrake, T. W. Zhang, F. Ming-fai and H. S. Sueng, "Actuating a simple 3D passive dynamic walker," in *IEEE International Conference on Robotics and Automation*, New Orleans, 2004.

[7] S. O. Anderson, M. Wisse, C. G. Atkeson, J. K. Hodgkin, G. J. Zeglin and B. Moyer, "Powered Bipeds Based on Passive Dynamic Principles," in *IEEE-RAS International Conference on Humanoid Robots,* Tsukuba, 2005.

[8] M. M. Williamson, Series Elastic Actuators, Boston: M.Sc Thesis, Massachusetts Institute of Technology, 1995.

[9] M. Wisse and F. J. V., "Design and Construction of MIKE; a 2-D Autonomous Biped Based on Passive Dynamic Walking," *Adaptive Motion of Animals and Machines,* vol. 4, pp. 143-154, 2006.

[10] P. Bhounsule, J. Cortell and A. Ruina, "Design and Control of Ranger: An Energy-Efficient, Dynamic Walking Robot," in *Climbing and Walking Robots and the Support Technologies for Mobile Machines,* , Baltimore, 2012.

[11] J. Schmiedeler and B. Knox, "A Unidirectional Series-Elastic Actuator Design Using a Spiral Torsion Spring," *Journal of Mechanical Design*, vol. 131, no. 12, 2009.

[12] D. Hobbelen, T. de Boer and M. Wisse, "System overview of bipedal robots Flame and TUlip: tailor-made for Limit Cycle Walking," in *2008 IEEE/RSJ International Conference on Intelligent Robots and Systems*, Nice, France, 2008.

[13] M. Wisse, F. V. Frankenhuyzen and B. Moyer, "Passive-based walking robot; denise, a simple, efficient, and lightweight biped.," *IEEE Robotics Automation Magazine*, vol. 14, no. 2, pp. 52-62, 2007.

[14] M. Yong, J. Wang, S. Li and Z. Han, "Energy-Efficient Control of Pneumatic Muscle Actuated Biped Robot Joints," in *The Sixth World Congress on Intelligent Control and Automation*, Dalian, 2006.

[15] K. Hosoda, T. Takuma and M. Ishikawa, "Design and Control of a 3D Biped Robot Actuated by Antagonistic Pairs of Pneumatic Muscles," in *3rd Int. Conf. of Adaptive Motion of Animals and Machines*, Ilmenau, 2005.

[16] B. Verrelst, "The pneumatic biped ”lucy” actuated with Pleated Pneumatic Artificial Muscles," *Autonomous Robots*, vol. 18, no. 2, pp. 201-213, 2005.

[17] A. Kuo, "Energetics of actively powered locomotion using the simplest walking model," *J. Biomech. Eng.*, vol. 124, pp. 113-120, 2002.

[18] J. Choi and J. Grizzle, "Feedback control of an underactuated planar bipedal robot with impulsive foot action," *Robotica*, vol. 23, no. 5, pp. 567-580, 2005.

[19] D. Haeufle, M. Taylor, S. Schmitt and H. Geyer, "A clutched parallel elastic actuator concept: towards energy efficient powered legs in prosthetics and robotics," *IEEE RAS & EMBS International Conference.*, 2012.

[20] E. Yazdi and A. Alasty, "Stabilization of Biped Walking Robot Using the Energy Shaping Method," *Journal of Computational and Nonlinear Dynamics*, vol. 3, 2008.

[21] A. Sanyal and A. Goswami, "Stabilization of Biped Walking Robot Using the Energy Shaping Method," *Journal of Computational and Nonlinear Dynamics*, vol. 3, 2008.

[22] A. Ohta, M. Yamakita and F. K., "From Passive to Active Dynamic Walking," in *IEEE Conference on Decision and Control*, Phoenix, 1999.

[23] S. Suzuki, K. Hta, Y. Pan and S. Hatakeyama, "Biped Walking Robot Control with Passive Walker Model by new VSC servo," in *Proceedings of the American Control Conference*,

Arlington, 2001.

[24] M. W. Spong and F. Bullo, "Controlled Symmetries and Passive Walking," *IEEE Transactions on Automatic Control,* vol. 50, no. 7, pp. 1025-1031, 2005.

[25] Q. Wu and N. Sabet., "An experimental study of passive dynamic walking," *Robotica,* vol. 22, pp. 251-262, 2004.

[26] Q. Wu and J. Chen, "Effects of ramp angle and mass distribution on passive dynamic gait-an experimental study," *International Journal of Humanoid Robotics,* vol. 7, no. 1, pp. 55-72, 2010.

[27] J. Chen, Design and dynamic analysis of four-legged passive dynamic walker with knees, Winnipeg: B.Sc Thesis, University of Manitoba, 2007.

[28] K. Rushdi, D. Koop and Q. Wu, "Experimental studies on passive dynamic bipedal walking," *Robotics and Autonomous Systems,* vol. 62, no. 4, pp. 446-455, 2014.

[29] S. O'Brien, Experimental Stabililty Analysis of Passive Dynamic Walking, Winnipeg: B.Sc Thesis, University of Manitoba, 2009.

[30] D. Koop and Q. Wu, "Passive Dynamic Biped Walking Part I: Development and Validation of an Advanced Model," *ASME Computational and Nonlinear Dynamics,* vol. 8, no. 4, 2013.

[31] D. Koop and Q. Wu, "Passive Dynamic Biped Walking Part II: Stability Analysis of the Passive Dynamic Gait," *ASME Computational and Nonlinear Dynamics,* vol. 8, no. 4, 2013.

[32] R. Ghorbani and Q. Wu, "On improving bipedal walking energetics through adjusting the stiffness of elastic elements at the ankle joint," *International Journal of Humanoid Robotics,* vol. 6, no. 1, pp. 23-48, 2009.

[33] R. Ghorbani and Q. Wu, "Conceptual Design of The Adjustable Stiffness Artificial Tendons for Legged Robotics," *Mechanism and Machine Theory,* vol. 44, pp. 140-161, 2009.

[34] X. Mu and Q. Wu, "Impact Dynamics and Contact Events for Biped Robots via Impact Effects," *IEEE Transactions on Systems, Man and Cybernetics,* vol. 36, no. 6, pp. 1364-1372, 2006.

[35] C. Yang, Q. Wu and G. Joyce, "Effects of Constraints on Bipedal Balancing during Standing," *International Journal of Humanoid Robotics,* vol. 4, no. 4, pp. 735-775, 2007.

[36] M. Alghooneh, On Exploration of Mechanical Insights into Bipedal Walking: Gait Characteristics, Energy Efficiency, and Exploration, Winnipeg: Ph.D Thesis, University of Manitoba, 2014.

[37] M. Alghooneh and Q. Wu, "Single-support heel-off: a crucial gait event helps realizing agile and energy-efficient bipedal walking," *Robotica*, p. Accepted for Publication, 2014.

[38] D. Koop, Dynamics and Stability of Passive Dynamic Biped Walking Using an Advanced Mathematical Model, Winnipeg: M.Sc Thesis, University of Manitoba, 2012.

[39] L. B. Freidovich, U. Mettin, A. S. Shiriaev and M. W. Spong, "A passive 2DOF walker: Finding gait cycles using virtual holonomic constraints," in *47th IEEE Conference on Decision and Control*, Cancun, 2008.

[40] A. Goswami, B. Espiau and A. Keramane, "Limit cycles and their stability in a passive bipedal gait," in *IEEE International Conference on Robotics and Automation*, Minneapolis, 1996.